# SANDIA REPORT

SAND89—2558 • UC—814
Unlimited Release
Printed February 1992

# Groundwater Flow Code Verification "Benchmarking" Activity (COVE-2A): Analysis of Participants' Work

R. C. Dykhuizen, R. W. Barnard

**Prepared by**
**Sandia National Laboratories**
**Albuquerque, New Mexico 87185 and Livermore, California 94550**
**for the United States Department of Energy**
**under Contract DE-AC04-76DP00789**

HYDROLOGY DOCUMENT NUMBER 680

SF2900Q(8-81)

Issued by Sandia National Laboratories, operated for the United States Department of Energy by Sandia Corporation.

**NOTICE:** This report was prepared as an account of work sponsored by an agency of the United States Government. Neither the United States Government nor any agency thereof, nor any of their employees, nor any of their contractors, subcontractors, or their employees, makes any warranty, express or implied, or assumes any legal liability or responsibility for the accuracy, completeness, or usefulness of any information, apparatus, product, or process disclosed, or represents that its use would not infringe privately owned rights. Reference herein to any specific commercial product, process, or service by trade name, trademark, manufacturer, or otherwise, does not necessarily constitute or imply its endorsement, recommendation, or favoring by the United States Government, any agency thereof or any of their contractors or subcontractors. The views and opinions expressed herein do not necessarily state or reflect those of the United States Government, any agency thereof or any of their contractors.

Printed in the United States of America. This report has been reproduced directly from the best available copy.

Available to DOE and DOE contractors from
Office of Scientific and Technical Information
PO Box 62
Oak Ridge, TN 37831

Prices available from (615) 576-8401, FTS 626-8401

Available to the public from
National Technical Information Service
US Department of Commerce
5285 Port Royal Rd
Springfield, VA 22161

NTIS price codes
Printed copy: A04
Microfiche copy: A01

SAND89-2558
Unlimited Release
Printed February 1992

Distribution
Category UC-814

# Groundwater Flow Code Verification "Benchmarking" Activity (COVE-2A): Analysis of Participants' Work

R. C. Dykhuizen
Thermal and Fluid Engineering Division
R. W. Barnard
Repository Performance Assessment Division
Sandia National Laboratories
Albuquerque, New Mexico 87185

## Abstract

The Code Verification Project (COVE) is a series of benchmarking calculations designed to verify numerical procedures for hydrologic flow and contaminant transport through a variably saturated porous medium. The COVE-2A problem set is a subset of the COVE series. COVE-2A compared the outputs from five hydrologic flow computer codes in the analysis of a one-dimensional water infiltration problem set. Initial comparisons between the codes showed very good agreement when comparing the pressure profiles through the domain. Saturations, which are directly derived from the pressures, also agreed well. However, a second round of calculations was required before all the codes could agree on calculated quantities that were derived from the gradient of the pressure.

The work contained in this report was under WBS Element 1.2.1.4.9.


## ACKNOWLEDGMENT

This work was conceived and directed by R. W. Prindle, 6312, who is now a principal of Deuel and Associates, Inc. The authors would like to acknowledge the detailed review of this report provided by P. L. Hopkins,1511, and H. A. Dockery, 6312.

## Contents


1 INTRODUCTION . . . . . 1
1.1 The COVE Project . . . . . 1
1.2 Participants . . . . . 5
1.3 Descriptions of Codes . . . . . 5
2 SUMMARY OF PARTICIPANTS' REPORTED RESULTS . . . . . 8
2.1 TOSPAC . . . . . 8
2.2 TRACR3D . . . . . 8
2.3 TRUST . . . . . 9
2.4 LLUVIA . . . . . 9
2.5 NORIA . . . . . 10
2.6 Code Performance Comparison . . . . . 10
3 DISCUSSION OF RESULTS . . . . . 13
3.1 Steady-State Cases . . . . . 13
3.2 Transient Cases . . . . . 31
4 SUMMARY AND CONCLUSIONS . . . . . 48
5 REFERENCES . . . . . 50
Appendix A. Reference Information Base . . . . . 52

## Figures


1 Stratigraphy for COVE-2A Problems . . . . . 2
2 Case 1: Initial Results for Steady-State Pressure Profile . . . . . 14
3 Case 1: Initial Results for Steady-State Normalized Flux Profile . . . . 15
4 Case 1: Initial Results for Steady-State Fracture Velocity Profile . . . . 15
5 Case 1: Initial Results for Steady-State Matrix Velocity Profile . . . . 16
6 Case 1: Initial Results for Steady-State Hydraulic Conductivity Profile . 16
7 Case 1: Initial Results for Steady-State Saturation Profile . . . . . 17
8 Case 1: Final Results for Steady-State Pressure Head Profile . . . . . 17
9 Case 1: Final Results for Steady-State Fracture Velocity Profile . . . . 18
10 Case 1: Final Results for Steady-State Hydraulic Conductivtiy Profile . . 18
11 Case 2: Final Results for Steady-State Fracture Velocity Profile . . . . 19
12 Case 3: Initial Results for Steady-State Fracture Velocity Profile . . . . 20
13 Case 3: Initial Results for Steady-State Normalized Flux Profile . . . . 21
14 Case 3: Final Results for Steady-State Normalized Flux Profile . . . . 21
15 Case 3: Final Results for Steady-State Fracture Velocity Profile . . . . 22
16 Case 4: Initial Results for Steady-State Pressure Head Profile . . . . . 23
17 Case 4: Initial Results for Steady-State Normalized Flux Profile . . . . 23
18 Case 4: Initial Results for Steady-State Fracture Velocity Profile . . . . 24
19 Case 4: Final Results for Steady-State Normalized Flux Profile . . . . 24
20 Case 4: Final Results for Steady-State Fracture Velocity Profile . . . . 25
21 Case 5: Initial Results for Steady-State Fracture Velocity Profile . . . . 26
22 Case 5: Final Results for Steady-State Fracture Velocity Profile . . . . 26
23 Case 6: Final Results for Steady-State Pressure Head Profile . . . . . 27
24 Case 6: Final Results for Steady-State Normalized Flux Profile . . . . 28
25 Case 6: Final Results for Steady-State Hydraulic Conductivity Profile . . 28
26 Case 6: Final Results for Steady-State Saturation Profile . . . . . 29
27 Case 6: Final Results for Steady-State Fracture Velocity Profile . . . . 29
28 Case 6: Final Results for Steady-State Matrix Velocity Profile . . . . 30
29 Case 7: Final Results for Pressure Head Profile at 100,000 Years . . . . 32
30 Case 7: Final Results for Normalized Flux Profile at 100,000 Years . . . 32
31 Case 7: Final Results for Hydraulic Conductivity Profile at 100,000 Years 33
32 Case 7: Final Results for Saturation Profile at 100,000 Years . . . . . 33
33 Case 7: Final Results for Fracture Velocity Profile at 100,000 Years . . . 34
34 Case 7: Final Results for Matrix Velocity Profile at 100,000 Years . . . 34
35 Case 7: Final Results for Pressure Head at 219.5 Meters . . . . . 35

36 Case 7: Final Results for Normalized Flux at 219.5 Meters . . . . . 35
37 Case 7: Final Results for Hydraulic Conductivity at 219.5 Meters . . . 36
38 Case 7: Final Results for Saturation at 219.5 Meters . . . . . 36
39 Case 7: Final Results for Fracture Velocity at 219.5 Meters . . . . . 37
40 Case 7: Final Results for Matrix Velocity at 219.5 Meters . . . . . 37
41 Case 8: Final Results for Normalized Flux Profile at 100,000 Years . . . 38
42 Case 9: Final Results for Normalized Flux Profile at 300 Years . . . . 39
43 Case 9: Final Results for Fracture Velocity Profile at 300 Years . . . . 40
44 Case 9: Final Results for Pressure Head at 219.5 Meters . . . . . 40
45 Case 9: Final Results for Normalized Flux at 219.5 Meters . . . . . 41
46 Case 9: Final Results for Hydraulic Conductivity at 219.5 Meters . . . 41
47 Case 9: Final Results for Saturation at 219.5 Meters . . . . . 42
48 Case 9: Final Results for Fracture Velocity at 219.5 Meters . . . . . 42
49 Case 9: Final Results for Matrix Velocity at 219.5 Meters . . . . . 43
50 Case 10: Final Results for Pressure Head at 250 Years . . . . . 44
51 Case 11: Final Results for Normalized Flux at 0.5 Years . . . . . 45
52 Case 11: Final Results for Normalized Flux at 1.5 Years . . . . . 46
53 Case 12: Final Results for Normalized Flux at 100 Years . . . . . 47

## Tables

1 COVE-2A Problem Set . . . . . 3
2 Material Properties . . . . . 4
3 COVE-2A Participants . . . . . 5
4 Timing Information for COVE-2A . . . . . 11

# 1 INTRODUCTION

The Nuclear Waste Repository Technology Department at Sandia National Laboratories (SNL) is investigating the suitability of Yucca Mountain as a potential site for underground burial of nuclear wastes. One element of the investigations is to assess the potential long-term effects of groundwater flow on the integrity of a potential repository.

A number of computer codes are being used to model groundwater flow through geologic media in which the potential repository would be located. These codes compute numerical solutions for problems that are usually analytically intractable. Consequently, independent confirmation of the correctness of the solution is often not possible. Code verification is a process that permits the determination of the numerical accuracy of codes by comparing the results of several numerical solutions for the same problem. The international nuclear waste research community uses benchmarking for intercomparisons that partially satisfy the Nuclear Regulatory Commission (NRC) definition of code verification (Silling, 1983). This report presents the results from the COVE-2A (Code Verification) project, which is a subset of the COVE project (Hayden, 1985).

## 1.1 The COVE Project

The COVE series of benchmarking projects have been designed to verify numerical procedures for hydrologic flow and contaminant transport in porous media. COVE-1 investigated a small-scale problem of water flow and contaminant transport through a variably saturated porous medium (Hayden, 1985). COVE-2 problems involve a more complex set of conditions by investigating the performance of codes on problems of repository-site scale. COVE-2A uses a one-dimensional (1-D) geometry with five homogeneous geologic layers. COVE-2B uses a two-dimensional (2-D) geometry with two layers, and COVE-2C specifies two layers and an explicitly modeled fault. Both COVE-1 and COVE-2 problems assume one-phase, isothermal groundwater flow; COVE-3 considers two-phase, nonisothermal, 2-D problems on a repository-site scale. The COVE-1 work has been completed (Hayden, 1985). This report describes COVE-2A activities; the remaining COVE-2 and COVE-3 problems are in various stages of planning and execution.

### COVE-2A Problem Definition

The following is a brief description of the COVE-2A problem. Complete details are provided in the original Problem Definition Memo (PDM) written by Prindle, 1986.

The COVE-2A problem used a 1-D geometry with five hydrogeologic zones (Figure 1). The geologic data were taken from a description of the variably saturated, fractured volcanic tuffs underlying Yucca Mountain, Nye County, Nevada (Peters et al., 1984). The hydrologic model used for the analyses was a composite fracture-matrix continuum (Peters et al., 1988; Dudley et al., 1988). A zero pressure (saturated) boundary condition

was imposed for all COVE-2A cases at the lower boundary. The water flux imposed at the top boundary varied from case to case. The material characterizations of the hydrogeologic zones were provided to the participants. The problem set consisted of twelve cases. These were composed of combinations of three different imposed fluxes, two different material property sets, and a steady or transient boundary condition. The three different imposed water fluxes were 0.1, 0.5 and 4.0 mm/yr. The lowest flux resulted in most of the groundwater flowing through the matrix, and the highest resulted in a fracture-dominated system.

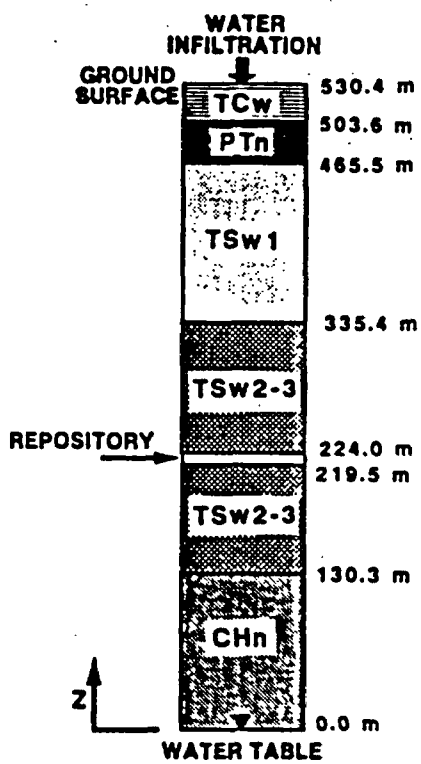


**Figure 1.** Stratigraphy for COVE-2A Problems

For each of the imposed fluxes, there were two hydrologic property sets provided for the Calico Hills (CHn) hydrogeologic zone. The purpose of using different hydrologic properties was to investigate the sensitivity of the numerical solution techniques to sharp contacts between materials of greatly different hydrologic characteristics. For one property set, the Calico Hills zone was considered to be zeolitized (CHnz) and to have hydrologic properties very similar to the Topopah Spring unit directly above. For the other property set, the Calico Hills unit was assumed to be vitrified (CHnv) and to have properties orders of magnitude different from the overlying Topopah Spring. The above resulted in six steady-state cases.

Finally, the six steady-cases were used as initial conditions for six transient cases where the imposed flux was doubled in a step change. This resulted in six transient cases. The twelve total cases allowed for code comparisons for both steady and transient conditions with various combinations of matrix and fracture flow. The 12 cases defining the problem set are listed in Table 1.

**Table 1.** COVE-2A PROBLEM SET

| Case | Imposed Flux (mm/yr) | Materials Properties | Time Domain |
|---|---|---|---|
| 1 | 0.1 | zeolitic | steady |
| 2 | 0.1 | vitric | steady |
| 3 | 0.5 | zeolitic | steady |
| 4 | 0.5 | vitric | steady |
| 5 | 4.0 | zeolitic | steady |
| 6 | 4.0 | vitric | steady |
| 7 | 0.1 to 0.2 | zeolitic | step change |
| 8 | 0.1 to 0.2 | vitric | step change |
| 9 | 0.5 to 1.0 | zeolitic | step change |
| 10 | 0.5 to 1.0 | vitric | step change |
| 11 | 4.0 to 8.0 | zeolitic | step change |
| 12 | 4.0 to 8.0 | vitric | step change |

The requirement that all the analyses be based on the hydrologic equations and input data specified in the PDM was made to ensure a meaningful comparison among all the results. Input data were taken from characterizations of Yucca Mountain tuffs (Peters et al., 1984), and are listed in Table 2. Physical constants, such as the gravitational acceleration, duration of a calendar year, and the compressibility of water, were also provided to ensure consistency among the participants. The extreme detail provided in the problem statement was a result of difficulties encountered in COVE-1 where the problems solved by the individual participants were not identical (especially in their choice of boundary and initial conditions). Participants were not requested to interpret the physical implications of their work (except as the phenomena relate to the performance of their codes), although several did provide interpretations.

Potential computational difficulties were expected to arise from the strong variations of the hydraulic properties as a function of pressure head. Such effects often cause numerical instabilities (Dykhuizen, 1989) or failure of convergence, especially at interfaces where material properties change significantly. The cases where the fractures were partially saturated proved to be the most difficult to calculate due to the more rapid variation of hydraulic conductivity with pressure.

## Table 2. MATERIAL PROPERTIES

| | TCw | PTn | TSw1 | TSw2-3 | CHnv | CHnz |
|---|---|---|---|---|---|---|
| $n_m$ | 0.08 | 0.40 | 0.11 | 0.11 | 0.46 | 0.28 |
| $K_m$ (m/s) | $9.7 \times 10^{-12}$ | $3.9 \times 10^{-7}$ | $1.9 \times 10^{-11}$ | $1.9 \times 10^{-11}$ | $2.7 \times 10^{-7}$ | $2.0 \times 10^{-11}$ |
| $S_{r,m}$ | 0.002 | 0.100 | 0.080 | 0.080 | 0.041 | 0.110 |
| $\alpha_m$ (1/m) | $0.821 \times 10^{-2}$ | $1.5 \times 10^{-2}$ | $0.567 \times 10^{-2}$ | $0.567 \times 10^{-2}$ | $1.600 \times 10^{-2}$ | $0.308 \times 10^{-2}$ |
| $\beta_m$ | 1.558 | 6.872 | 1.798 | 1.798 | 3.872 | 1.602 |
| $n_f$ | $1.4 \times 10^{-4}$ | $2.7 \times 10^{-5}$ | $4.1 \times 10^{-5}$ | $1.8 \times 10^{-4}$ | $4.6 \times 10^{-5}$ | $4.6 \times 10^{-5}$ |
| $K_f$ (m/s) | $5.3 \times 10^{-9}$ | $1.6 \times 10^{-8}$ | $0.9 \times 10^{-9}$ | $3.1 \times 10^{-9}$ | $9.2 \times 10^{-9}$ | $9.2 \times 10^{-9}$ |
| $S_{r,f}$ | 0.0395 | 0.0395 | 0.0395 | 0.0395 | 0.0395 | 0.0395 |
| $\alpha_f$ (1/m) | 1.285 | 1.285 | 1.285 | 1.285 | 1.285 | 1.285 |
| $\beta_f$ | 4.23 | 4.23 | 4.23 | 4.23 | 4.23 | 4.23 |
| $\alpha'_{bulk}$ (1/m) | $6.2 \times 10^{-7}$ | $8.2 \times 10^{-6}$ | $1.2 \times 10^{-6}$ | $5.8 \times 10^{-7}$ | $3.9 \times 10^{-6}$ | $2.6 \times 10^{-6}$ |
| $\frac{\partial n_f}{\partial \sigma'}$ (1/m) | $1.32 \times 10^{-6}$ | $1.9 \times 10^{-7}$ | $5.6 \times 10^{-8}$ | $1.2 \times 10^{-7}$ | $2.8 \times 10^{-8}$ | $2.8 \times 10^{-8}$ |

Nomenclature:

$K$ saturated hydraulic conductivity
$n$ porosity
$\alpha$ van Genuchten parameter
$\alpha'_{bulk}$ coefficient of consolidation
$S$ saturation
$\sigma'$ rock mass stress
$\beta$ van Genuchten parameter

Subscripts:

$f$ fracture
$m$ matrix
$r$ residual

## 1.2 Participants

Participants in the COVE-2A project and the documentation of their work are shown in Table 3:

Table 3. COVE-2A PARTICIPANTS

| Laboratory | Code | COVE-2A Report |
|---|---|---|
| Sandia National Laboratories (SNL Division 6313) | TOSPAC | Dudley et al., 1988 |
| Los Alamos National Laboratory (LANL) | TRACR3D | Birdsell and Travis, 1991 |
| Lawrence Berkeley Laboratory (LBL) | TRUST | not yet available |
| Sandia National Laboratories (SNL Division 1511) | LLUVIA | Hopkins, 1989 |
| Sandia National Laboratories (SNL Divisions 6231 and 1511) | NORIA | Carrigan et al., 1991 |

## 1.3 Descriptions of Codes

The following descriptions of the codes used for COVE-2A are intended to highlight the differences among them. More comprehensive treatments are provided in the individual reports. Although there is no *a priori* indication that the different implementations can affect the results, this possibility must be considered when comparing the results.

### TOSPAC

The SNL Repository Performance Assessment Division used the code TOSPAC (Dudley et al., 1988) to solve the COVE-2A problems (Gauthier et al., 1991). TOSPAC is a one-dimensional, finite-difference code that solves coupled matrix-fracture isothermal liquid flow problems. In determining what output parameters would be available, the COVE-2A project leader investigated the capabilities of TOSPAC. Therefore, no modifications were required of this code to enable output of the requested variables. TOSPAC is capable of solving either the transient or the steady-state equations directly in one dimension.

### TRACR3D

Los Alamos National Laboratory (LANL) used the code TRACR3D (Travis, 1984) for the COVE-2A problems (Birdsell and Travis, 1991). TRACR3D is a finite-difference code that has the capability of modeling one- and two-phase flow in one, two, and three dimensions. TRACR3D uses tabular property data, so a preprocessor code was written to

calculate the characteristic properties in a format useable by TRACR3D. The preprocessor calculated tables of relative permeability and pressure as a function of total saturation using the van Genuchten relationships. The code could not include the effects of rock compressibility; however, they were determined to be small. For the one-dimensional, steady-state COVE-2A cases, the code was modified slightly to stop when it reached a steady-state condition. For transient problems, the code was modified to run starting from a time equal to the negative of the time necessary to reach steady-state; then at time zero, the flux change was imposed.

### TRUST

LBL used the code TRUST (Narasimhan et al., 1978) to solve the COVE-2A problems. This code uses an integral finite-difference method to solve the hydrologic mass conservation equation. Originally, TRUST did not include the ability to separately calculate water velocities in the matrix and fractures, nor did it include the effects of rock compressibility. Several modifications to TRUST were made to facilitate solving the different cases. These primarily included coding the governing and constitutive equations in a form identical with the specifications in the PDM. The TRUST code requires as input an estimate of the pressure head profile. Like TRACR3D, a false transient is solved to obtain the steady-state results for Cases 1 through 6. A preprocessor code was written to estimate the steady solution in order to minimize the execution time requirement. This code also attempted to optimize the calculational mesh sizes.

### LLUVIA

The SNL Computational Fluid Dynamics Division used LLUVIA (Hopkins and Eaton, 1989) to solve the COVE-2A problems (Hopkins, 1989). This code solves problems of one-dimensional, isothermal, steady-state fluid flow through saturated or partially saturated rock. LLUVIA starts with a user-defined mesh on which output is requested. The code actually solves the governing equation on a much finer mesh. The mesh is automatically adapted to maintain accuracy. The code outputs the results at some of these intermediate locations if it is found that the conductivity is changing rapidly. This enables more accurate evaluation of the auxiliary output quantities. The steady-state formulation in LLUVIA allowed quick solution of Cases 1 through 6. However, since LLUVIA only performs steady-state calculations, the six transient COVE-2A cases were calculated as steady-state problems with the fluxes set equal to the final values.

### NORIA

The SNL Geophysics Division (in conjunction with the SNL Computational Fluid Dynamics Division) used the code NORIA (Bixler, 1985) to solve the COVE-2A problems (Carrigan et al., 1991). This code is a two-dimensional, finite-element heat- and mass-transport code designed to solve multiphase transport problems in porous media. For the COVE-2A problems, the full capabilities of NORIA were not required, so a "stripped

down" version was used that considered only single phase flow. NORIA is not capable of performing true one-dimensional problems. Consequently, material properties were set to be transversely uniform, and appropriate side boundary conditions were used to simulate one dimension. Because NORIA does not solve steady-state problems directly, a false transient was simulated to the steady-state condition. The code LLUVIA was run to provide estimates of the steady profile at the NORIA mesh locations in order to reduce the NORIA execution times.

# 2 SUMMARY OF PARTICIPANTS' REPORTED RESULTS

All the participants' calculations produced approximately the same results, although there were some notable differences. They all observed that as the imposed flux increases, the pressure heads increase, resulting in higher total saturations, higher hydraulic conductivities, and higher velocities (matrix and fracture). For the transient problems, they all calculated approximately the same times to achieve the new steady-state, and found that the vitric layer property set resulted in increased times to obtain the new steady state. Their reports stressed different aspects of the problem. As a rule, comparisons were excellent for the primary parameter calculated, the pressure head. Agreement was also good for the saturation level, which is directly derived from the pressure head. However, for quantities that are derived from the gradient of the pressure head (e.g., flux and velocities), the calculations showed noticeable differences. Most of these differences were corrected between the initial results and the final results. Section 3 of this report will detail all of the computational differences that were found.

Initial results were sent in memorandum form to the principal investigator. In these initial results, differences arose mostly from reporting results that contained undetected errors. In future calculations, greater care should be taken to check the results.

This section will compare the results from the different codes in a general fashion. It will identify the types of discrepancies and how they were resolved between the initial and final results. Some observations will also be made about the execution times for the different codes. The next section will compare the results case by case.

## 2.1 TOSPAC

TOSPAC solved every case. An error in the determination of fracture water velocity was found from examining the initial results. Numerical instabilities were also observed. Modifications of the code corrected these errors. One consequence of these modifications was to triple the number of mesh nodes used in the problem to enhance accuracy and stabilize the results. However, efficiency improvements allowed execution times to decrease despite the additional mesh points.

The TOSPAC report provided an extensive analysis and interpretation of the COVE-2A cases.

## 2.2 TRACR3D

TRACR3D successfully computed all of the COVE-2A cases. Solutions did not oscillate at boundary interfaces; therefore, the numerical solution was considered stable. TRACR3D neglected rock compressibility effects in its calculations, but showed that the effect of this omission was small. The authors included an analysis of the difference between cases contrasting the inclusion of vitric and zeolitic zones. They observed that

the high matrix conductivity of the vitric tuff prevented fracture-dominated flow in this unit at all flux rates investigated.

The TRACR3D work initially had problems calculating matrix and fracture velocity for the COVE-2A problems. Originally, these values were calculated by multiplying the pressure gradient between two nodes by the matrix or fracture hydraulic conductivity at the lower node. For locations with high gradients (such as at stratigraphic interfaces), this method is unsatisfactory because the conductivity can differ greatly between the nodes. For the final results, the velocity calculation was modified to obtain more consistent results.

Problems were also encountered because of insufficient accuracy in the tabulated hydraulic properties and an insufficient convergence criterion for the pressure variable. These were identified by LANL, and corrected, before the final code comparisons.

## 2.3 TRUST

TRUST was also able to solve all the cases. The results for water velocities (especially in the fractures) differed from other codes in several of the cases. Additionally, for some of the transient cases, numerical instabilities occurred. The numerical instabilities were probably caused by a mesh that was too coarse (Dykhuizen, 1989).

The coarse mesh probably also contributed to the water velocity discrepancies. However, it is possible that TRUST suffered from the same problem as one identified by LANL in TRACR3D. When solving a false transient to a steady-state condition, pressure is used as the dependent variable, and the calculations are stopped when the pressure converges to a near steady value. Very small changes in the pressure can cause noticeable changes in the local flux. This may have accounted for TRUST showing good agreement for pressure, but noticeable differences for fracture velocities.

Initially TRUST had an error in calculating fluid velocities due to an indexing error. This was corrected for the final TRUST results.

## 2.4 LLUVIA

Originally, LLUVIA was designed to evaluate groundwater travel time, and consequently reported outputs such as saturation, velocity, and conductivity as approximate averages over the internodal cells. This resulted in small errors in the initial results that were reported for LLUVIA. LLUVIA was modified to evaluate the requested output as point values to enable comparisons with the other participants. This produced better results for the flux and velocity profiles.

LLUVIA is a one-dimensional, steady-state code; therefore, Cases 7 through 12 were solved with constant imposed fluxes equal to the respective final values. Transient results were not available for comparison with the other participants.

## 2.5 NORIA

NORIA is a two-dimensional finite-element code that successfully computed all the COVE-2A cases. Some cases converged slowly. To improve convergence, adjustment of some of the code input variables was made. For the steady-state problems it was found that increasing the liquid compressibility reduced the computational effort required to obtain the steady-state. For transient problems it was found that two modifications allowed faster solutions. The first was to reduce the magnitude of the error tolerance. The second was to not allow the hydraulic conductivity of the two-dimensional elements to vary in the horizontal direction when solving these one-dimensional problems. Carrigan et al., 1991 provided an analysis of the results, including an analysis of the mass balance considerations for the steady and transient cases.

## 2.6 Code Performance Comparison

Table 2 lists the execution times for the codes to reach solutions for the various cases. TRACR3D, TRUST, and NORIA were run on a Cray X-MP super computer. LLUVIA and TOSPAC were run on a VAX 8650. For each code, the total reported execution times for each case are listed, as well as a "normalized time" consisting of the execution time divided by the number of nodes for each problem. Additionally the normalized execution times reported for the VAX 8650 computer were also divided by a factor of 10. This nominally corrects for the fact that the VAX 8650 is significantly slower than the Cray X-MP. This normalization somewhat accounts for the different meshes and computers used by the different participants. However, because the participants were not told that execution time comparisons were going to be made, it is unfair to rate the codes based on execution times alone. No value judgments were given in the problem definition that allowed the participants to weight accuracy against efficiency.

As can be seen from Table 4, Cases 1 through 6 are most efficiently solved by LLUVIA or TOSPAC, which solve steady-state equations directly. The other codes obtain the steady-state solution through the computation of a false transient.

Calculations for flux values in the transition from predominantly matrix flow to predominantly fracture flow commonly encounter computational difficulties. For the COVE-2A problem, these were Cases 3 and 4, and Cases 9 and 10. As Table 2 shows, this is reflected in the longer execution times for these cases. The most inconsistent timing appears to be for the TRUST Cases 3 and 4, which are extraordinarily short compared with timings for other codes, and with timings for other TRUST cases. This, however, can be easily explained. TRUST employs a preprocessor code to calculate an initial condition. The pressure profile is easier to approximate for cases where the properties change rapidly (as in Cases 3 and 4). Therefore TRUST probably had a much better initial condition for calculating these steady-states conditions. For Cases 9 and 10, where all codes started with the same initial condition, TRUST had the same difficulty as the rest of the codes.

## Table 4. TIMING INFORMATION FOR COVE-2A

| LLUVIA Timing Information (Run on VAX 8650) | | | | TOSPAC Timing Information (Run on VAX 8650) | | | |
|---|---|---|---|---|---|---|---|
| Case | Nodes | CPU Time (s) | Time/Node ×0.1 | Case | Nodes | CPU Time (s) | Time/Node ×0.1 |
| 1 | 214 | 30.6 | 0.014 | 1 | 2303 | 160 | 0.007 |
| 2 | 211 | 20.4 | 0.010 | 2 | 2303 | 160 | 0.007 |
| 3 | 187 | 28.8 | 0.015 | 3 | 2303 | 160 | 0.007 |
| 4 | 207 | 21.8 | 0.011 | 4 | 2303 | 160 | 0.007 |
| 5 | 215 | 33.0 | 0.015 | 5 | 2303 | 160 | 0.007 |
| 6 | 281 | 46.9 | 0.017 | 6 | 2303 | 160 | 0.007 |
| | | | | 7 | 2303 | 1056 | 0.046 |
| | | | | 8 | 2303 | 985 | 0.043 |
| | | | | 9 | 2303 | 24142 | 1.05 |
| | | | | 10 | 2303 | 17389 | 0.76 |
| | | | | 11 | 2303 | 7301 | 0.32 |
| | | | | 12 | 2303 | 9164 | 0.40 |

| TRACR3D Timing Information (Run on Cray X-MP/48) | | | | TRUST Timing Information (Run on Cray X-MP) | | | |
|---|---|---|---|---|---|---|---|
| Case | Nodes | CPU Time (s) | Time/Node | Case | Nodes | CPU Time (s) | Time/Node |
| 1 | 362 | 39.6 | 0.11 | 1 | 183 | 104 | 0.57 |
| 2 | 362 | 33.2 | 0.09 | 2 | 134 | 62.0 | 0.46 |
| 3 | 362 | 148 | 0.41 | 3 | 338 | 3.9 | 0.01 |
| 4 | 362 | 159 | 0.44 | 4 | 315 | 4.2 | 0.01 |
| 5 | 362 | 67.7 | 0.19 | 5 | 240 | 14. | 0.06 |
| 6 | 362 | 114 | 0.31 | 6 | 308 | 7.4 | 0.02 |
| 7 | 362 | 151 | 0.42 | 7 | 183 | 290 | 1.58 |
| 8 | 362 | 137 | 0.38 | 8 | 134 | 211 | 1.57 |
| 9 | 362 | 462 | 1.28 | 9 | 338 | 3000 | 8.88 |
| 10 | 362 | 510 | 1.41 | 10 | 315 | 6720 | 21.3 |
| 11 | 362 | 307 | 0.85 | 11 | 240 | 149 | 0.62 |
| 12 | 362 | 679 | 1.88 | 12 | 308 | 7800 | 25.3 |

## TABLE 4 (CONTINUED) TIMING INFORMATION FOR COVE-2A

NORIA Timing Information
(Run on Cray X-MP)

| Case | Nodes | CPU Time (s) | Time/Node |
|---|---|---|---|
| 1 | 401 | 60 | 0.15 |
| 2 | 401 | 90 | 0.22 |
| 3 | 401 | 400 | 1.00 |
| 4 | 401 | 630 | 1.57 |
| 5 | 401 | 150 | 0.37 |
| 6 | 401 | 250 | 0.62 |
| 7 | 401 | 60 | 0.15 |
| 8 | 401 | 60 | 0.15 |
| 9 | 401 | 1030 | 2.57 |
| 10 | 401 | 840 | 2.09 |
| 11 | 401 | 360 | 0.90 |
| 12 | 401 | 215 | 0.54 |

# 3 DISCUSSION OF RESULTS

Results for each case from each participant have been plotted together in the figures presented in this report. The results identified as initial are the results obtained by the participants before any comparisons with the others were made. The initial results show greater variations among the participants. After some obvious errors were corrected, the final results exhibited much greater agreement.

The following discussion generally addresses the areas of disagreement among the codes. In part, the narrative refers to the steps taken by the participants to produce consistent results; these were summarized in the previous section. There is excellent agreement by all codes for calculations of pressure head (which is the primary dependent variable) and saturation (which is directly derived from the pressure). This is expected because the codes use the pressure value in calculating their error tolerances. Agreement for quantities derived from gradients of the pressure (such as fluxes and velocities) is not quite as good.

A large change in fracture saturation is required to conform to the boundary condition of complete saturation at the water table for many of the cases. This results in orders-of-magnitude changes in fracture conductivity near the water table. The equivalent porous medium model (Peters and Klavetter, 1988) assumes local pressure equilibrium between the matrix and fractures. Therefore, the gradient for both is the same at every point. At locations near the water table, the model predicts that the flow rapidly shifts from the matrix to the fractures, causing the fracture velocity to increase dramatically (sometimes by ten orders of magnitude). This causes a large spread in the reported values for the fracture velocity near the water table (within 1 m elevation). This difference is very localized, and therefore has little impact on travel times or water content of the mountain.

## 3.1 Steady-State Cases

For steady-state, one-dimensional problems, a good measure of the accuracy of a problem solution is when the ratio of the computed flux to the flux imposed at the boundary equals 1.0. This ratio was required output for all participants, and is referred to here as normalized flux. The higher imposed flux values, where fracture flow existed, resulted in the largest error in this measure, and the TRUST code typically reported the highest errors. However, for Cases 5 and 6 (the highest imposed steady flux), the TRUST code only exhibited 2 percent errors in this measure. For all of the other combinations of Cases and participants the errors were less than 1 percent. As mentioned earlier, the amount of deviation in this measure can be further reduced by decreasing mesh spacing, and decreasing the convergence tolerance in the calculations.

Agreement between all codes was very good for the steady-state problems.

## Case 1: Steady-state 0.1 mm/yr, zeolitic

Case 1 was the least demanding case for the codes. The flow was steady, and almost entirely contained within the matrix flow system. The initial results are shown in Figures 2 through 7. These show many discrepancies in the results when comparing the codes. TOSPAC initially exhibited errors in calculating fracture velocities (Figure 4); however, this is of little concern due to the dominance of the matrix flow system in this case. This error becomes more of a concern in other cases where the fracture flow is dominant. LLUVIA initially reported a small error in the normalized flux due to the coarse mesh and the computational procedure used (Figure 3). Very localized errors occurred in the TRUST results (see Figure 6 for the hydraulic conductivity) and in the TRACR3D results (see Figure 4 for the fracture velocity) at the Paintbrush Topopah Spring (PTn/TSw1) interface. These were so local that they would not cause any significant differences in the water content or travel time over the scale of the problem.

The final results corrected the above noted errors except for the very localized error by TRUST. Figure 8 shows that the pressure profile was unchanged due to the corrections put in place for the final calculations. Figures 9 and 10 exhibit the corrected output for the variables that did not agree in the initial comparison.

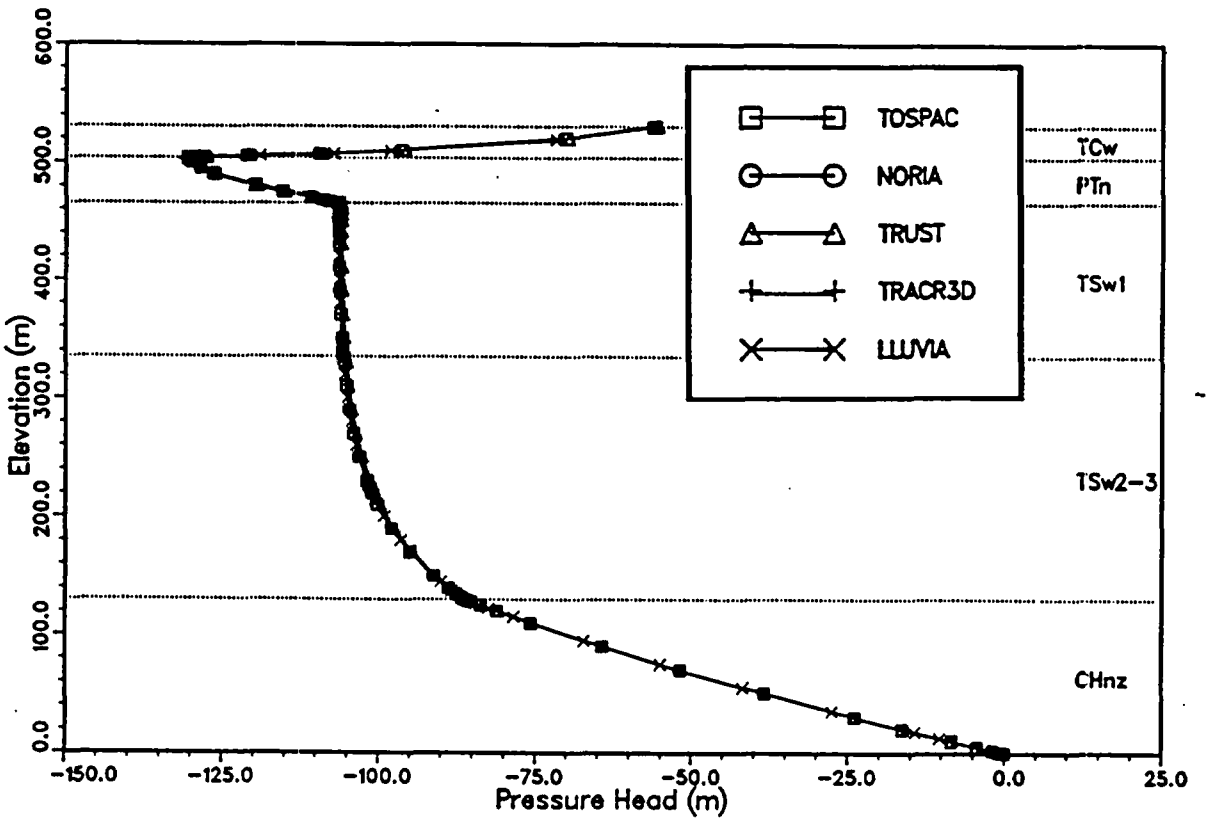


Figure 2. Case 1: Initial Results for Steady-State Pressure Profile

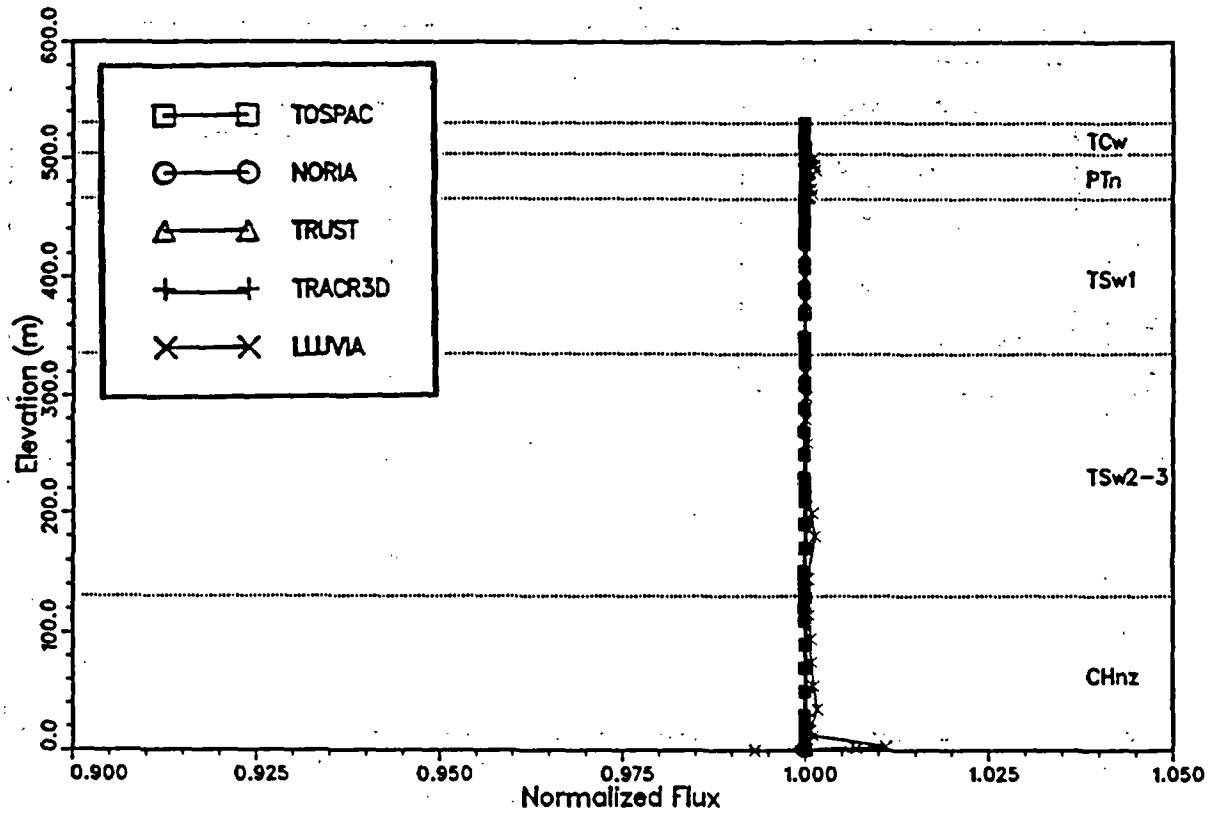


Figure 3. Case 1: Initial Results for Steady-State Normalized Flux Profile

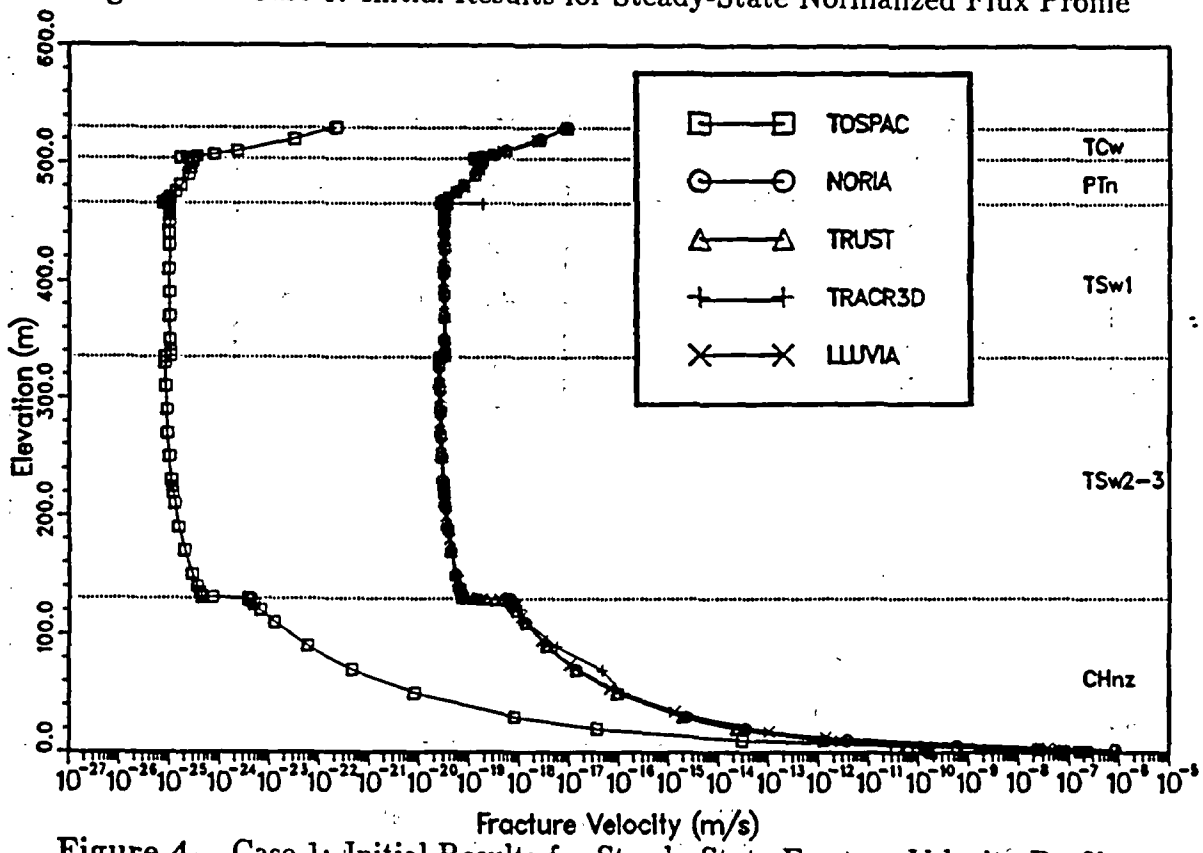


Figure 4. Case 1: Initial Results for Steady-State Fracture Velocity Profile

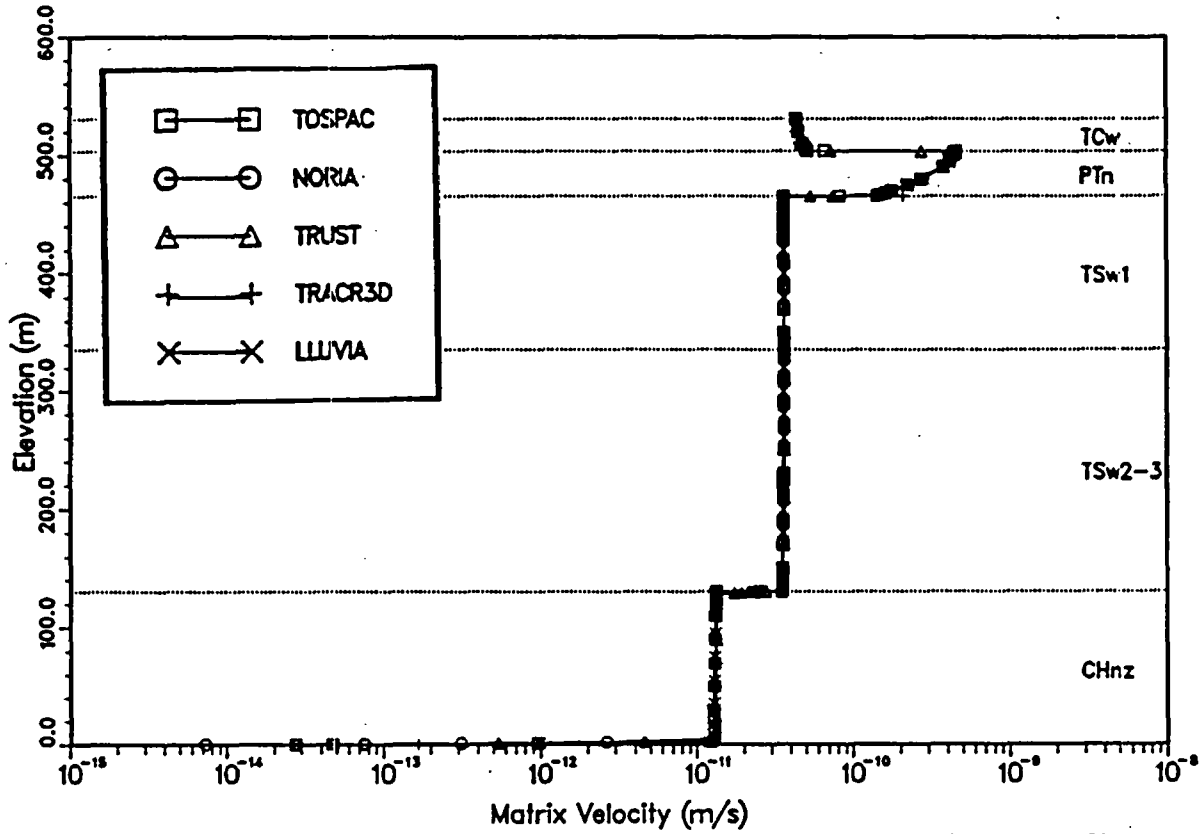


Figure 5. Case 1: Initial Results for Steady-State Matrix Velocity Profile

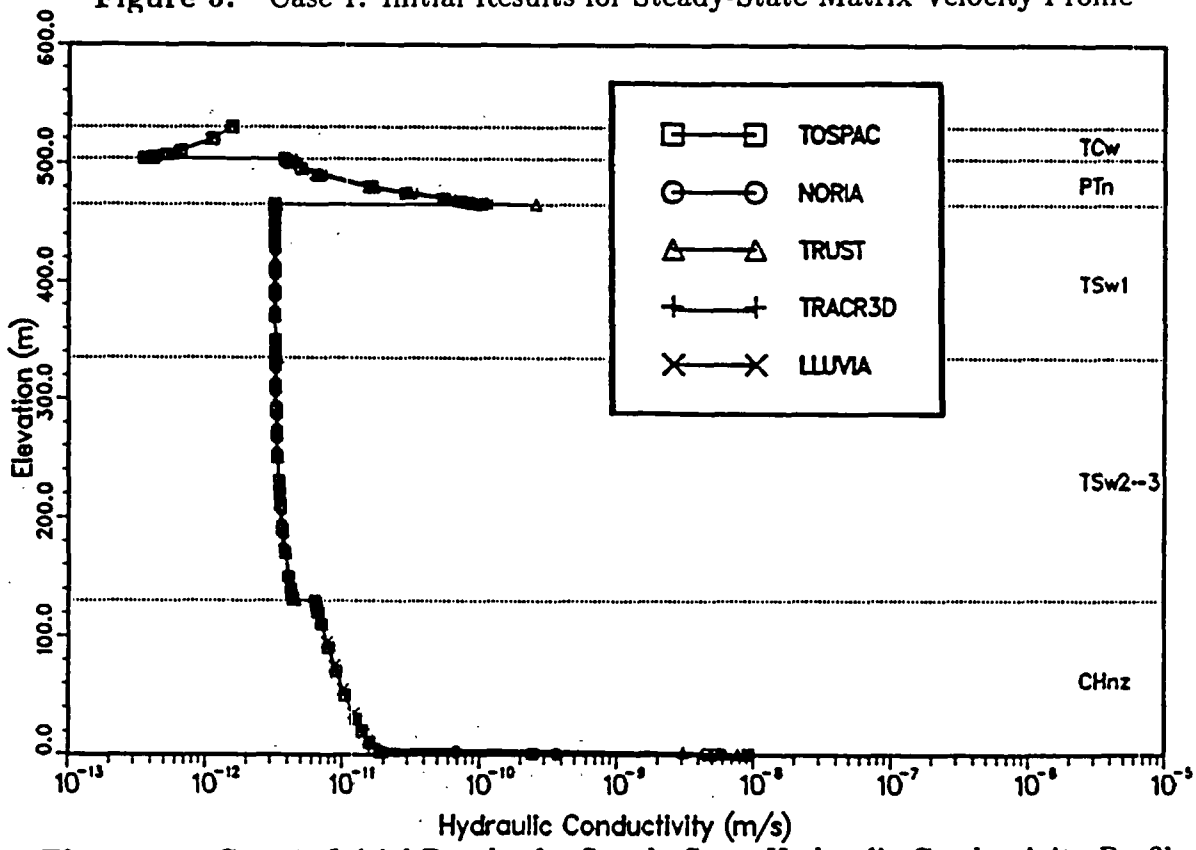


Figure 6. Case 1: Initial Results for Steady-State Hydraulic Conductivity Profile

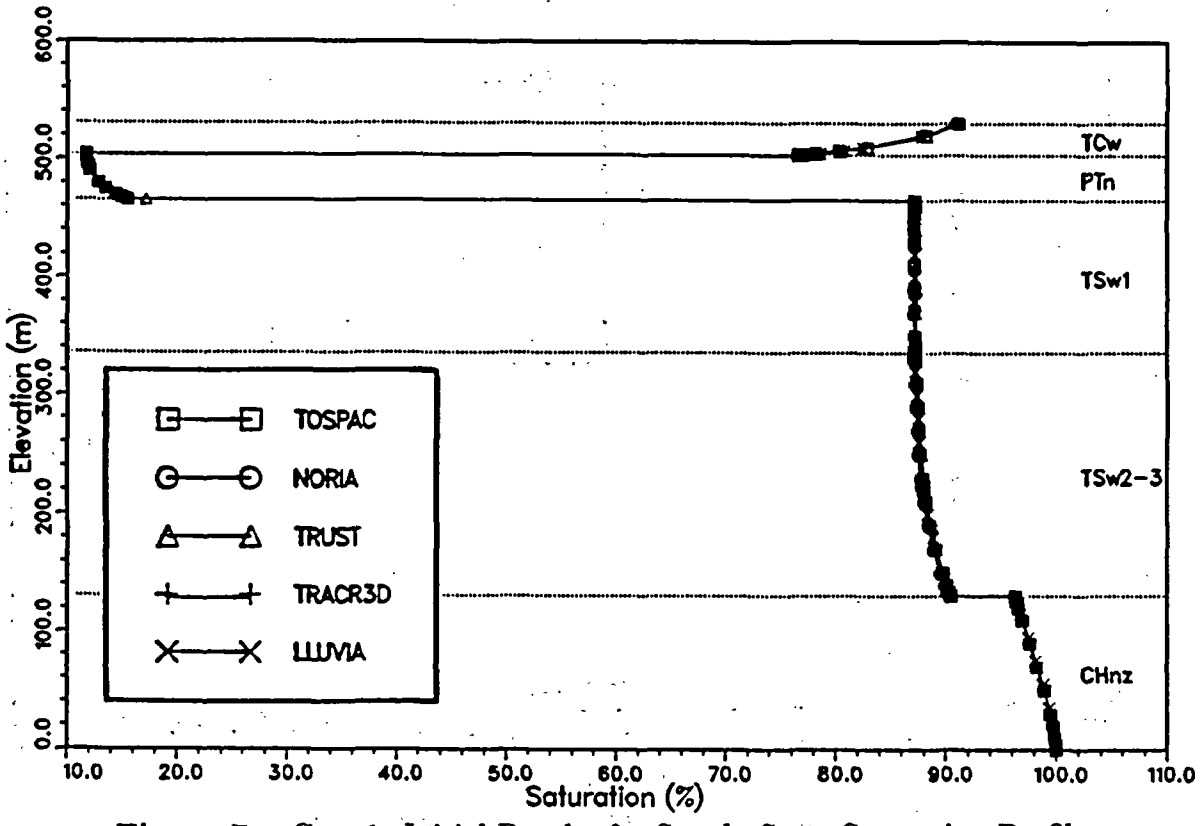


Figure 7. Case 1: Initial Results for Steady-State Saturation Profile

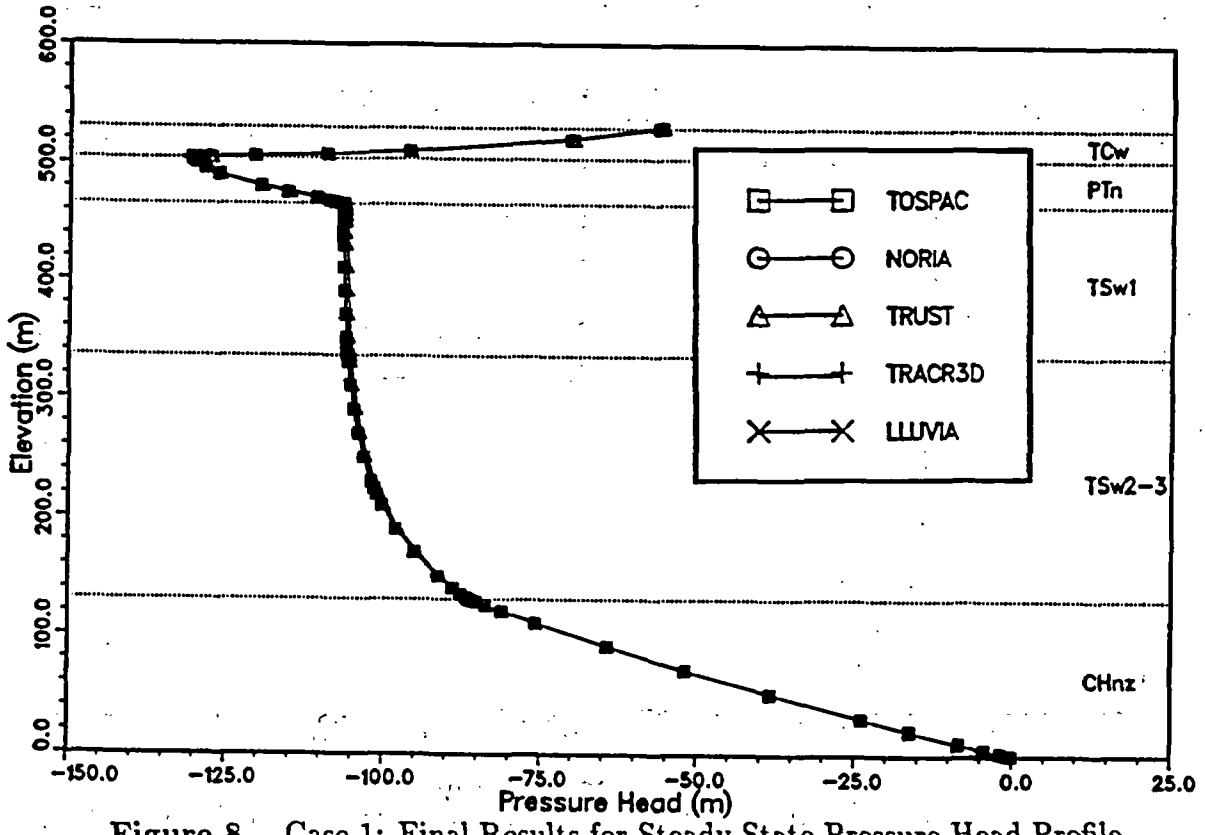


Figure 8. Case 1: Final Results for Steady-State Pressure Head Profile

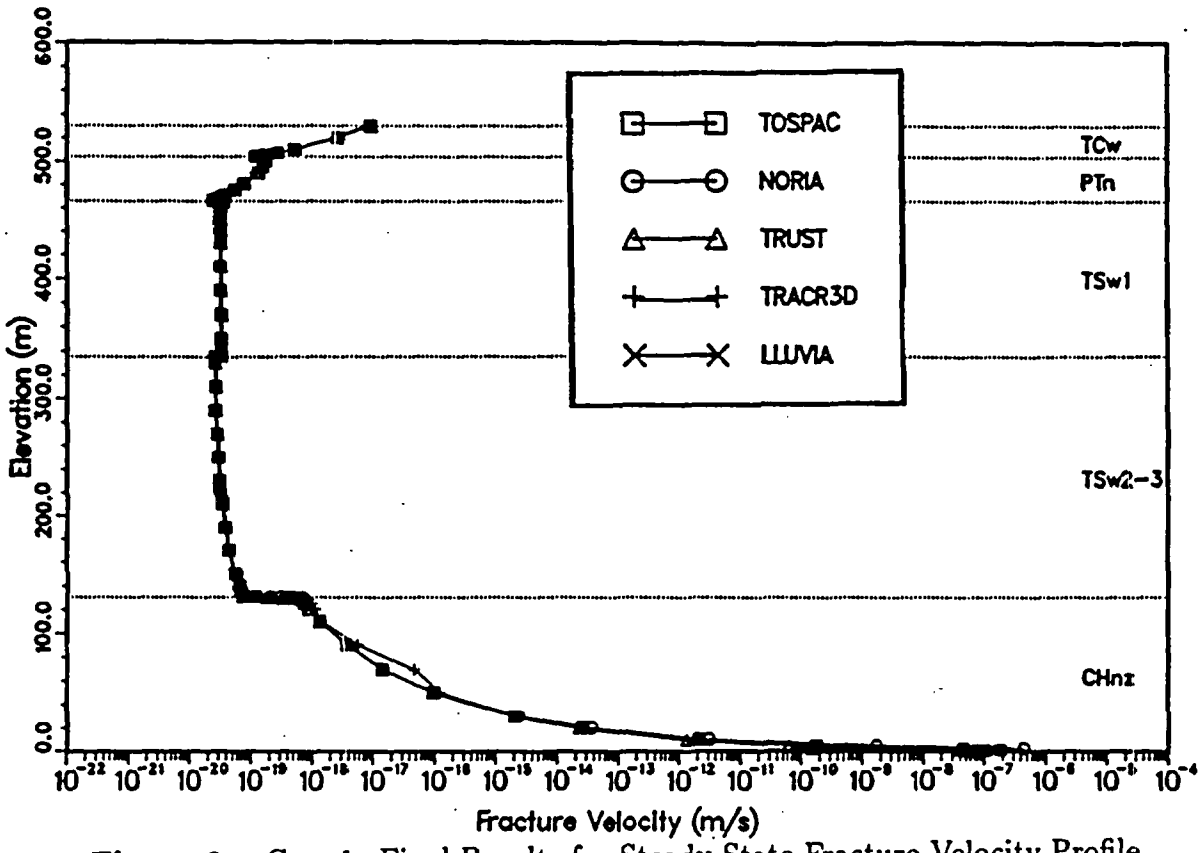


Figure 9. Case 1: Final Results for Steady-State Fracture Velocity Profile

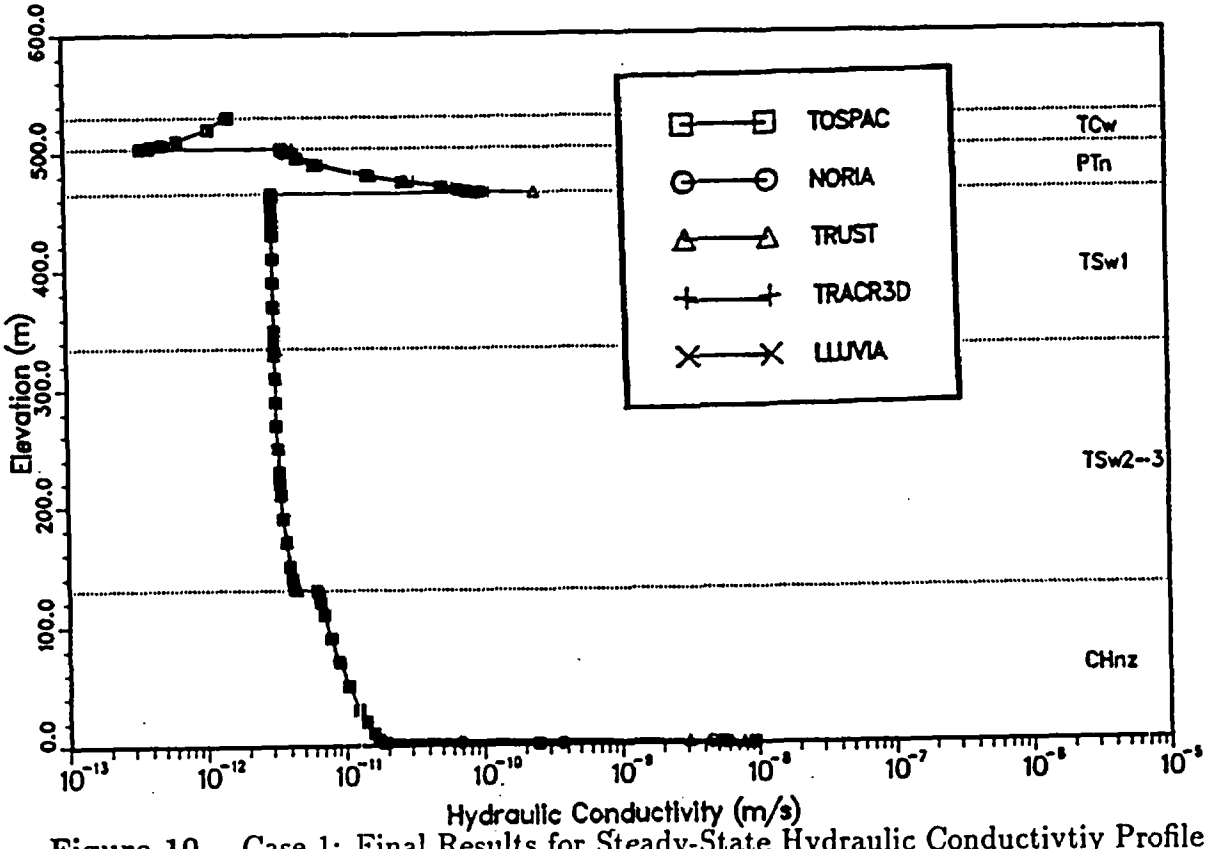


Figure 10. Case 1: Final Results for Steady-State Hydraulic Conductivtiy Profile

### Case 2: Steady-state 0.1 mm/yr, vitric

This case is identical to Case 1 except that the Calico Hills geologic unit is now defined as vitric. This results in a large change in the hydraulic conductivity at the Topopah Springs (TSw2-3) and Calico Hills (CHnv) interface. The initial and final results for this case are similar to those of Case 1. The new interface (TSw2-3/CHnv) introduced some new errors similar to the errors in Case 1 at the PTn/TSw1 interface. TRUST overestimated the hydraulic conductivity at the TSw2-3/CHnv interface, and TRACR3D overestimated the velocities at this interface. But again these errors were very localized. In the final calculations, these local effects were reduced by TRUST and eliminated by TRACR3D.

The TRUST results for fracture velocity diverged from the others in both the initial and the final calculations. The fracture velocity final result is shown in Figure 11. For all the COVE-2A results, the TRUST work was done with a coarser mesh than that used by the other participants. It is thought that a finer mesh and/or a tighter convergence criterion would help improve the TRUST results. A correction in the indexing of nodal values between the initial and the final results did not resolve the discrepancy in the fracture velocity between TRUST and the other codes. However, this correction did help in some of the later cases.

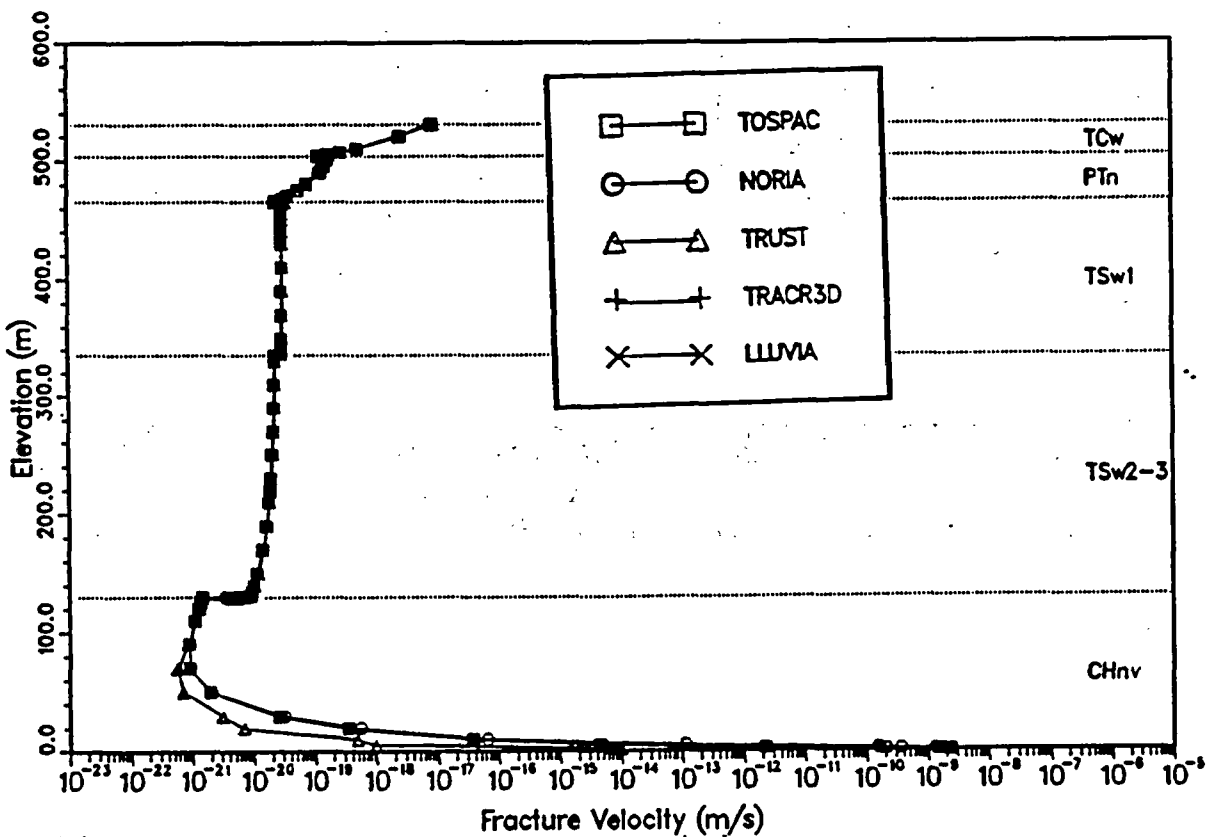


Figure 11. Case 2: Final Results for Steady-State Fracture Velocity Profile

### Case 3: Steady-state 0.5 mm/yr, zeolitic

This case is similar to Case 1 except that the flux has been increased. The initial results for this case were similar to Cases 1 and 2 in degree of divergence by some participants. This case resulted in some fracture flow in the TCw unit and the lower part of the CHn unit (Figure 12). This case resulted in a six orders of magnitude increase in fracture flux over Case 1 (where the fracture velocity was negligible). The occurrence of fracture flow increases the normalized flux errors (which are still small) in these units (Figure 13). In contrast to the prior cases, the participants were less successful at getting the normalized flux to be uniform (at unity) as shown in Figure 14, but the deviations are still less than 1 percent. The initial differences in the fracture velocity (due to the coding error in TOSPAC) were resolved (Figure 15).

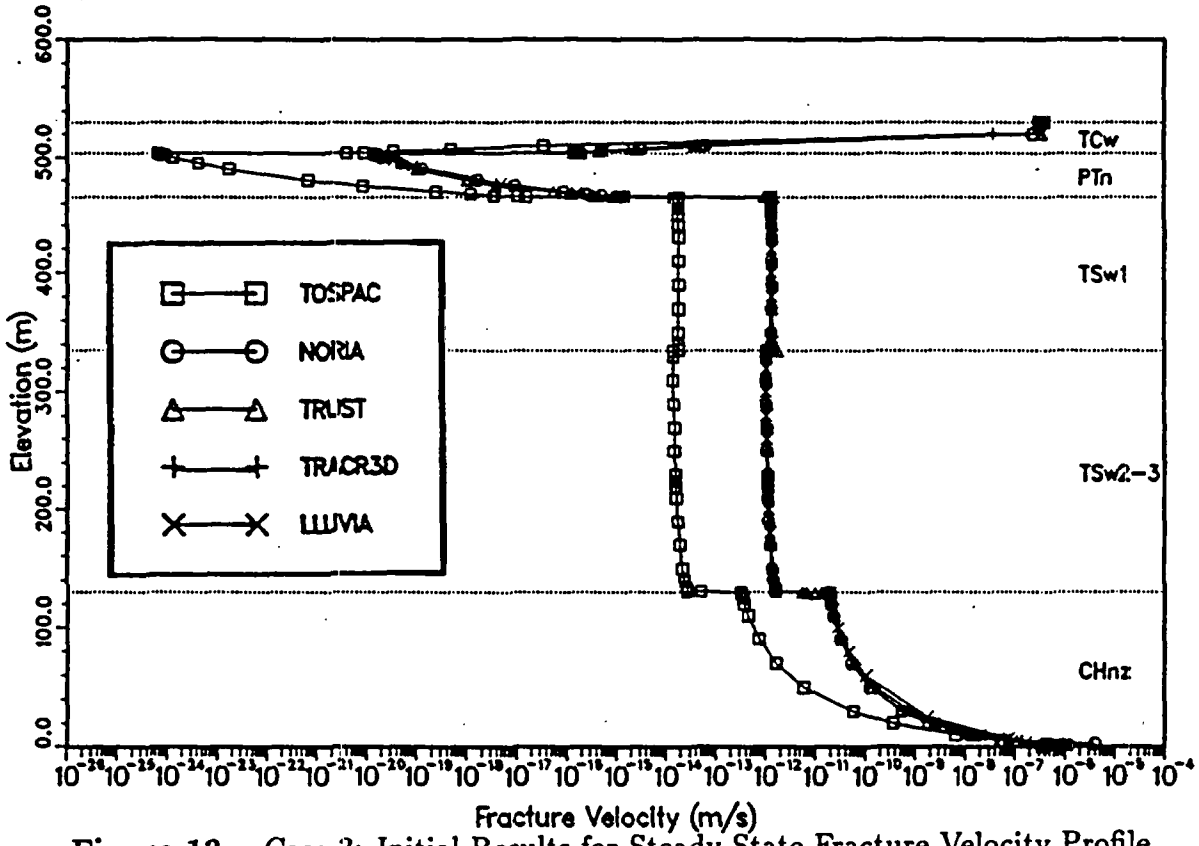


Figure 12. Case 3: Initial Results for Steady-State Fracture Velocity Profile

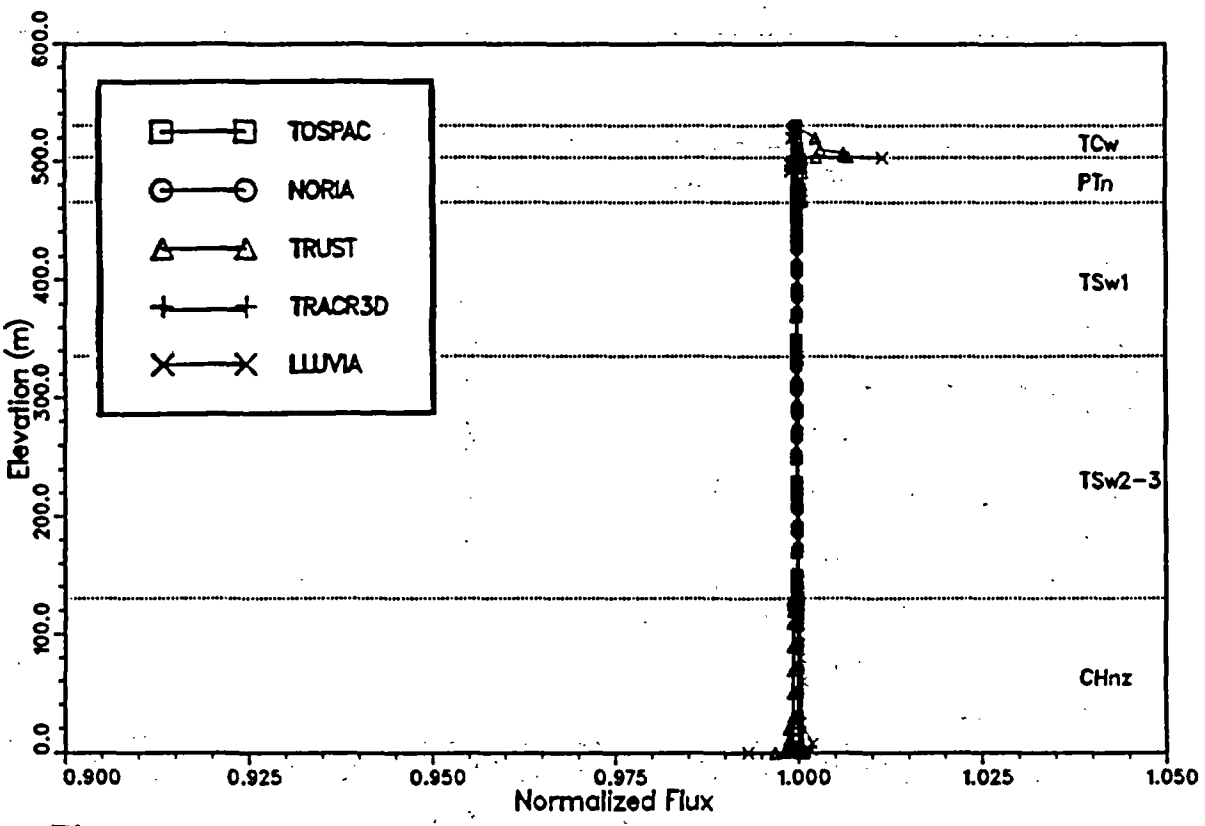


Figure 13. Case 3: Initial Results for Steady-State Normalized Flux Profile

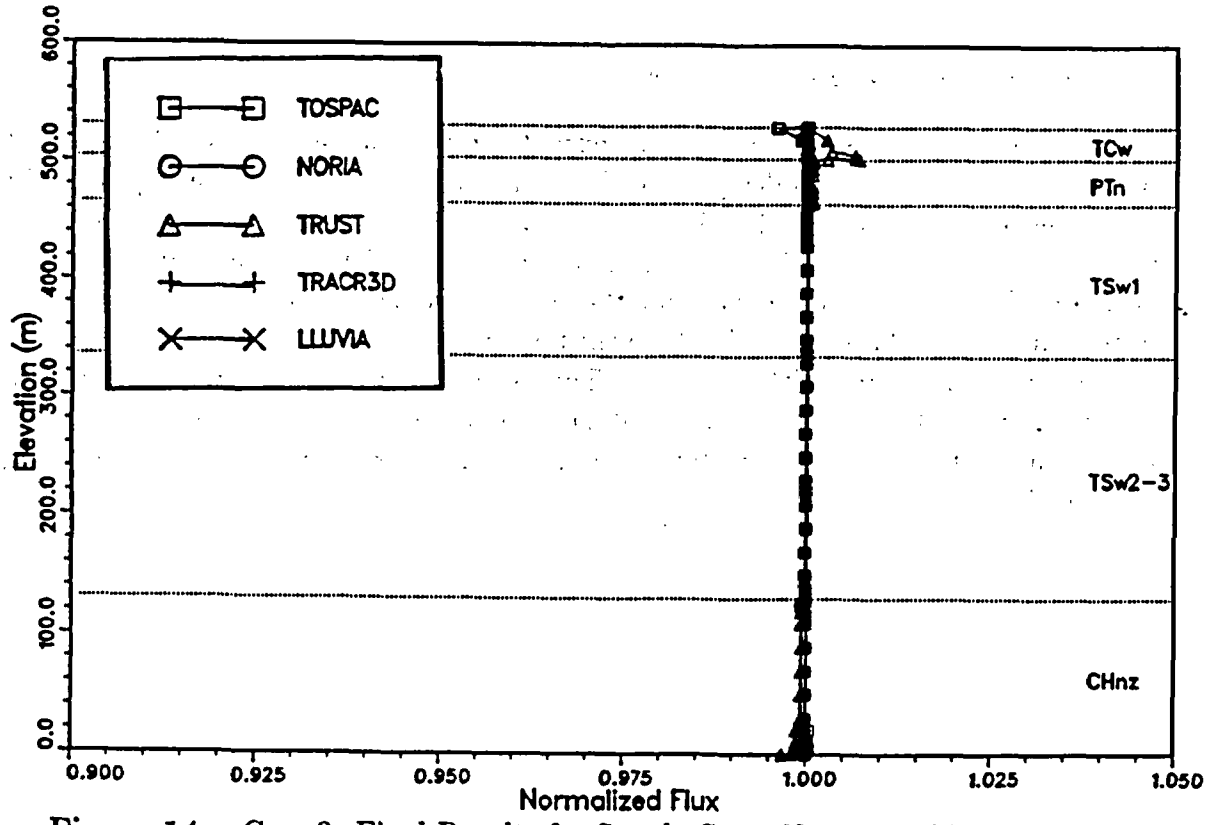


Figure 14. Case 3: Final Results for Steady-State Normalized Flux Profile

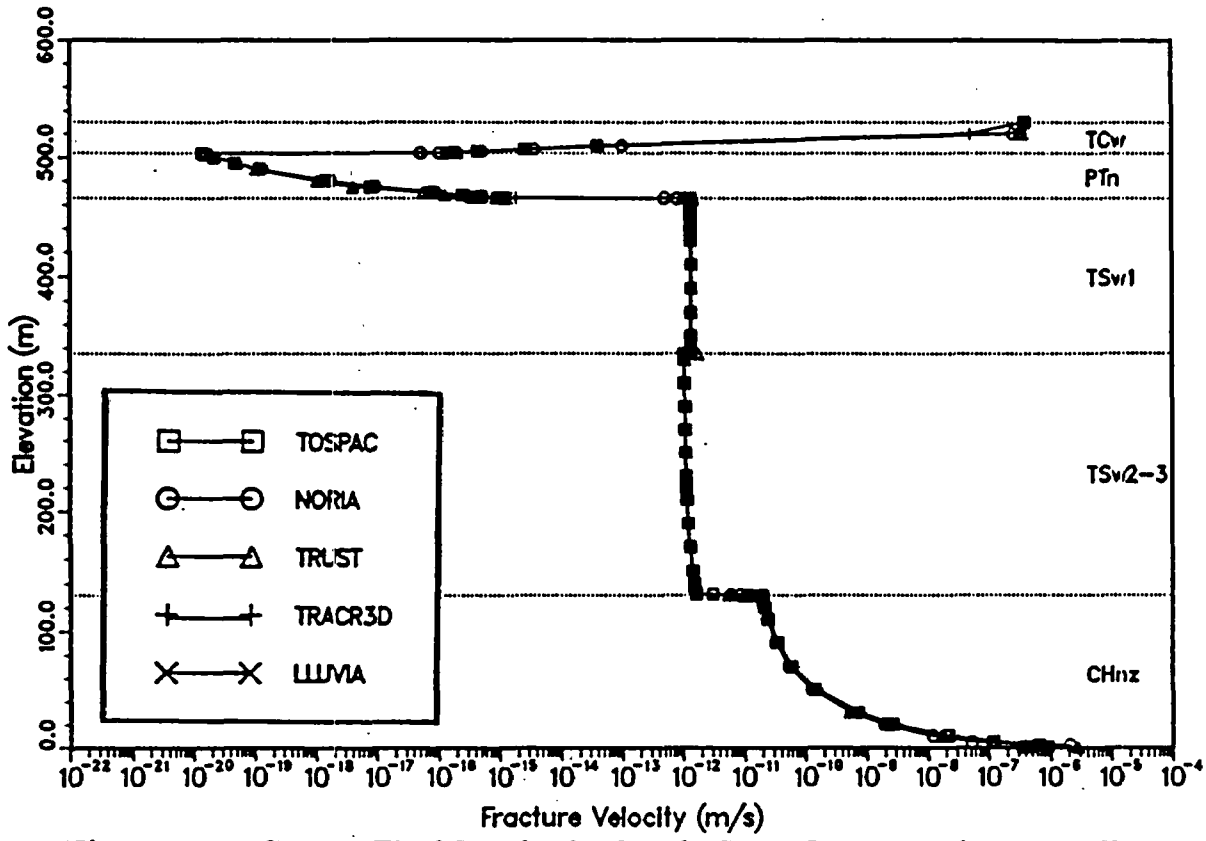


**Figure 15.** Case 3: Final Results for Steady-State Fracture Velocity Profile

### Case 4: Steady-state 0.5 mm/yr, vitric

This case is the same as Case 2, except for the increased flux. As in all of the previous cases, all of the codes produced identical results for the pressure profile (Figure 16). However, the initial TRUST results showed increased discrepancies in comparison to the other participants for the secondary variables. This is illustrated best by the normalized flux plot (Figure 17) and the fracture velocity plot (Figure 18). TRUST's initial calculation of fracture velocity in the bottom portion of the problem domain has the wrong sense, increasing with elevation. This is largely due to the previously mentioned indexing error. Correction of this coding error brought the TRUST results in better agreement with the others, but differences are still apparent in the final results (Figures 19 and 20).

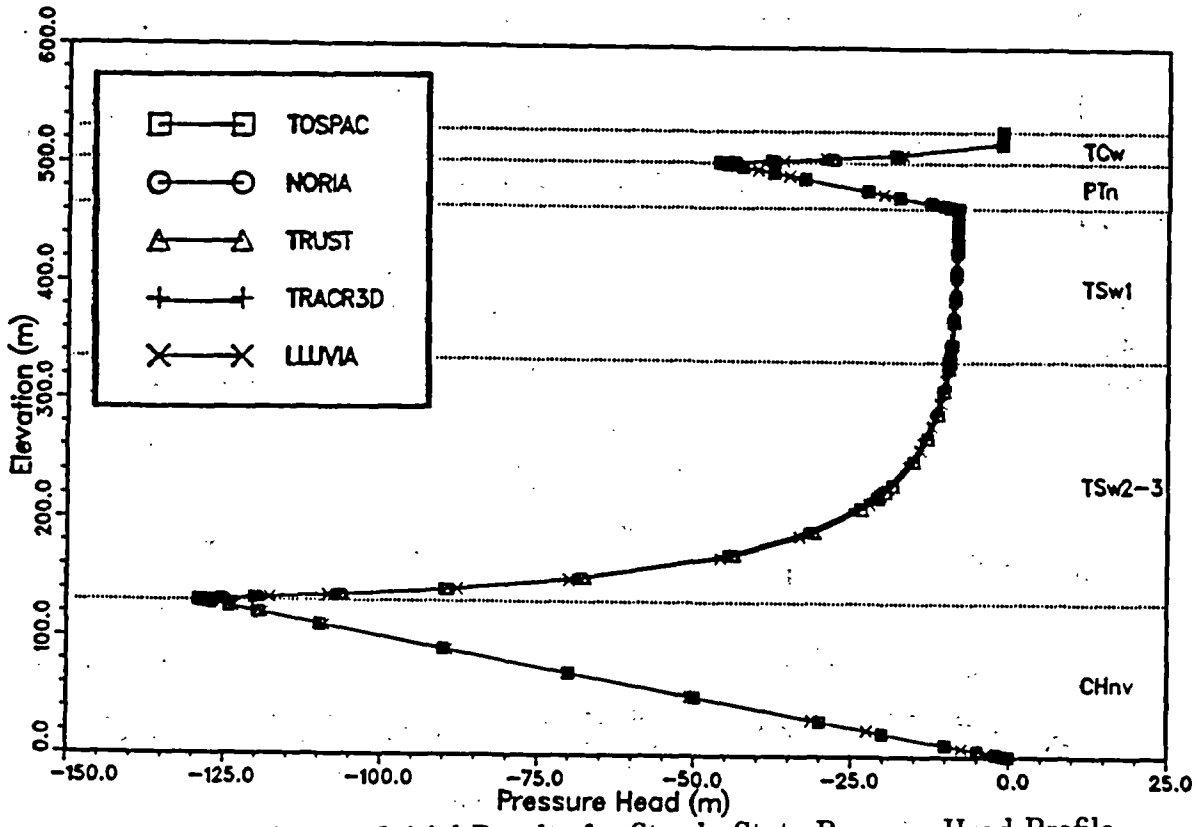


Figure 16. Case 4: Initial Results for Steady-State Pressure Head Profile

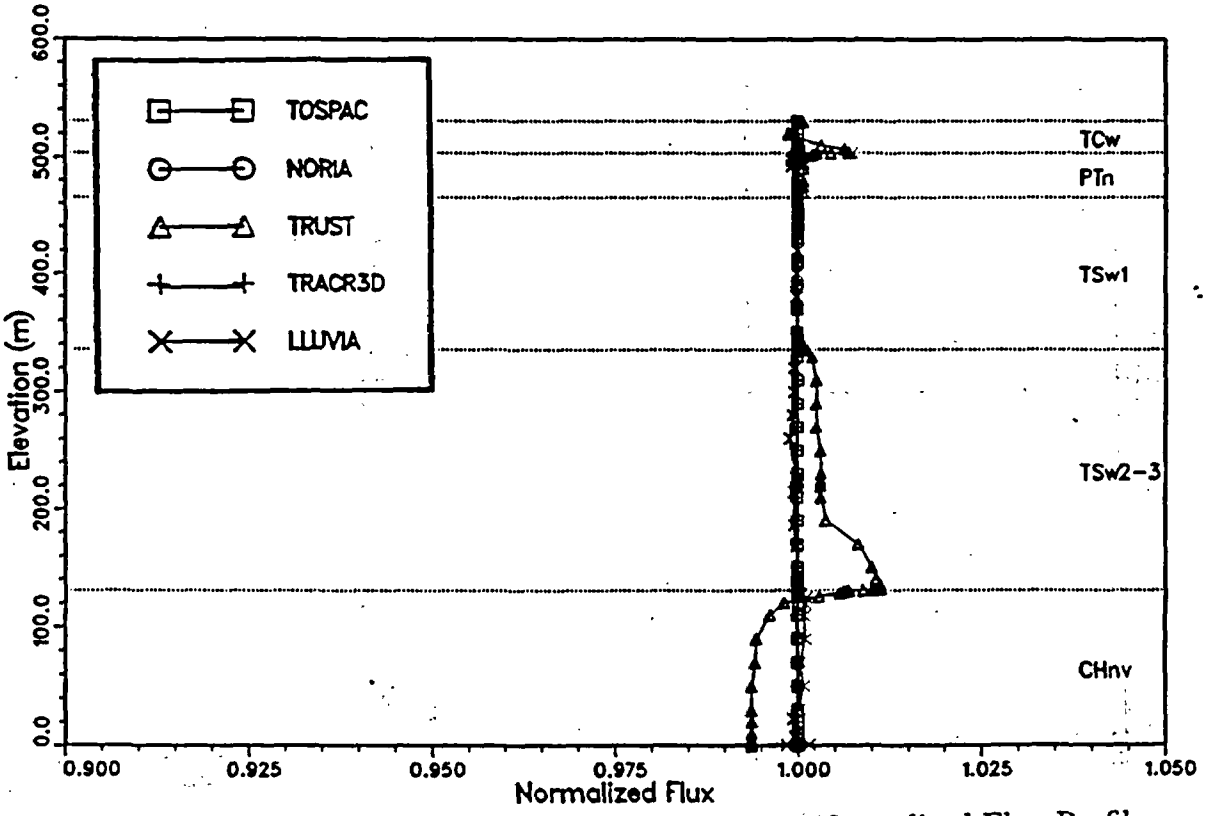


Figure 17. Case 4: Initial Results for Steady-State Normalized Flux Profile

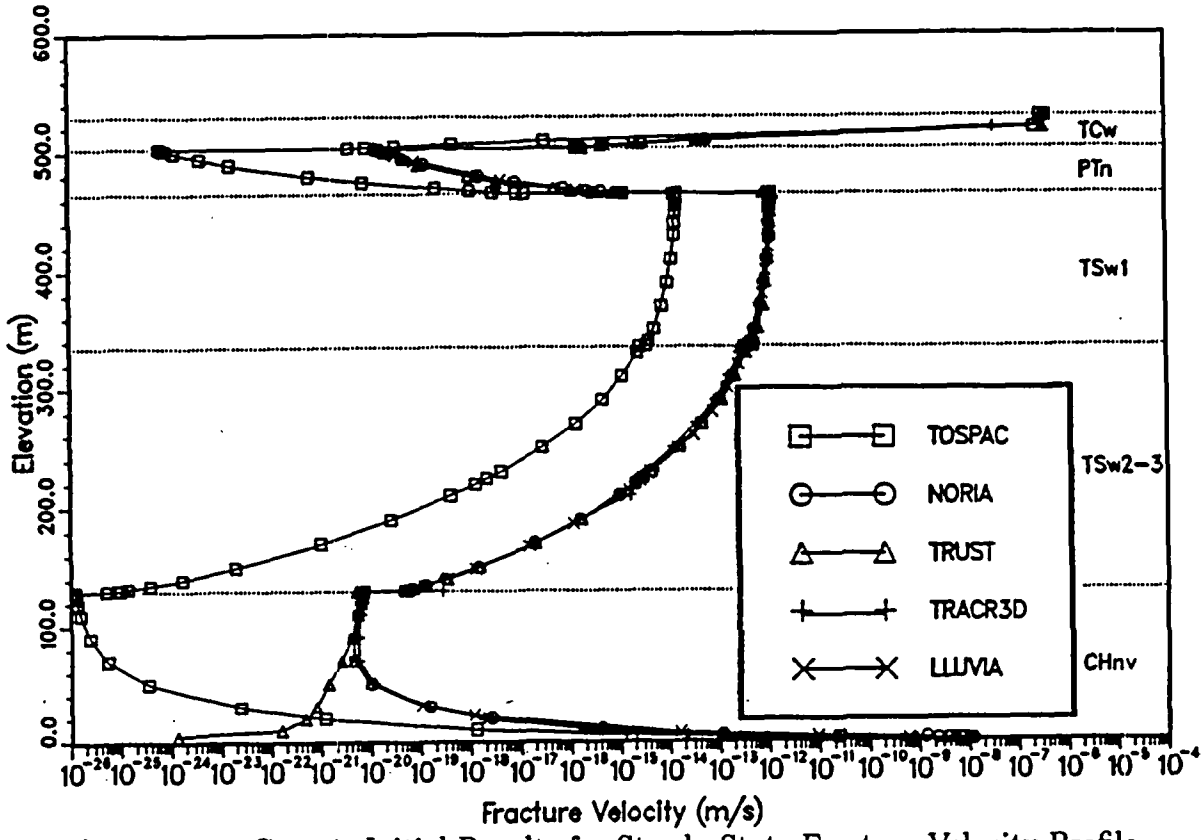


Figure 18. Case 4: Initial Results for Steady-State Fracture Velocity Profile

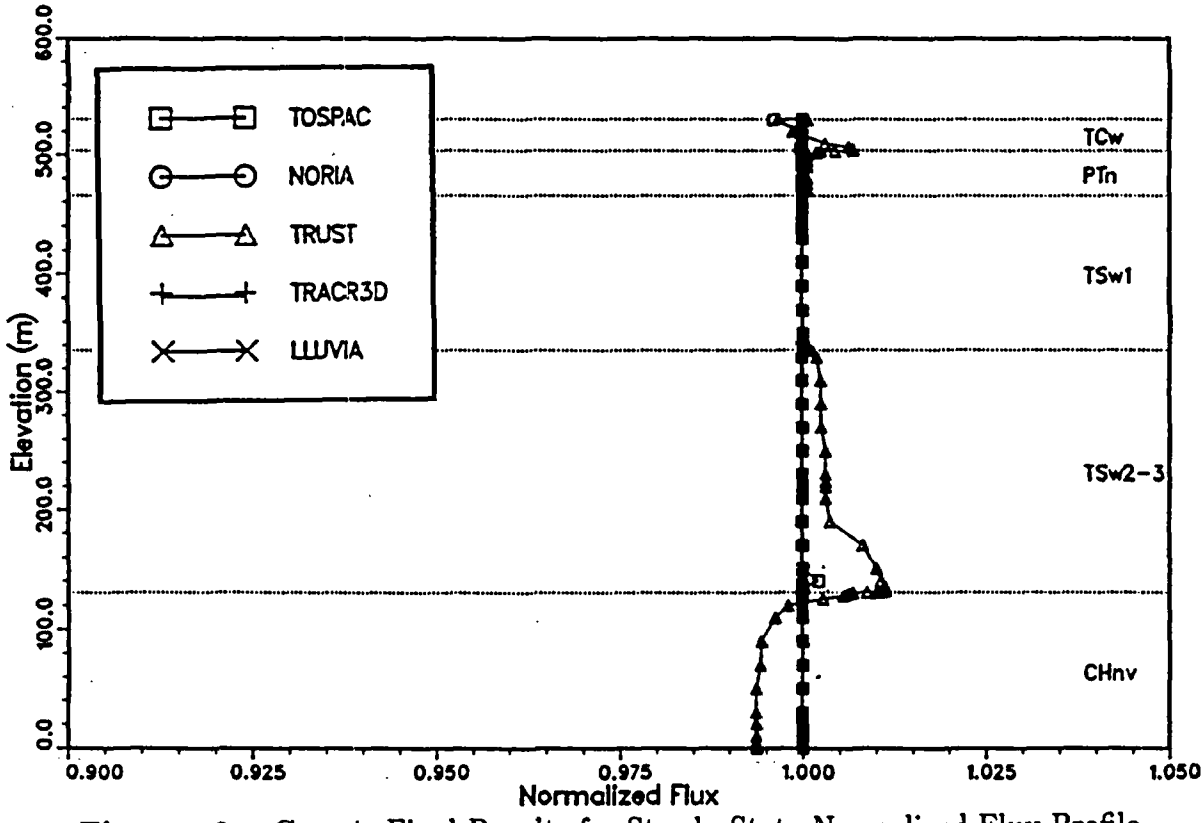


Figure 19. Case 4: Final Results for Steady-State Normalized Flux Profile

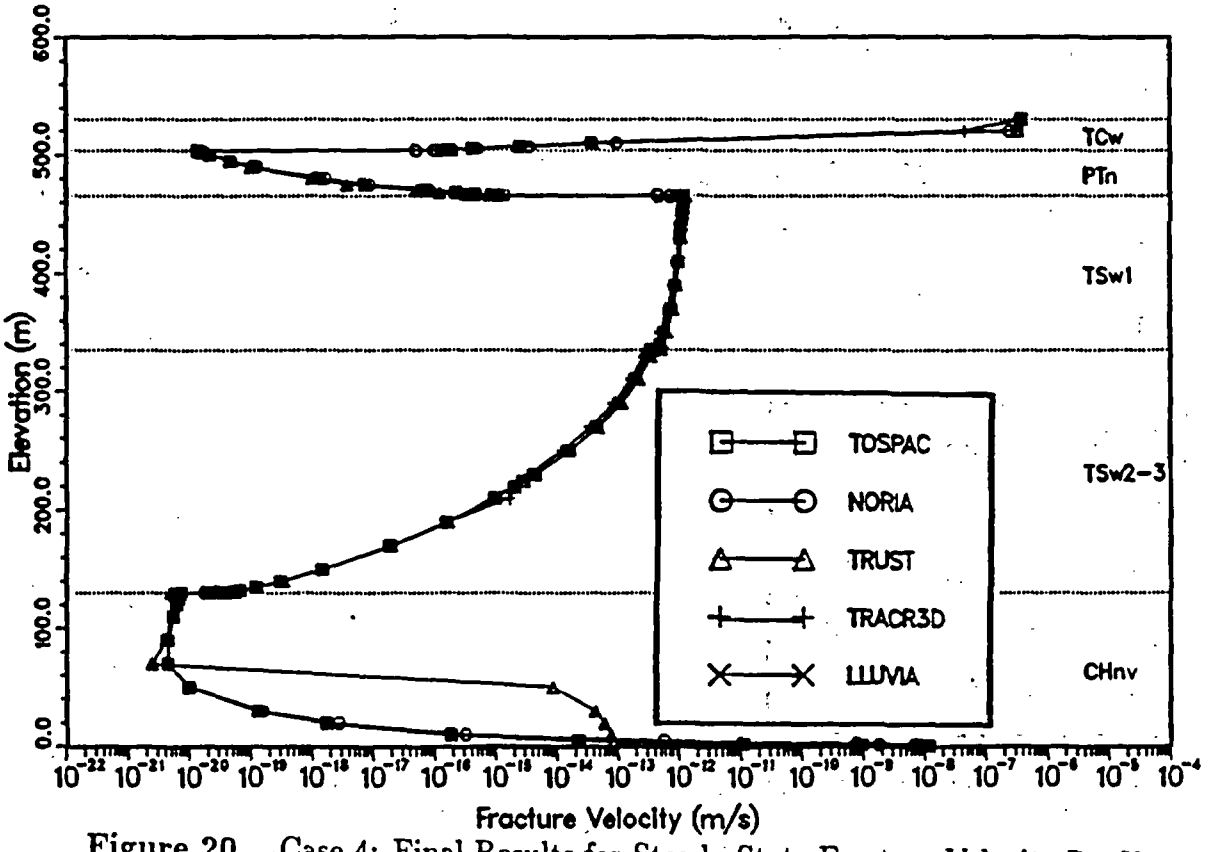


Figure 20. Case 4: Final Results for Steady-State Fracture Velocity Profile

### Case 5: Steady-state 4.0 mm/yr, zeolitic

In this case, significant fracture flow occurs in all layers. Again, the initial results for TRUST and TOSPAC diverged from those of the other participants due to coding errors. This is best shown in the fracture velocity plot (Figure 21). The final results showed better agreement, with TRUST still somewhat in disagreement (Figure 22). The improved agreement between TRUST and the other participants (in comparison to the previous cases) is due to the fact that the units are now nearly saturated. This results in low gradients in the pressure, so that a fine mesh is not as important.

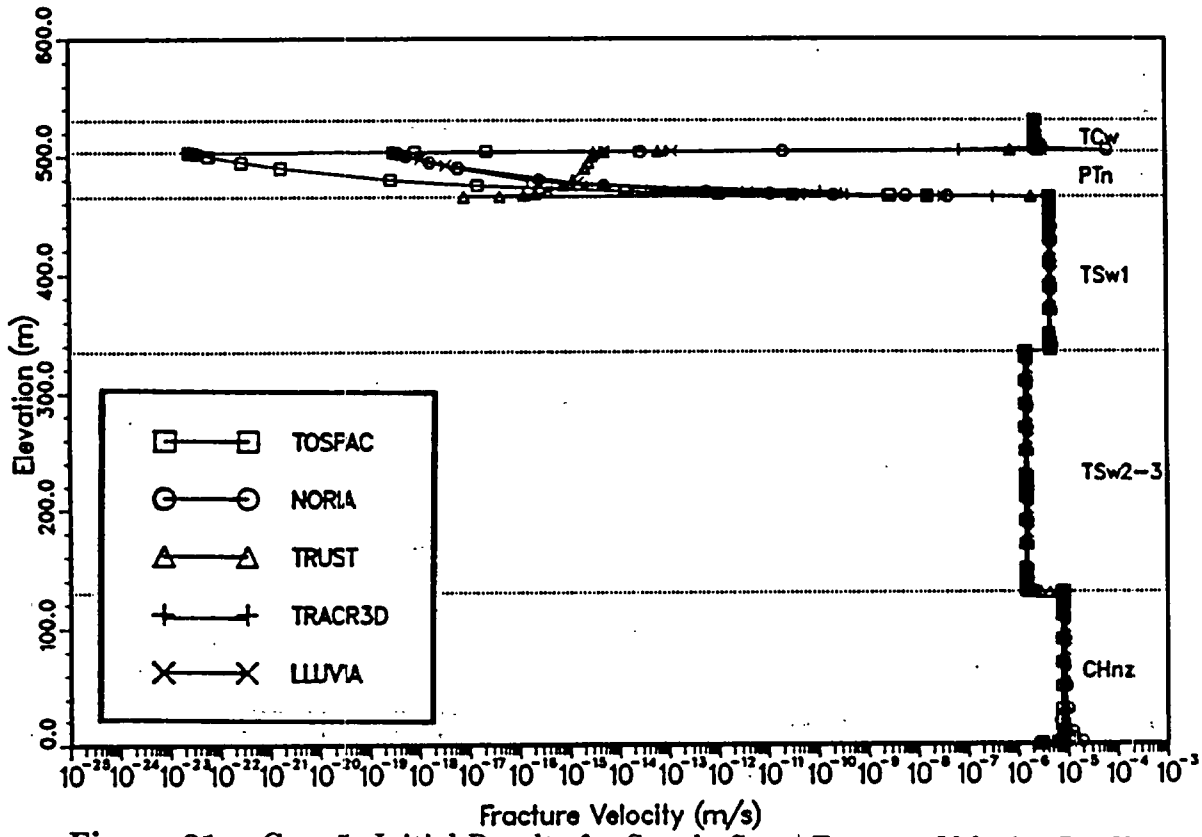


Figure 21. Case 5: Initial Results for Steady-State Fracture Velocity Profile

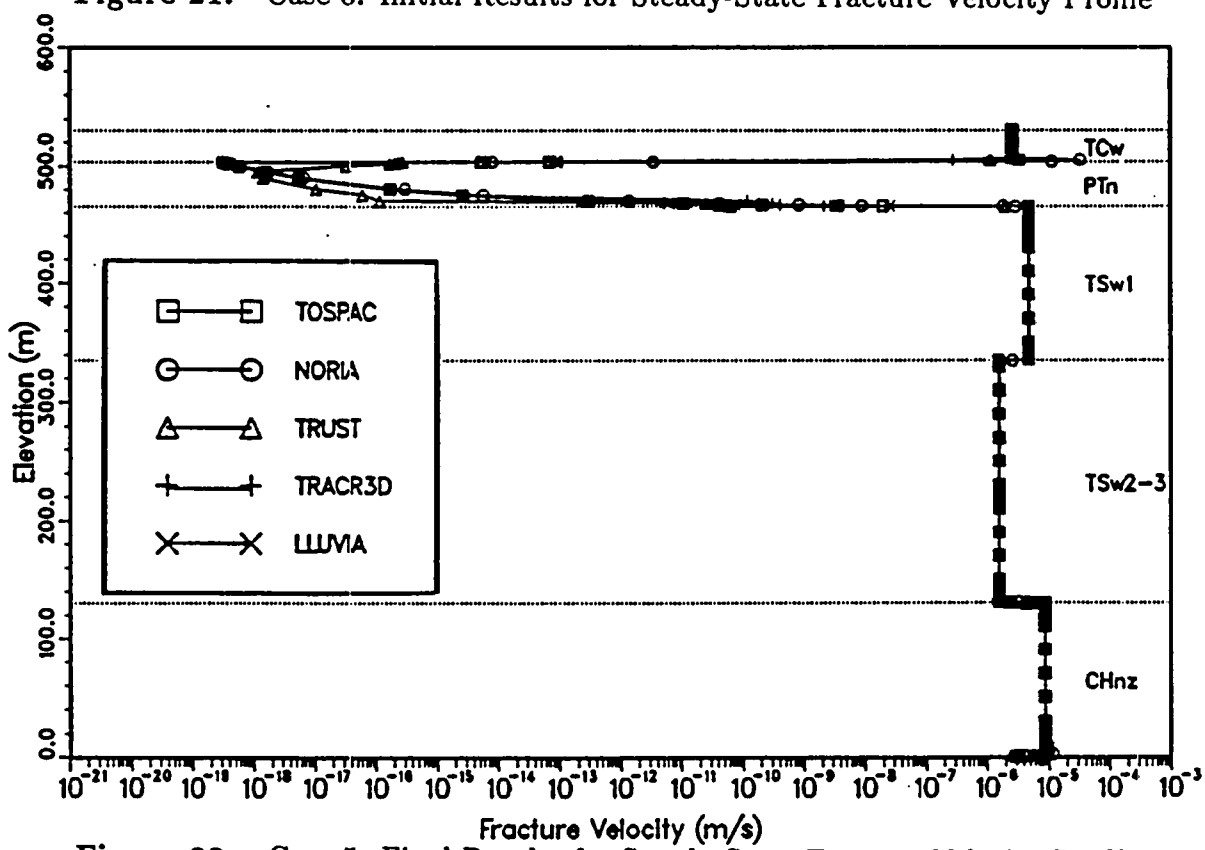


Figure 22. Case 5: Final Results for Steady-State Fracture Velocity Profile

### Case 6: Steady-state 4.0 mm/yr, vitric

Case 6 is the same as Case 5, except for the increased conductivity of the lowest layer. The comments made about Case 5 apply to this case. There are great divergences among the initial calculations, which are mostly improved for all participants by recalculation. The final results for TRUST are still somewhat different from the others. Figures 23 through 28 show the final results from all of the participants.

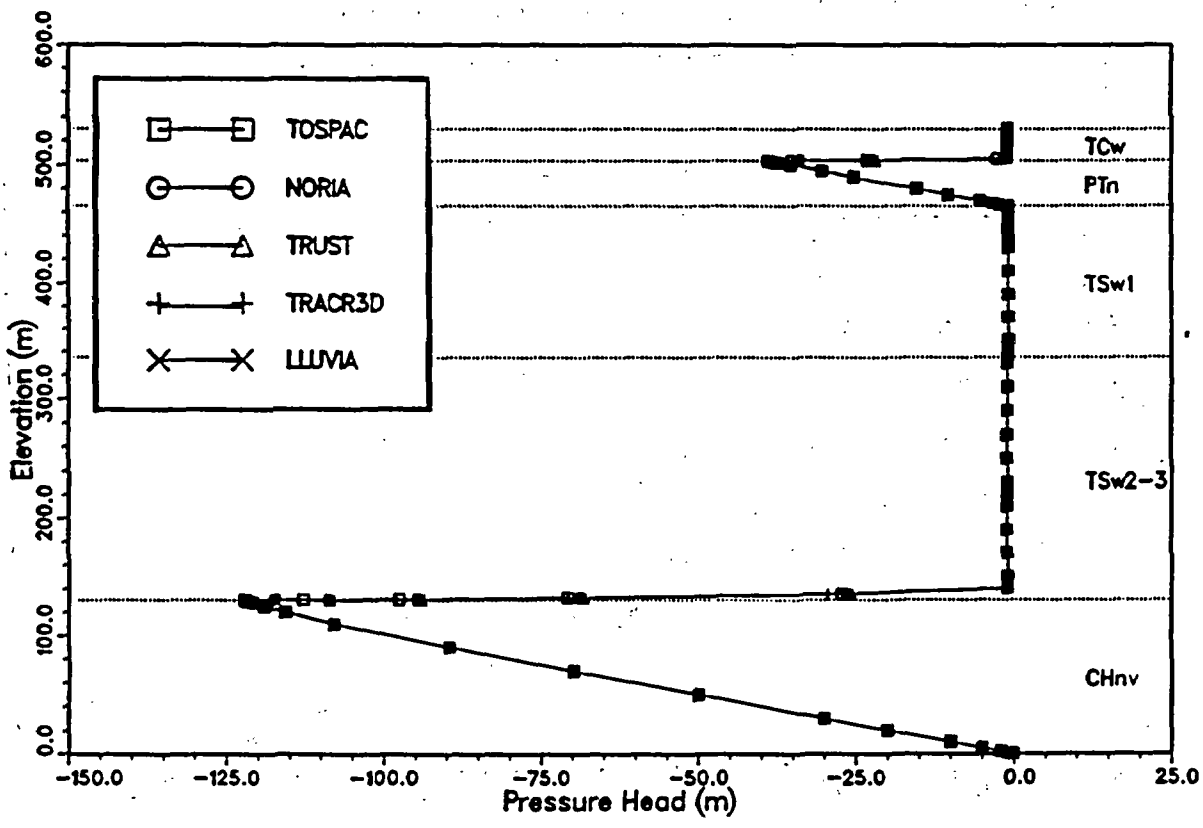


Figure 23. Case 6: Final Results for Steady-State Pressure Head Profile

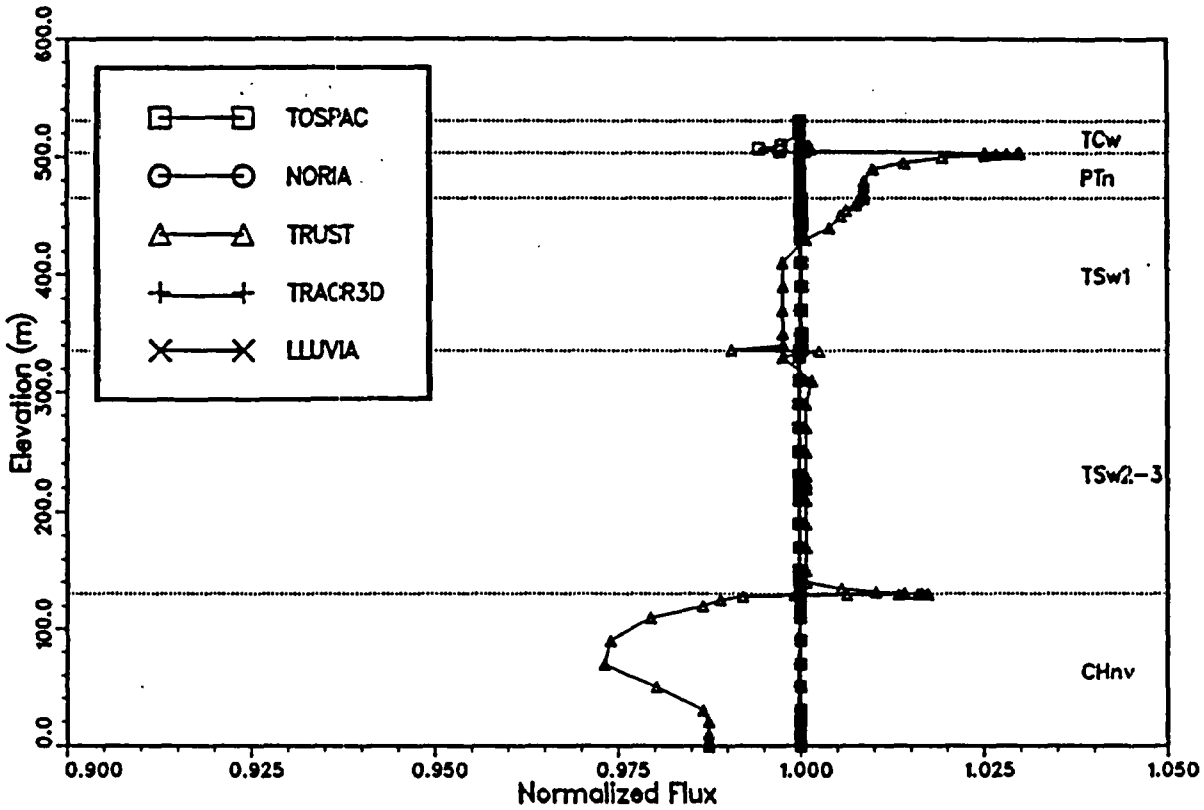


Figure 24. Case 6: Final Results for Steady-State Normalized Flux Profile

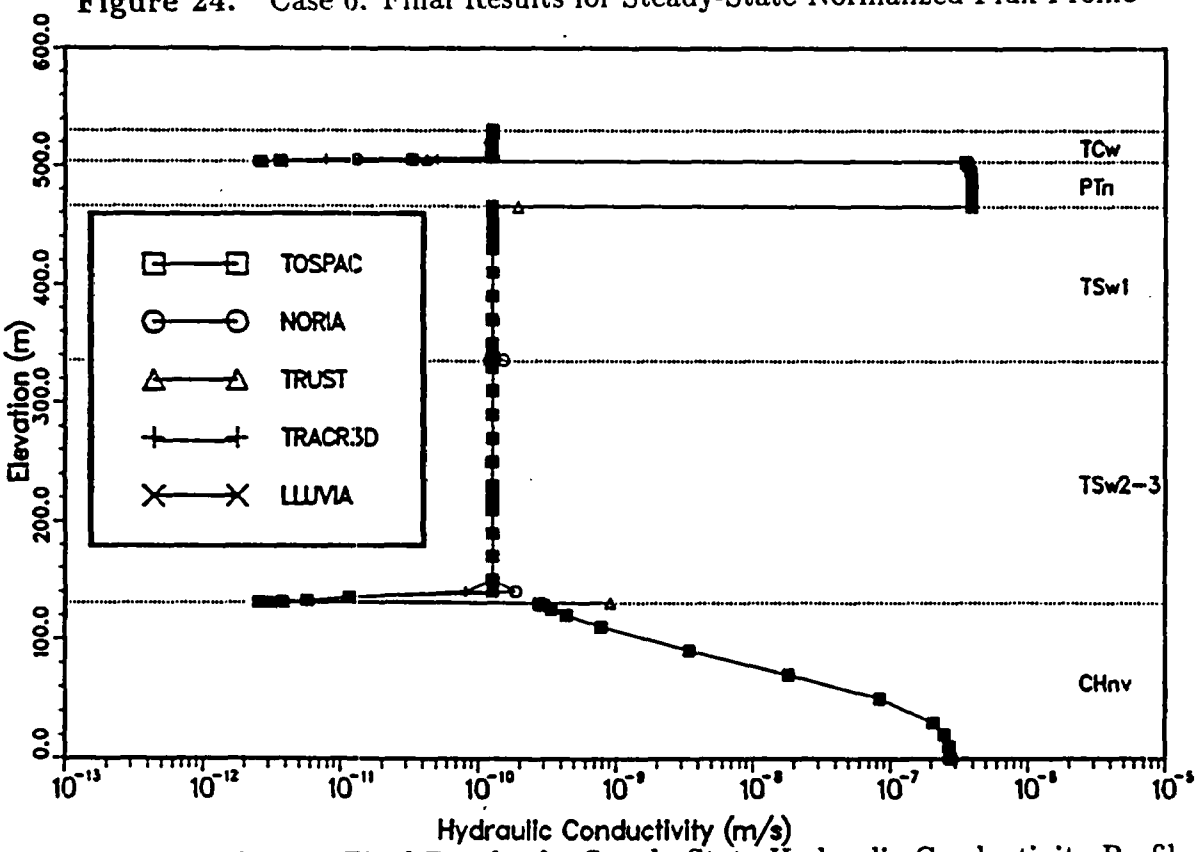


Figure 25. Case 6: Final Results for Steady-State Hydraulic Conductivity Profile

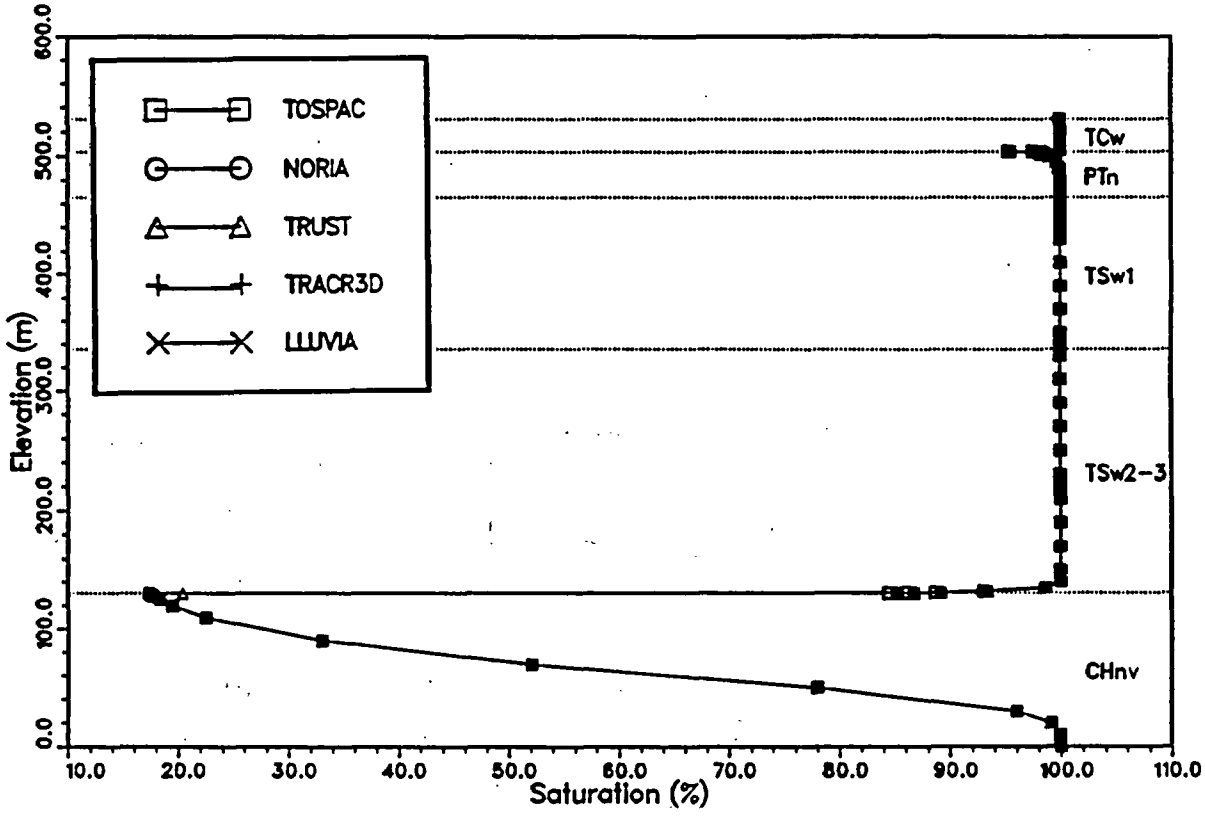


Figure 26. Case 6: Final Results for Steady-State Saturation Profile

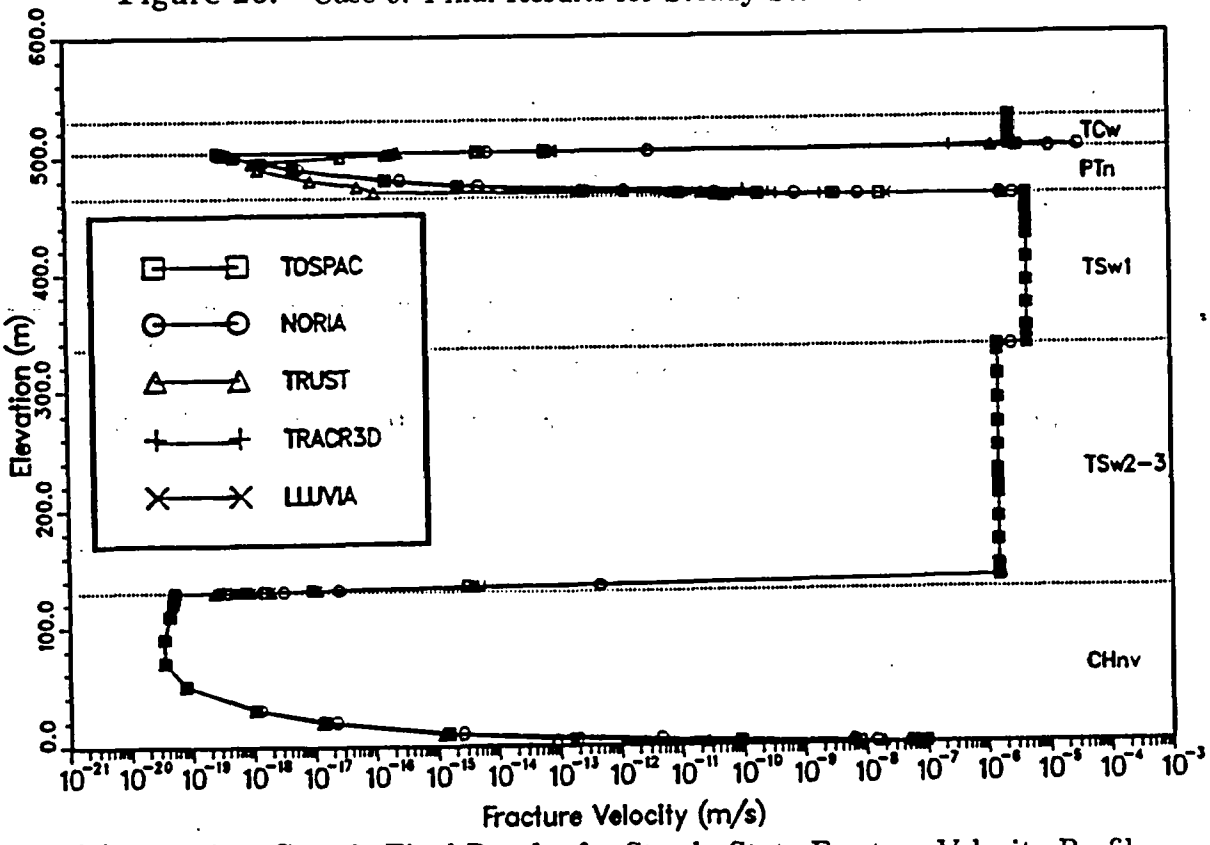


Figure 27. Case 6: Final Results for Steady-State Fracture Velocity Profile

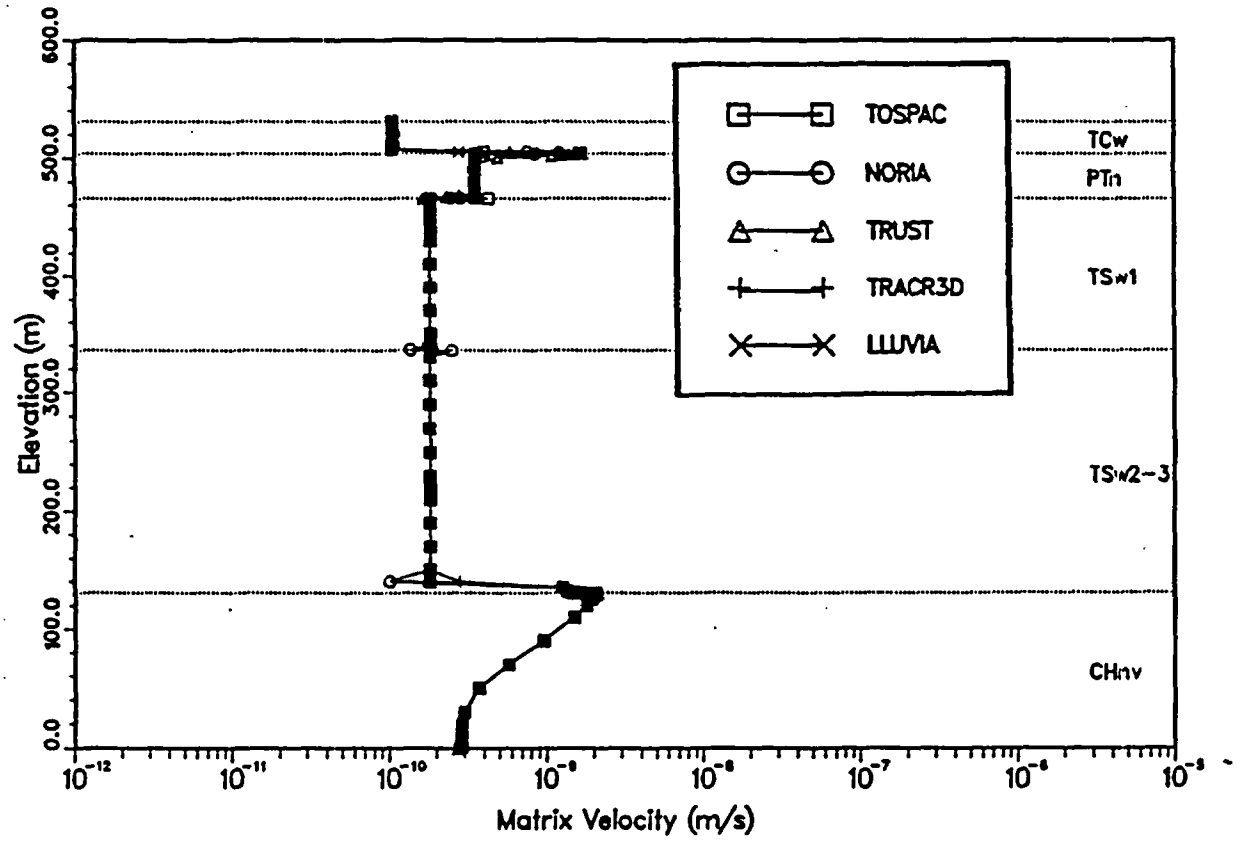


Figure 28. Case 6: Final Results for Steady-State Matrix Velocity Profile

## 3.2 Transient Cases

For the transient cases the participants were asked to provide the same six plots, discussed for the steady-state cases, at eight different times (The specified times varied from case to case.). In general, as time progresses, the differences among the results increases. Additionally, plots of the various calculated quantities as a function of time for various elevations were requested. The specified elevations were (with one exception) within a fraction of a meter of an interface. As was determined from the steady-state results, the interfaces are often the source of a very localized error that is not of global concern. The one exception is the time plots at the repository elevation (219.5 m). This is not at a stratigraphic interface and can be used as a fair test to show differences in the arrival times of the perturbed flux.

The same errors that were included in the initial results for the steady-state cases appeared in the initial results for these transient cases. Only two new errors were identified. The first was that some of the participants did not specify a small enough convergence criterion. This resulted in excess truncation errors. The second was that tabulated properties were not specified with enough precision for use by TRACER3D and therefore their results did not compare well with other participants. Birdsell and Travis (1991) provide an excellent discussion on the sensitivity of the transient non-linear finite-differenced equations to very small changes in the parameters and the convergence criterion. These errors were identified by early comparisons of results and were fixed for the final calculations. Therefore, the initial results for the transient cases will not be presented here.

Again the normalized flux plots proved to be a good vehicle for comparing codes. These plots as a function of elevation clearly show the progression of the flux perturbation.

Since LLUVIA is only a steady-state code, it could not produce the requested results for these transient cases.

### Case 7: Transient step change from 0.1 to 0.2 mm/yr, zeolitic

This transient involves very low fluxes that result in little fracture flow. All participants obtained very similar results for all of the requested output. Because all of the participants started from the same initial condition (Case 1), discrepancies among the codes increase with time. Figures 29 through 34 show a comparison of the results at 100,000 years, which is approaching the new steady-state. Except for very localized errors at interfaces (which are of no consequence), the agreement is very good. NORIA seems to be approaching the new steady-state at a slightly slower pace (Figure 30).

Figures 35 through 40 show the time plots for the output variables at the 219.5 meter elevation. Again it is shown that NORIA approaches the new steady-state at the slowest rate, but the difference in all of the results are on the order of a few percent (Figure 39).

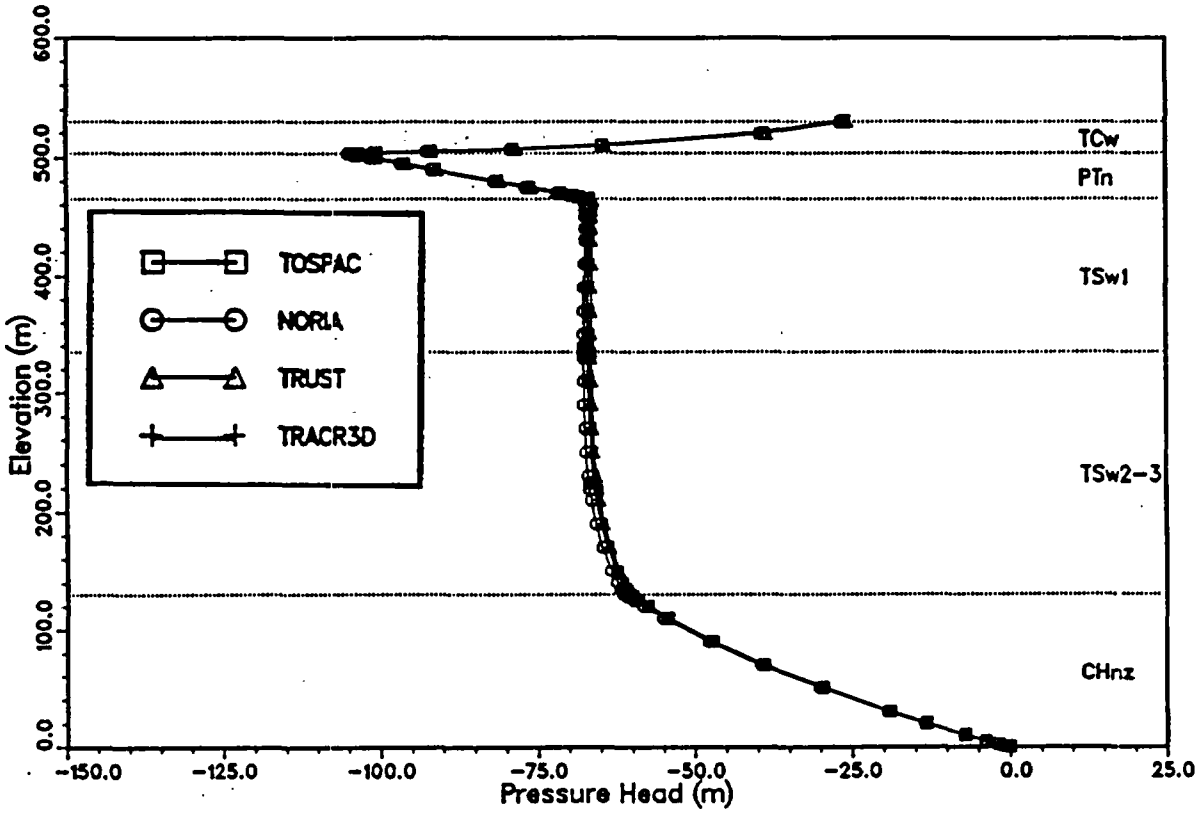


Figure 29. Case 7: Final Results for Pressure Head Profile at 100,000 Years

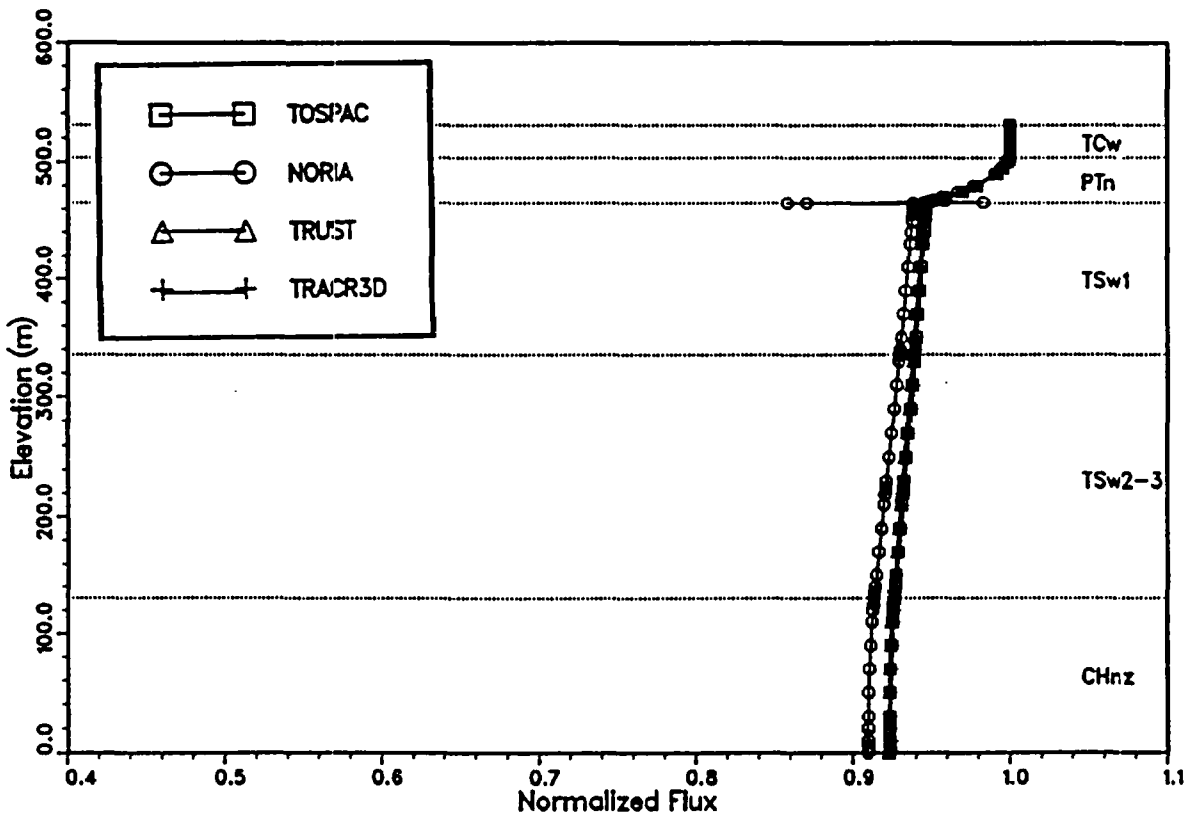


Figure 30. Case 7: Final Results for Normalized Flux Profile at 100,000 Years

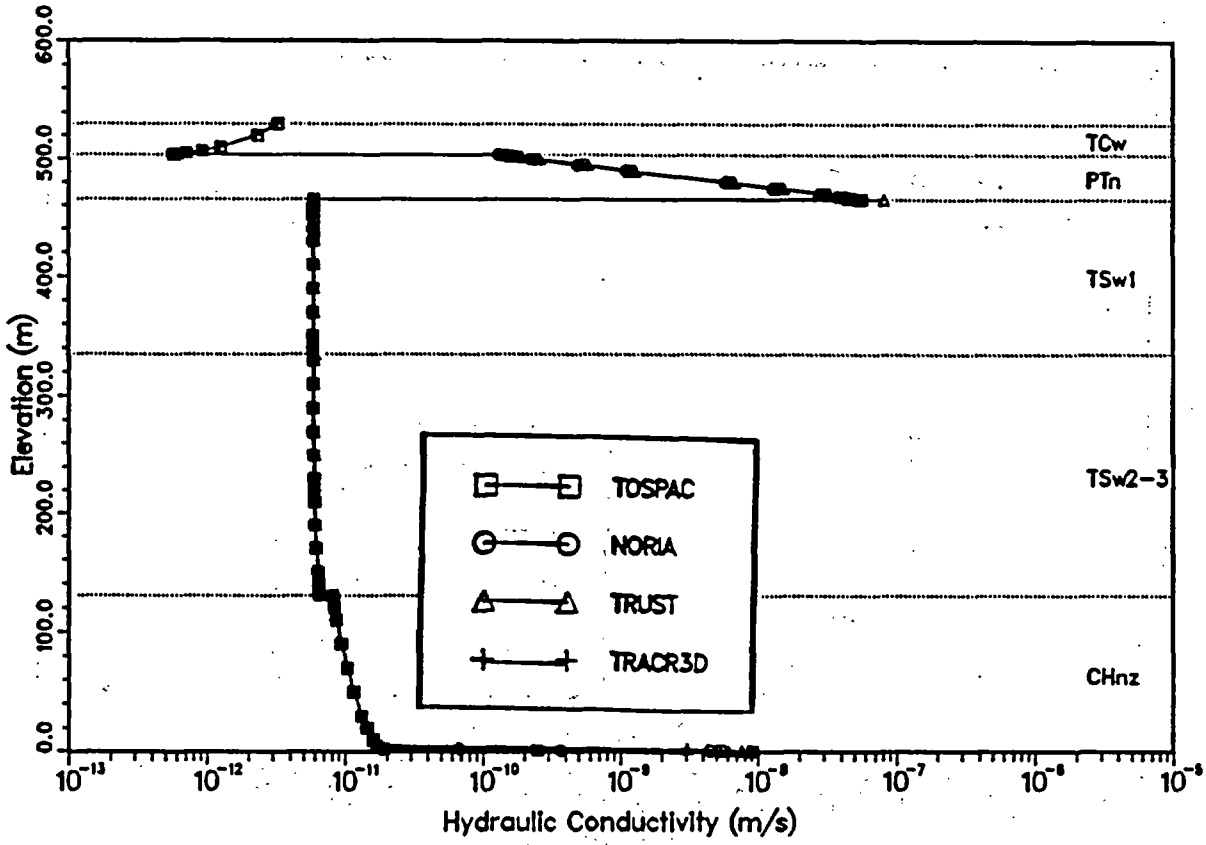


Figure 31. Case 7: Final Results for Hydraulic Conductivity Profile at 100,000 Years

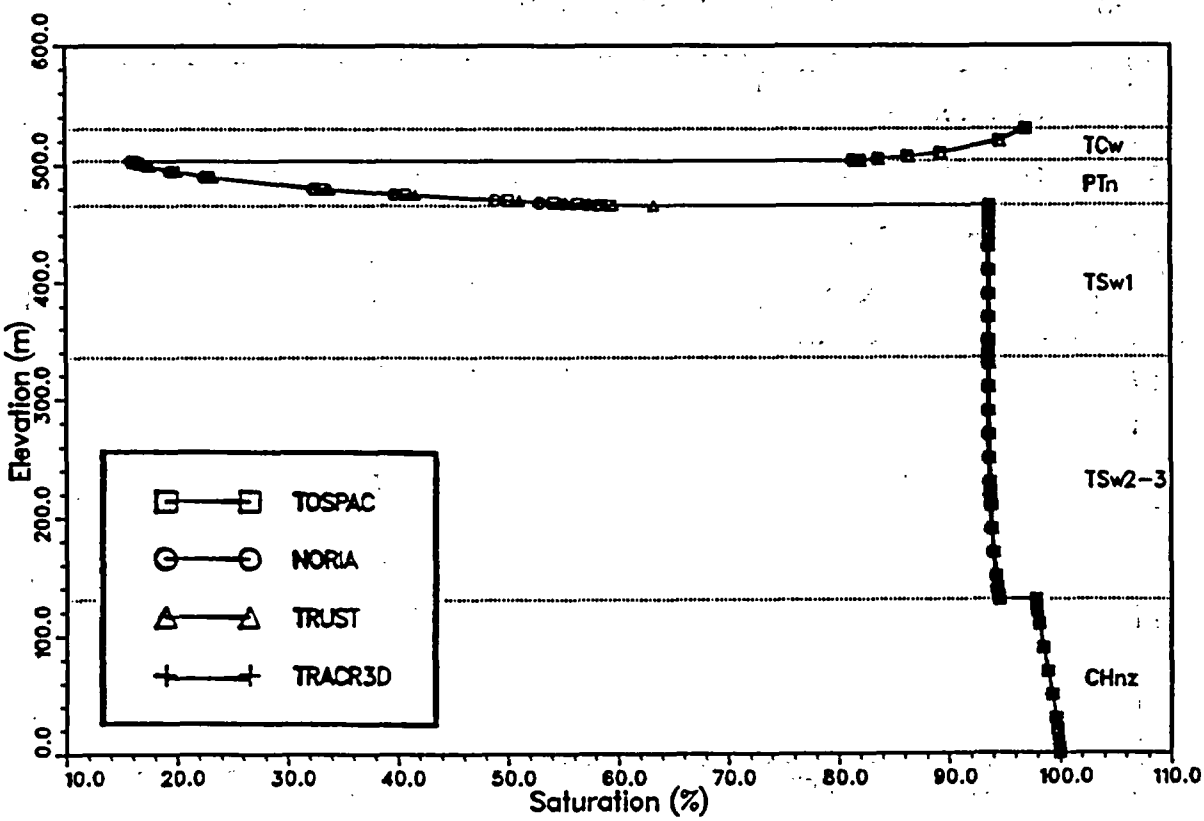


Figure 32. Case 7: Final Results for Saturation Profile at 100,000 Years

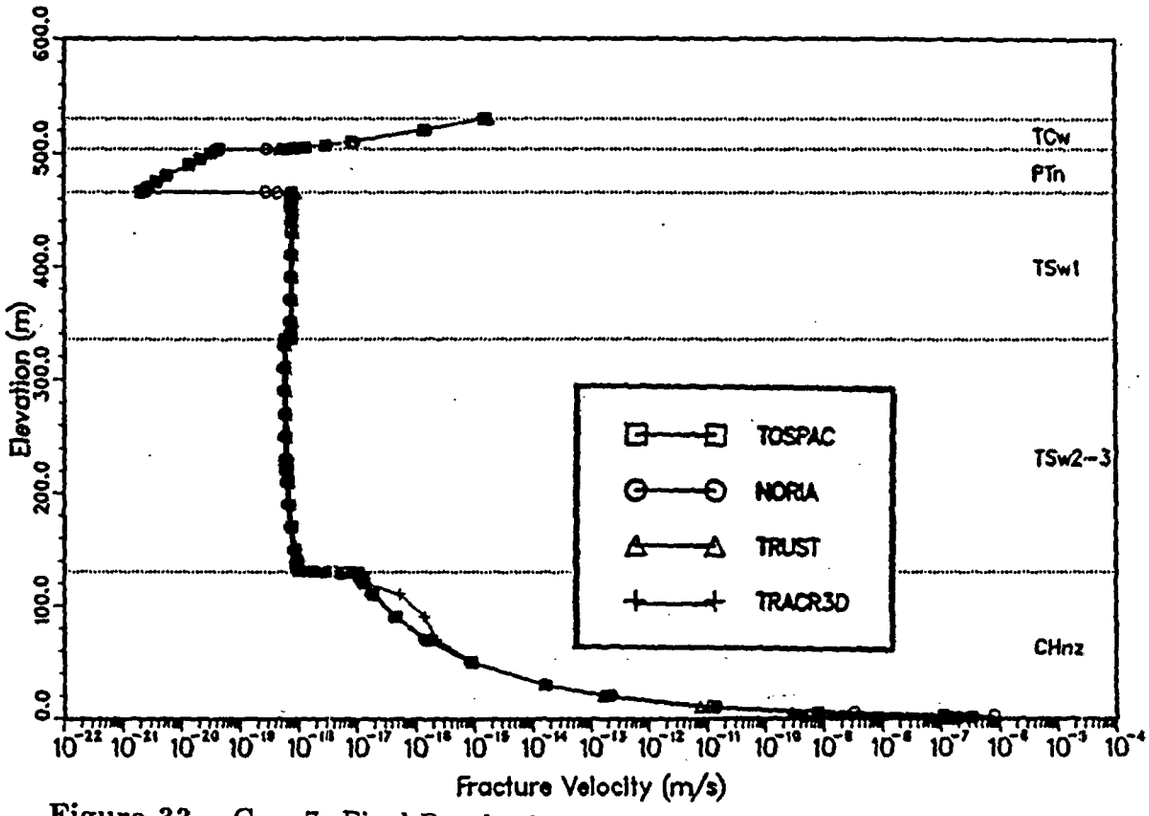


Figure 33. Case 7: Final Results for Fracture Velocity Profile at 100,000 Years

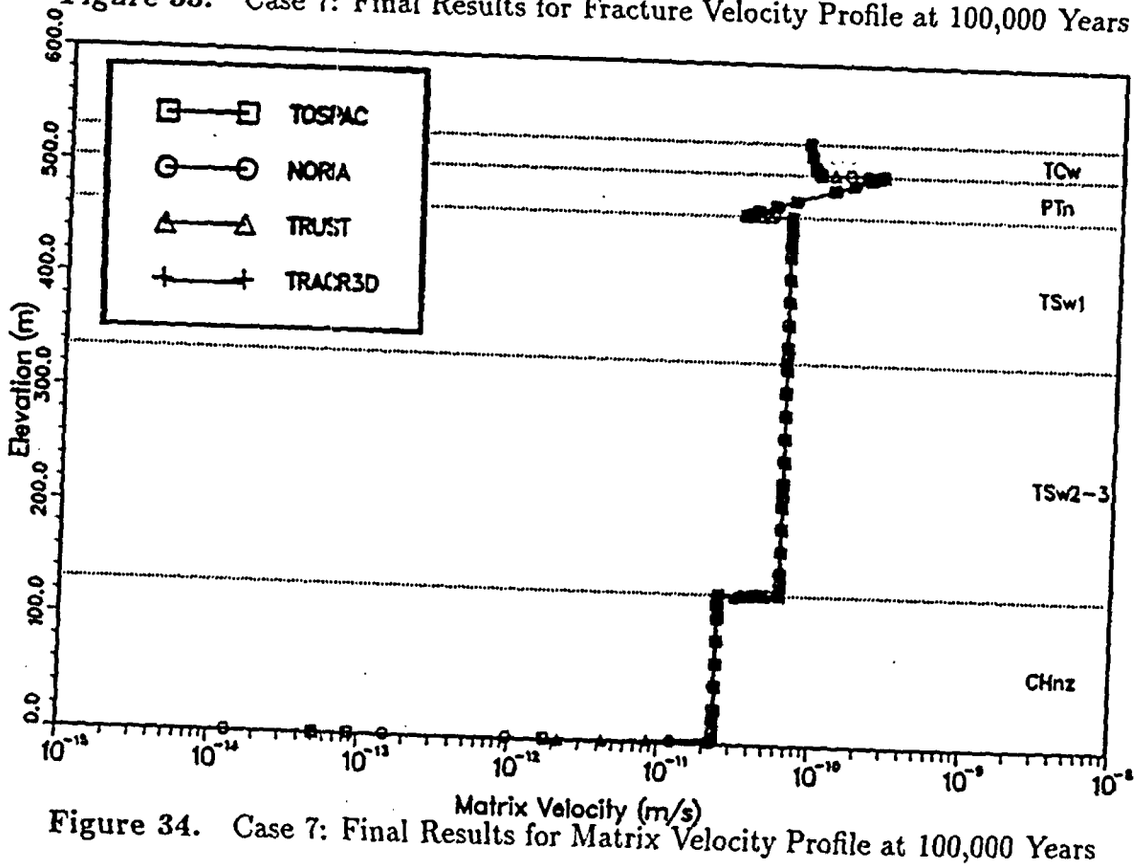


Figure 34. Case 7: Final Results for Matrix Velocity Profile at 100,000 Years

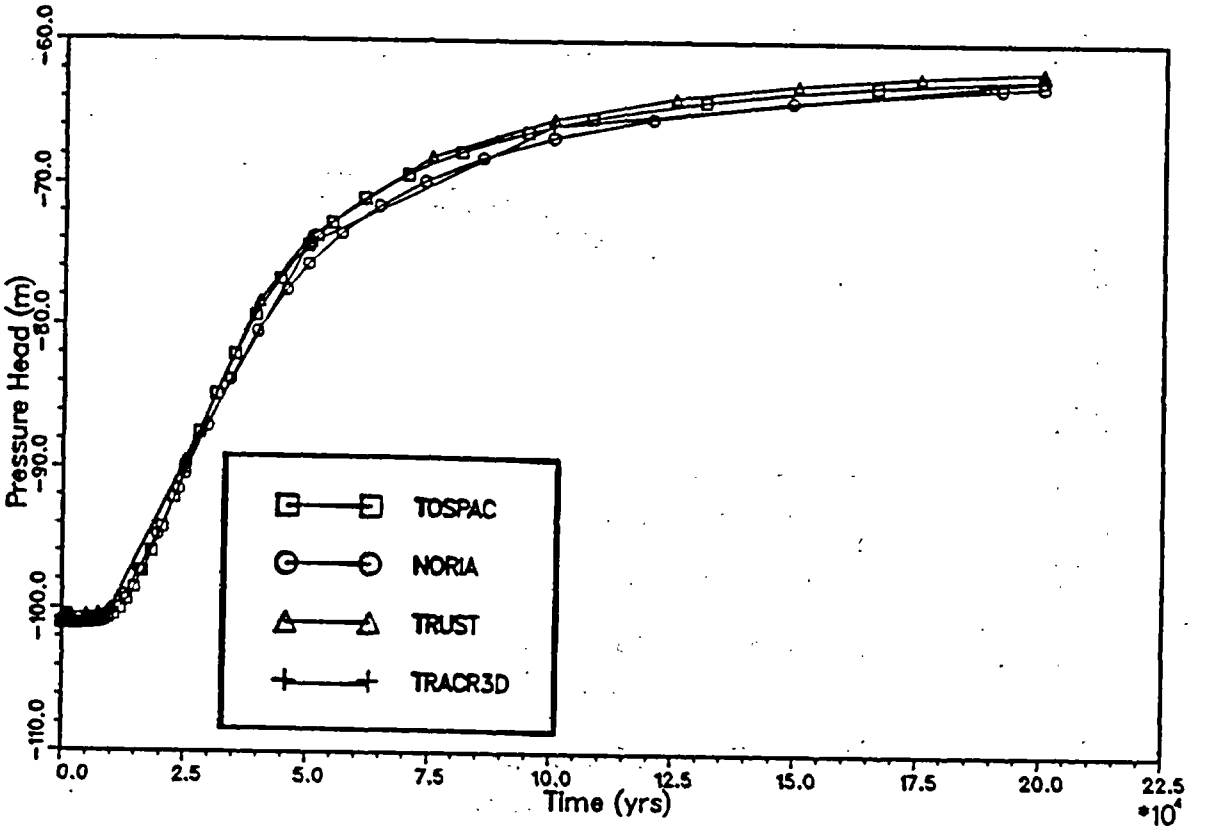


Figure 35. Case 7: Final Results for Pressure Head at 219.5 Meters

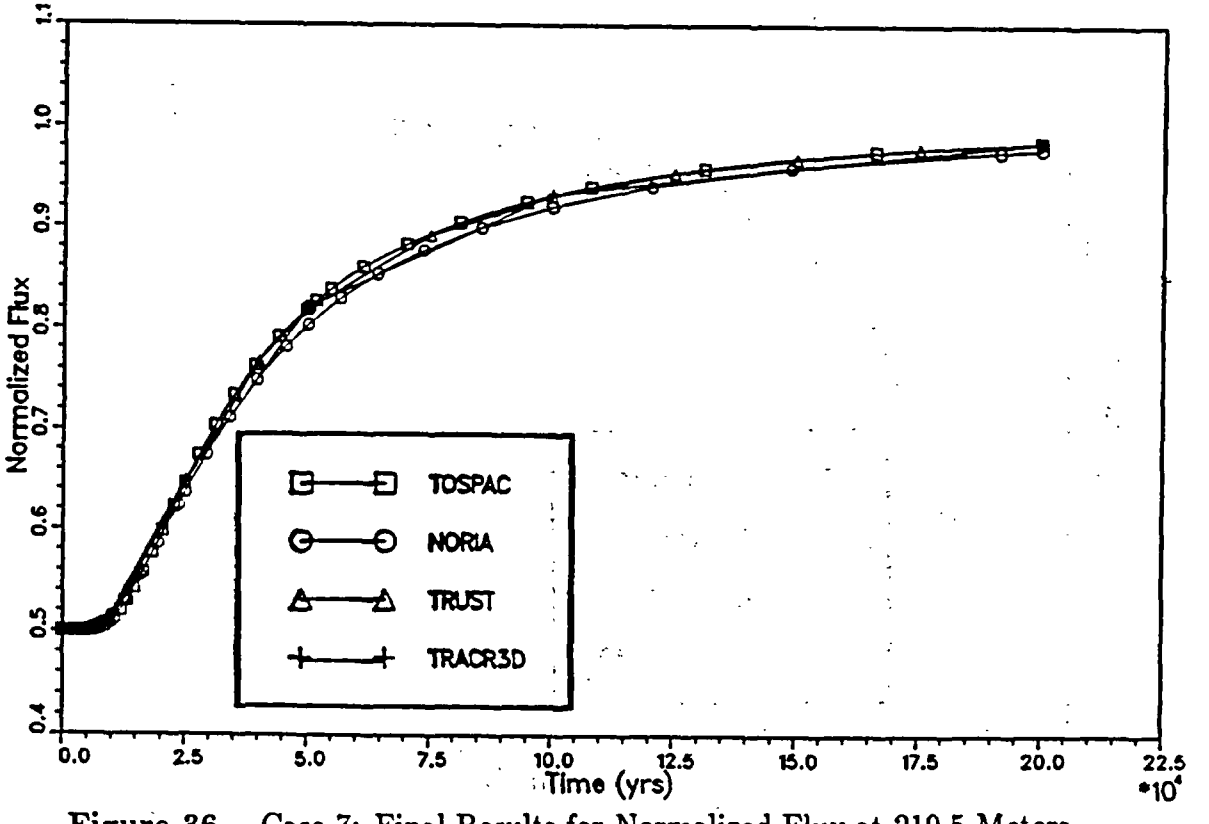


Figure 36. Case 7: Final Results for Normalized Flux at 219.5 Meters

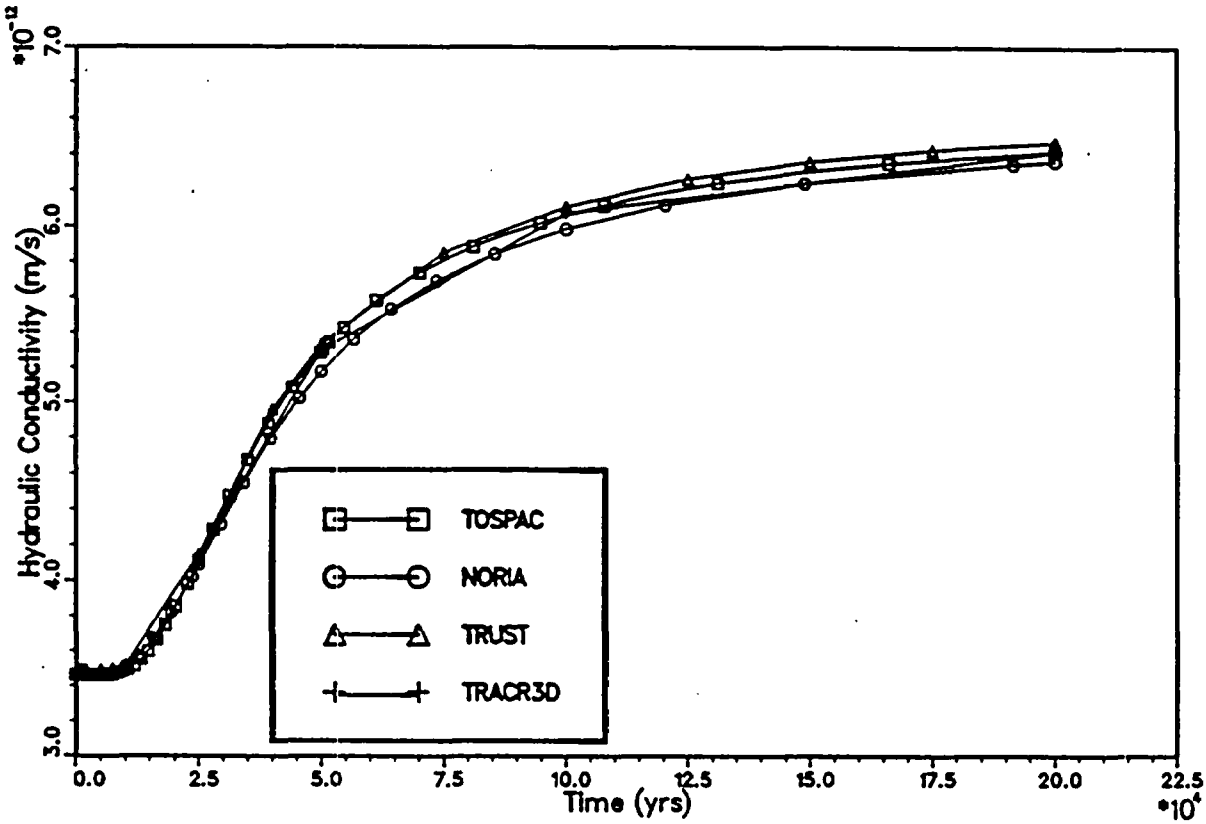


Figure 37. Case 7: Final Results for Hydraulic Conductivity at 219.5 Meters

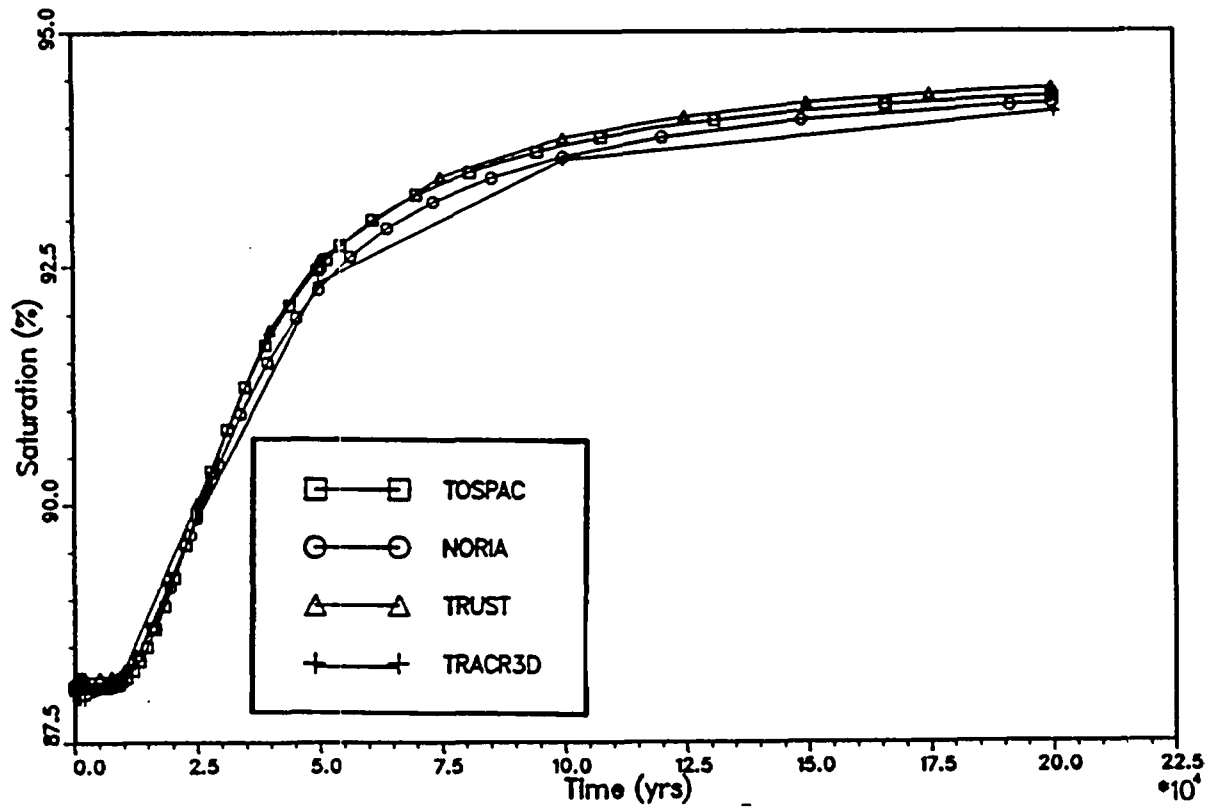


Figure 38. Case 7: Final Results for Saturation at 219.5 Meters

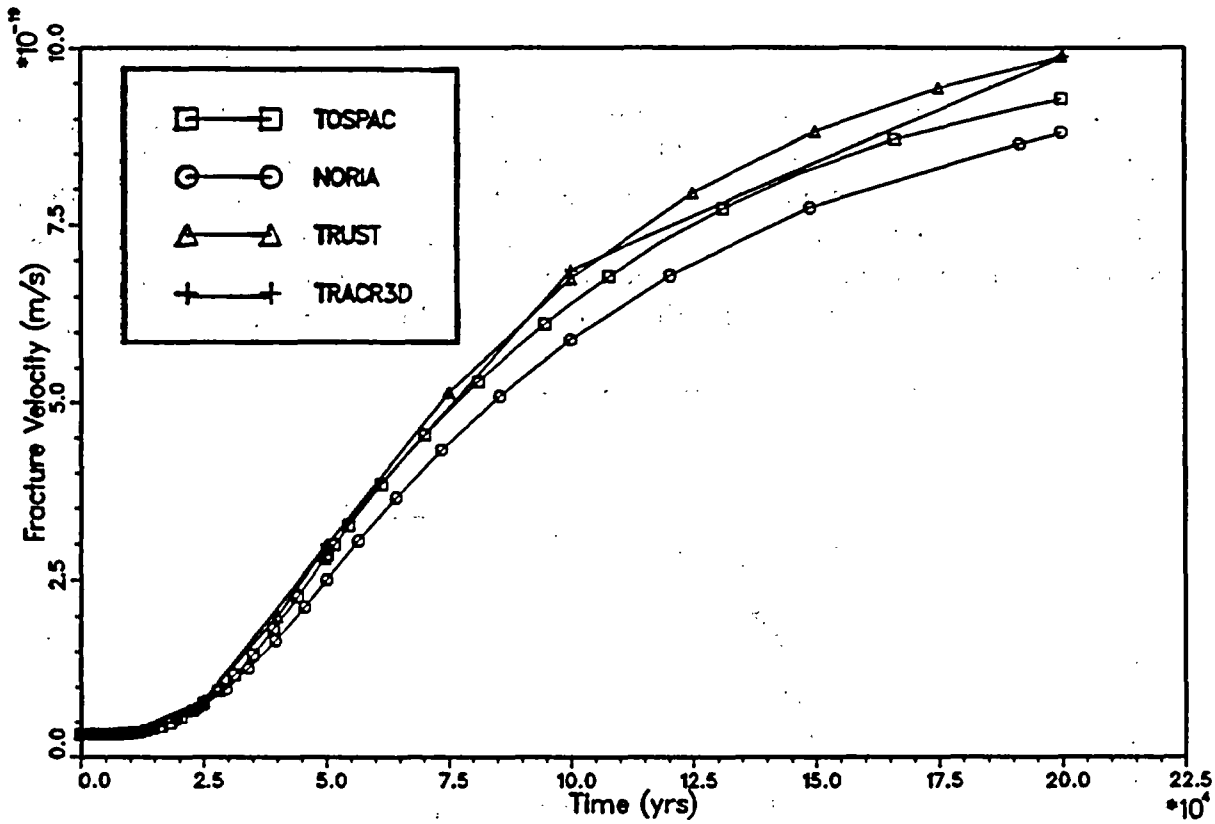


Figure 39. Case 7: Final Results for Fracture Velocity at 219.5 Meters

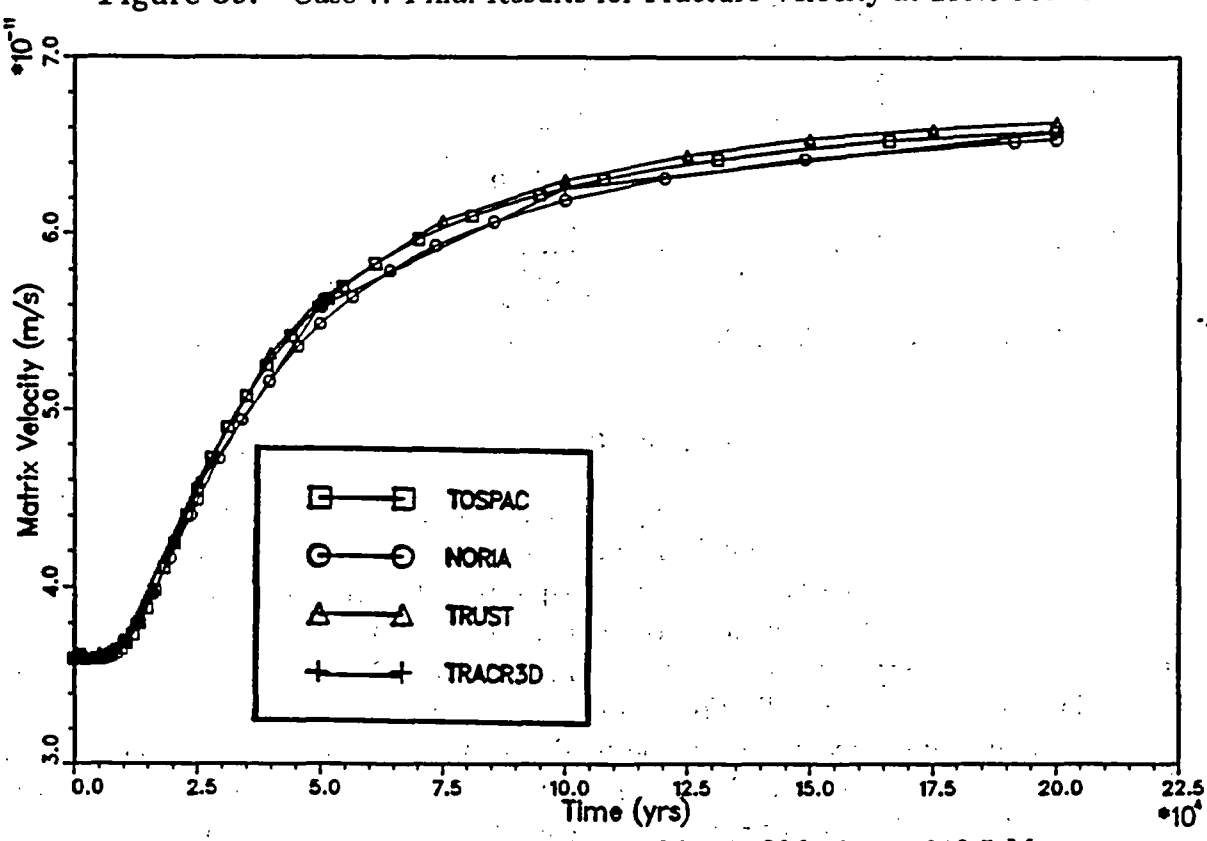


Figure 40. Case 7: Final Results for Matrix Velocity at 219.5 Meters

### Case 8: Transient step change from 0.1 to 0.2 mm/yr, vitric

This transient is very similar to the transient of Case 1, and therefore the results from the different participants could be compared in a similar manner. At 100,000 years, all codes predicted conditions close to a steady-state at the new flux level. Results from NORIA again lagged behind the other three codes, but the fluxes it predicted were only one percent lower (Figure 41). All codes show the increased time required to reach the new steady-state when the Calico Hills layer is defined by the vitric property set.

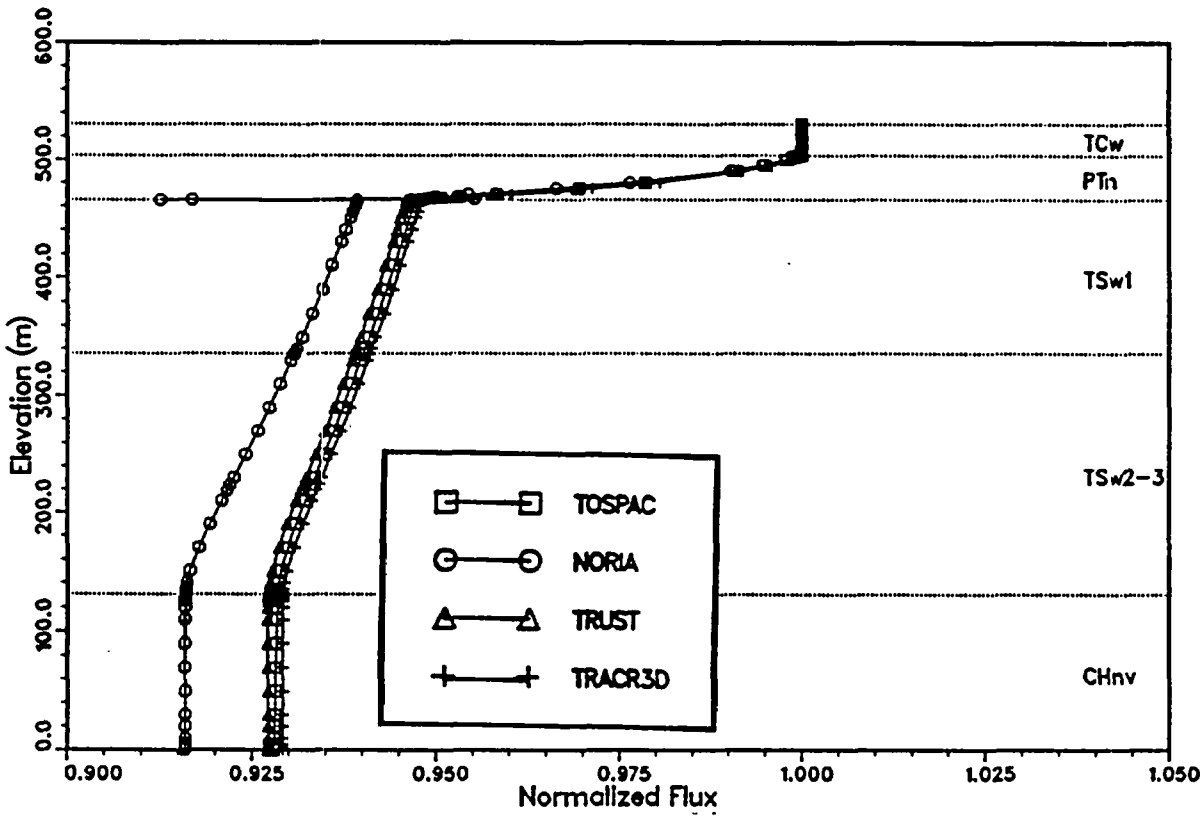


Figure 41. Case 8: Final Results for Normalized Flux Profile at 100,000 Years

### Case 9: Transient step change from 0.5 to 1.0 mm/yr, zeolotic

This transient is similar to Cases 7 and 8, but now fracture flow becomes more dominant. Again the participants' calculations agree very well. The transient reaches a new steady-state at the last time plane requested (450 years). The normalized flux exhibits a value of unity throughout the domain (Figure 42). However, Figure 42 does show a small offset error in the TRUST normalized flux (0.8 percent), and a local error in the TCw layer. The overall offset seems to begin at the elevation of the local error and is probably caused by the coarse mesh. Figure 43 shows the excellent agreement for the fracture velocity (the variable that exhibits the greatest variation among codes) at 300 years. The TRUST calculation shows a slightly greater penetration of the front into the domain. Figures 44 through 49 show the time history of the output variables at the

219.5-meter elevation. The agreement is very good. The apparent disparity among the codes is due to the fine scale of the y-axis, and the sparse data. TRUST and TRACR3D did not output data at a fine enough time scale to resolve the passage of the front.

Especially for this case, which involved a transition from matrix to fracture flow, the TRACR3D results were found to be very sensitive to the degree of precision in the permeability values that were tabulated for the code's use. This was determined and corrected before presentation of the final results.

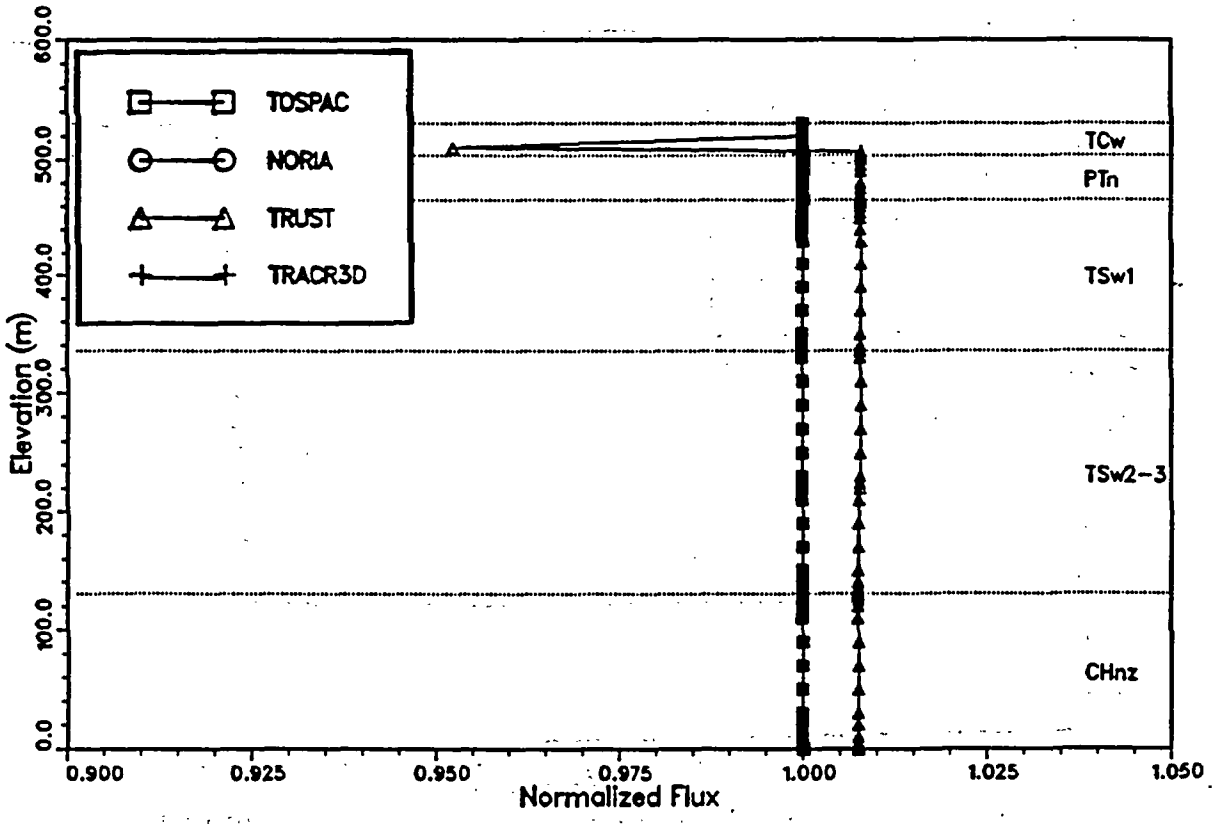


Figure 42. Case 9: Final Results for Normalized Flux Profile at 450 Years

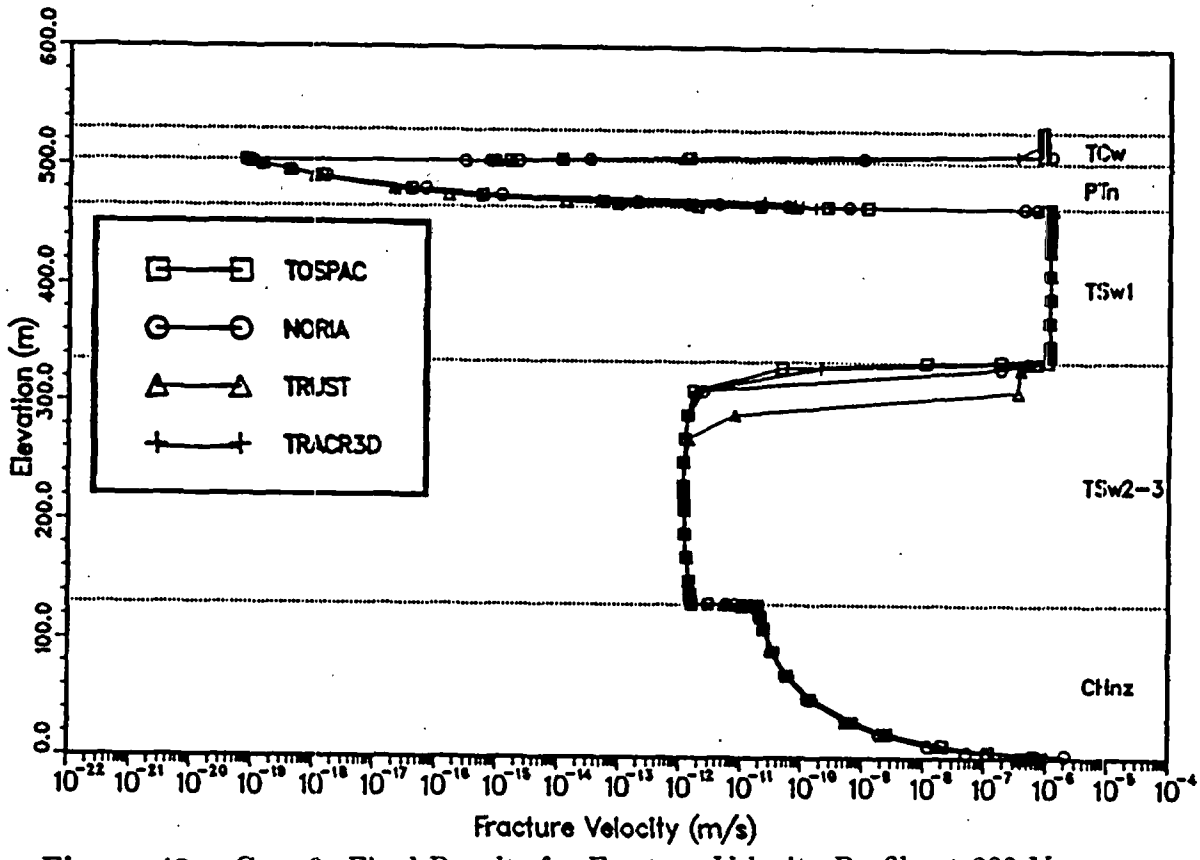


Figure 43. Case 9: Final Results for Fracture Velocity Profile at 300 Years

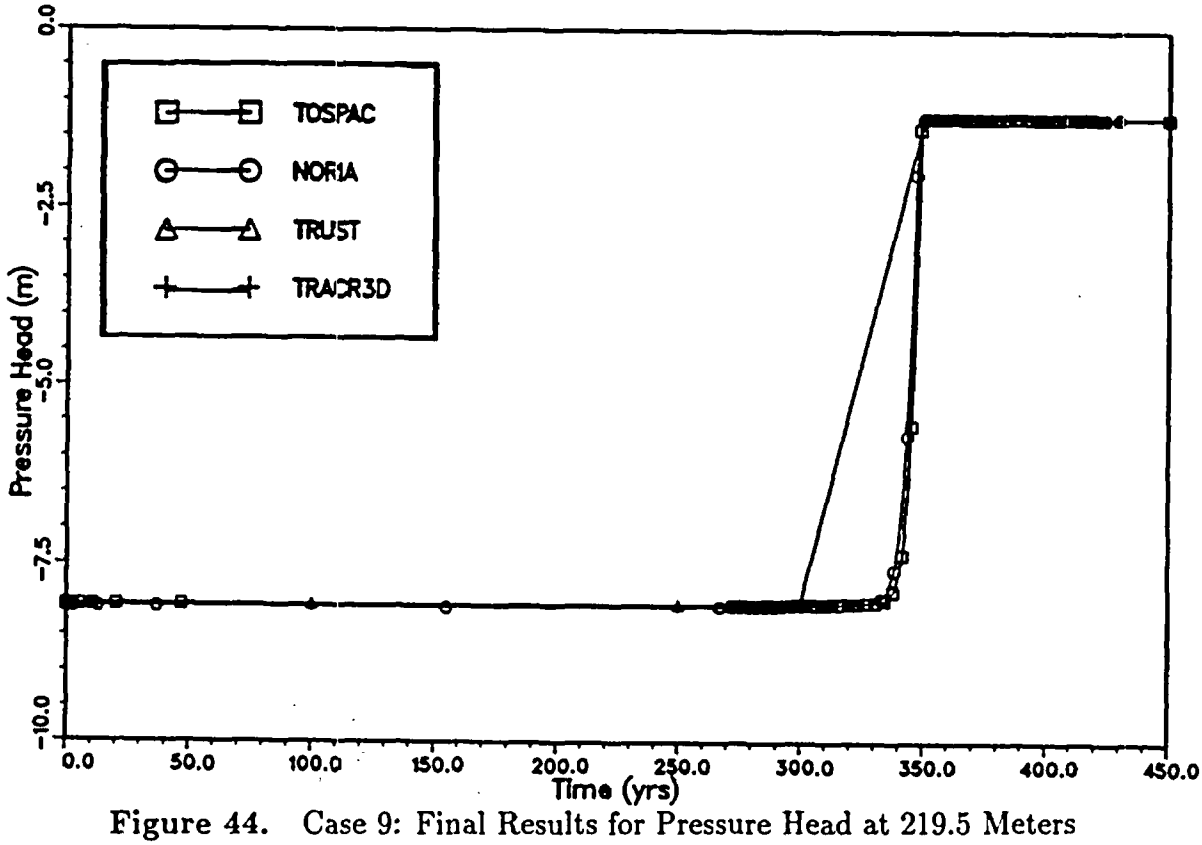


Figure 44. Case 9: Final Results for Pressure Head at 219.5 Meters

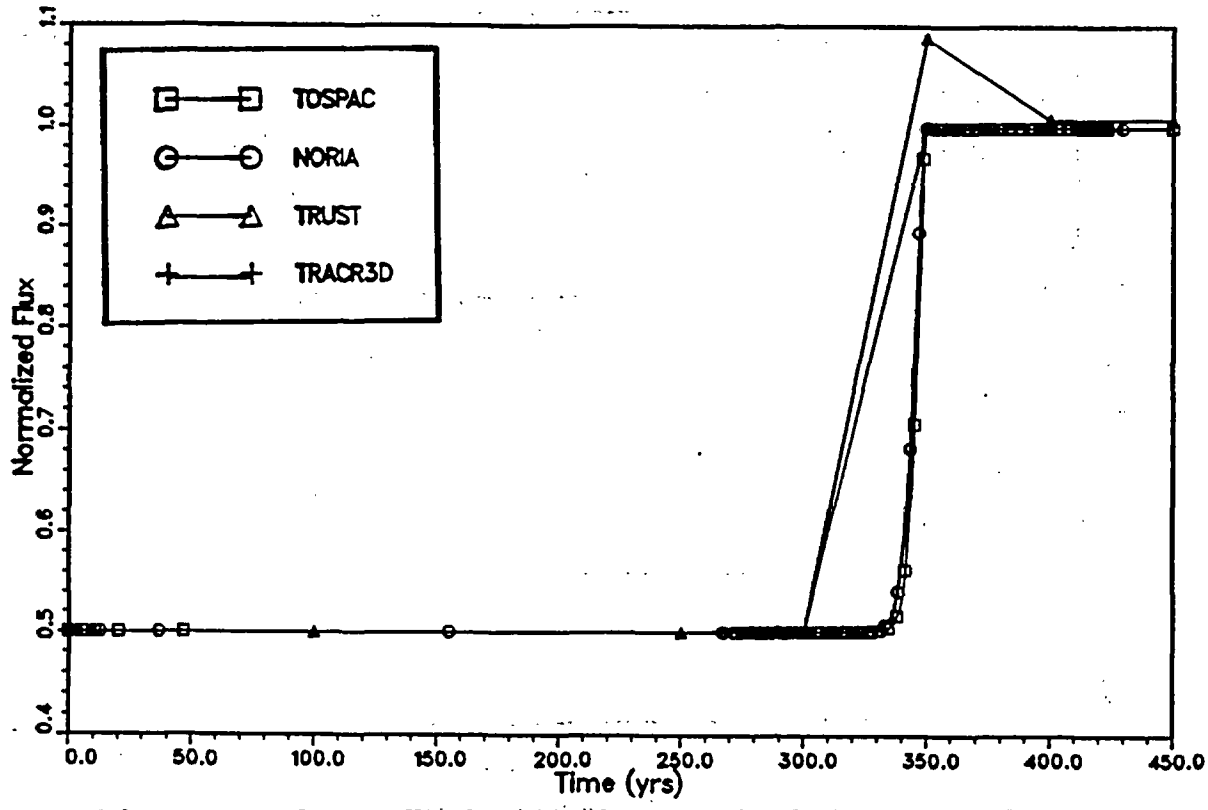


Figure 45. Case 9: Final Results for Normalized Flux at 219.5 Meters

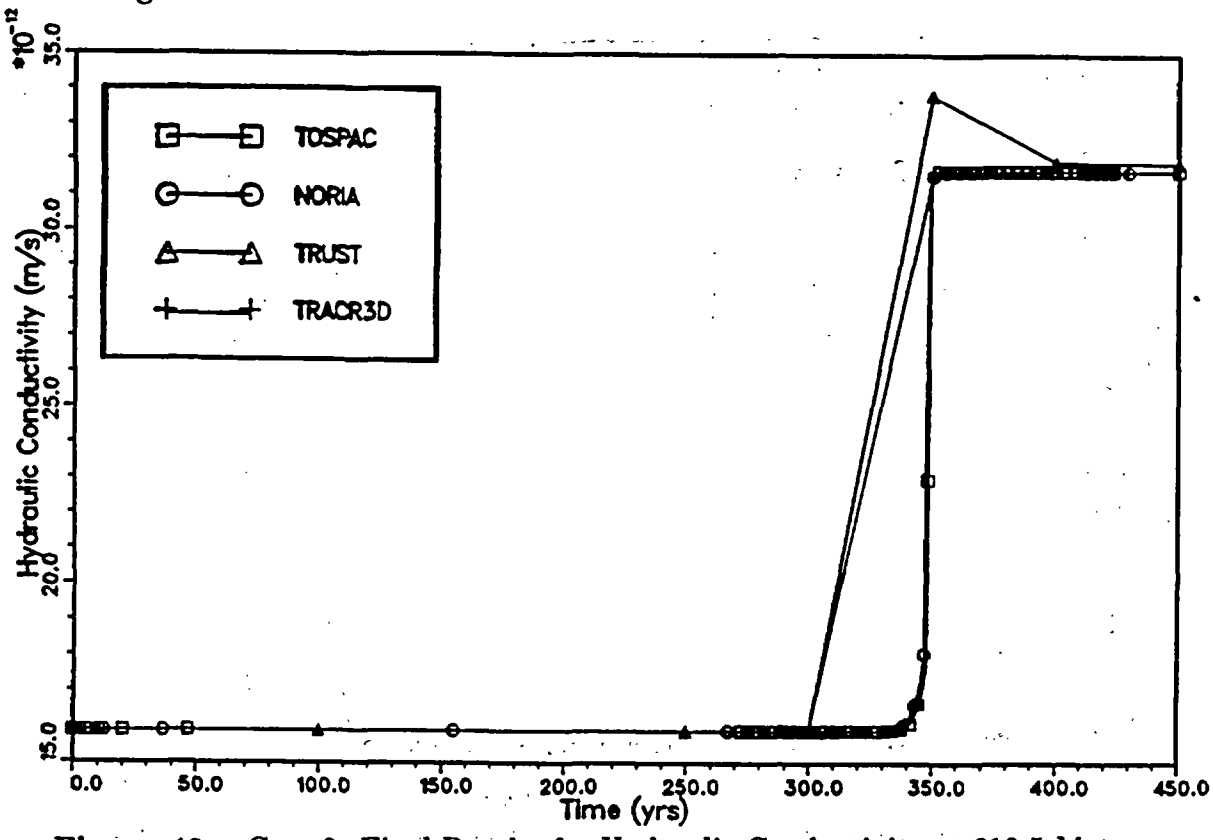


Figure 46. Case 9: Final Results for Hydraulic Conductivity at 219.5 Meters

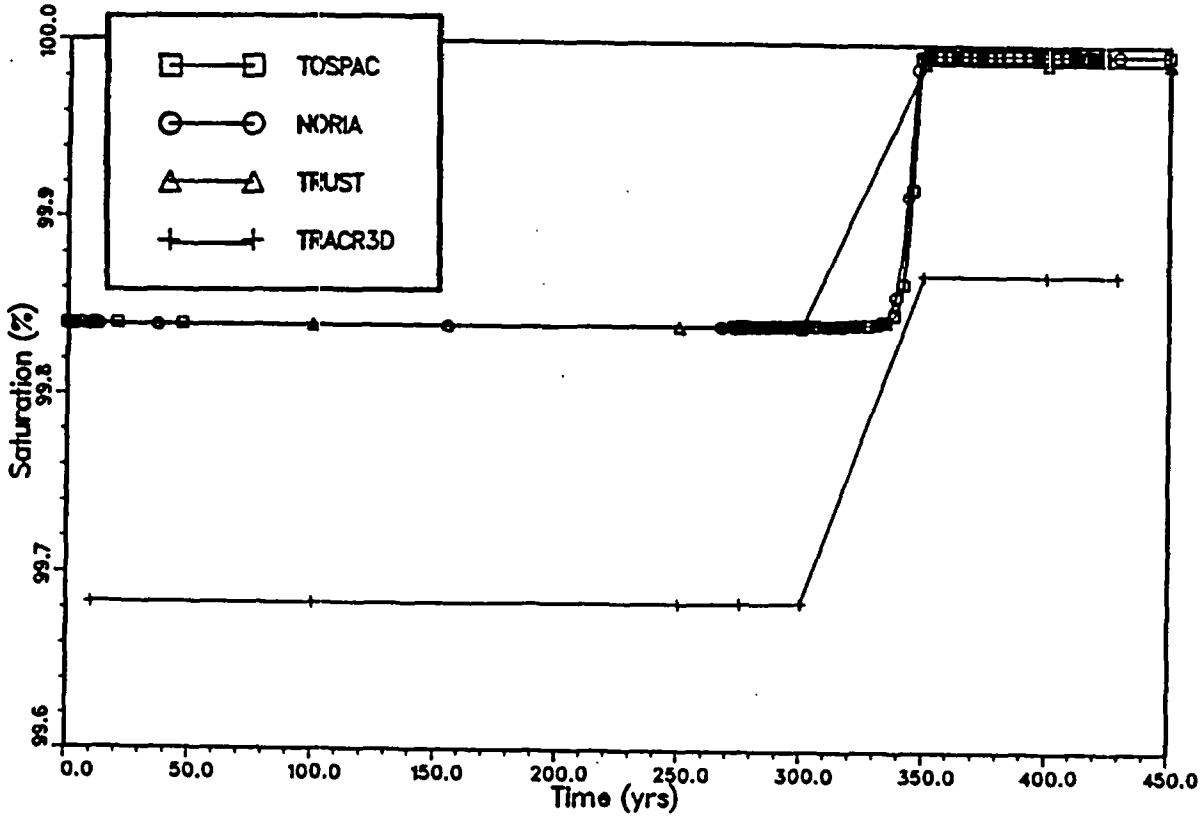


Figure 47. Case 9: Final Results for Saturation at 219.5 Meters

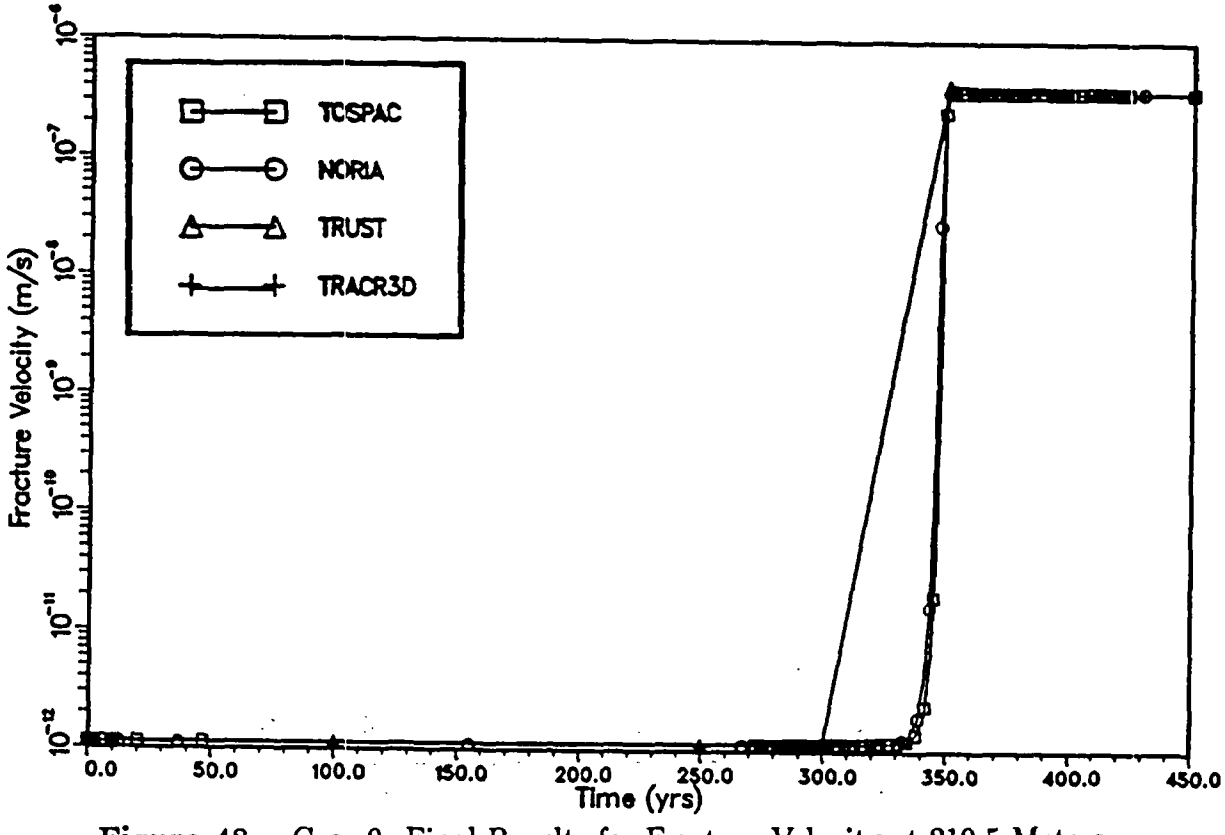


Figure 48. Case 9: Final Results for Fracture Velocity at 219.5 Meters

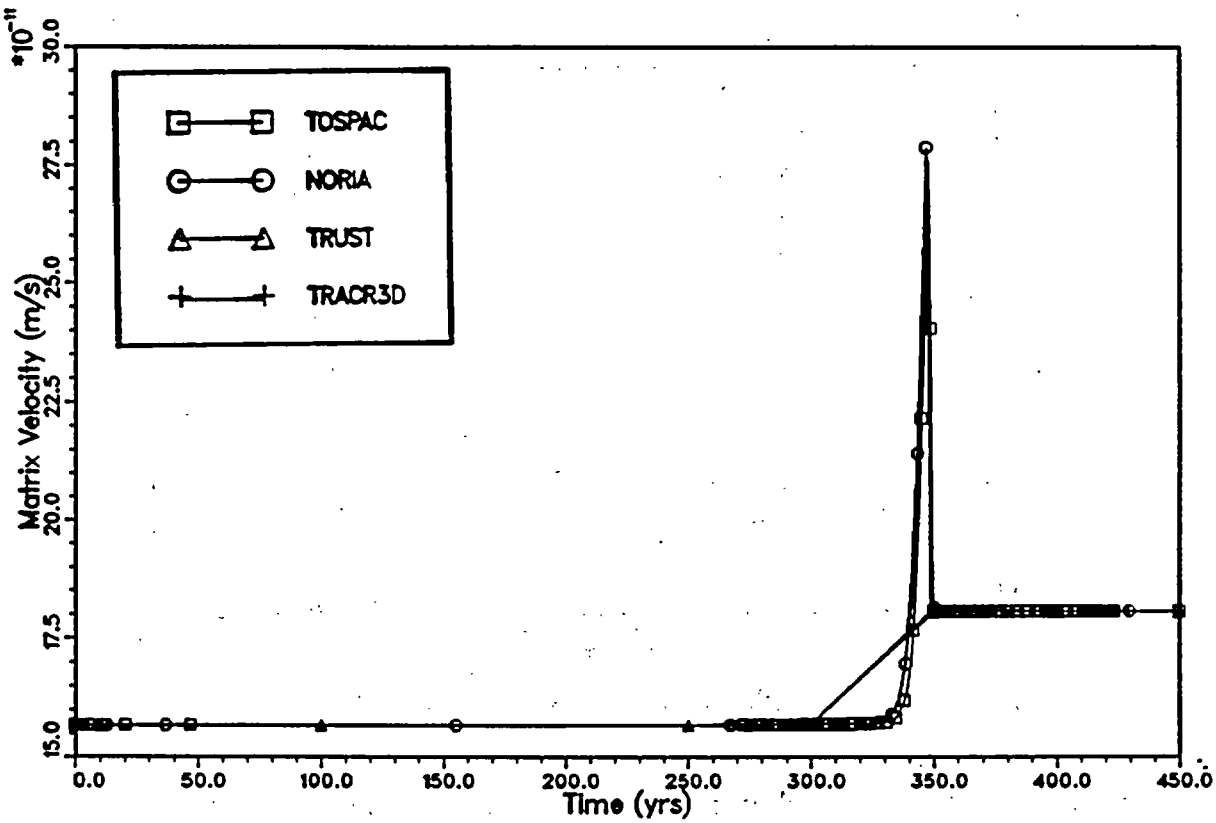


Figure 49. Case 9: Final Results for Matrix Velocity at 219.5 Meters

## Case 10: Transient step change from 0.5 to 1.0 mm/yr, vitric

This case is very similar to Case 9. The only change is that of the material properties for the Calico Hills geologic unit. The higher matrix conductivity for the vitric Calico Hills unit resulted in much more gradual changes in that layer when the front arrived. This made the calculations, in some sense, easier for the computer codes when the front reached the Calico Hills unit. However, not all of the codes required less CPU time for Case 10 than was required for Case 9. Again, the agreement among the codes was very good. Figure 50 is provided as a typical comparison of the codes for this case.

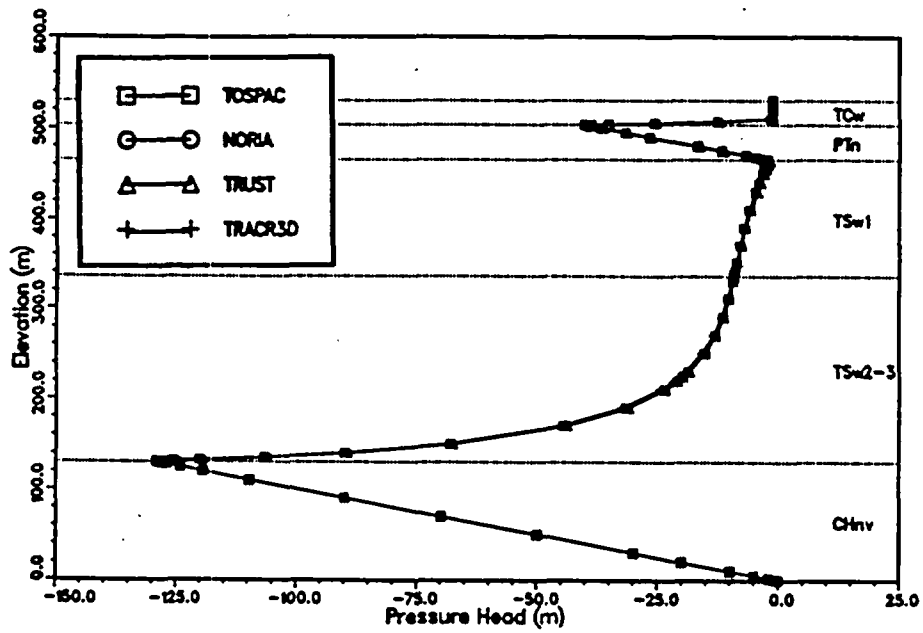


Figure 50. Case 10: Final Results for Pressure Head at 250 Years

## Case 11: Transient step change from 4.0 to 8.0 mm/yr, zeolitic

This case resulted in the fracture flow system transporting the majority of the flux throughout the transient. The matrix flow system is almost completely saturated, even at the beginning of the transient. The entire transient lasts only two years before the new steady condition is established. In general there was good agreement among the codes. Figures 51 and 52 show strong evidence of numerical oscillations in the TRUST results. Near the front, the flux oscillates with elevation. This oscillation is also apparent in the time plots where the oscillation appears as a function of time for one point (however, the low frequency of the temporal output prevents a detailed depiction of the oscillation). It is interesting to note that this instability does not seem to effect the progression of the front through the domain, for TRUST predicts about the same behavior for the motion of the front. As was noted earlier, the numerical instability probably arose from the coarse calculational mesh used for this code.

TRACR3D had problems computing the passage of the wetting front through the problem domain, especially for Cases 11 and 12. These cases had relatively small changes in pressure as the wetting front advanced. Because TRACR3D (as do the other codes) uses pressure changes to determine the time step, the time step increased to the point that the wetting front could not be accurately followed. A similar problem was also identified in the initial NORIA results for Case 11. Forcing smaller time steps in both of these codes resulted in a more accurate simulation of this transient.

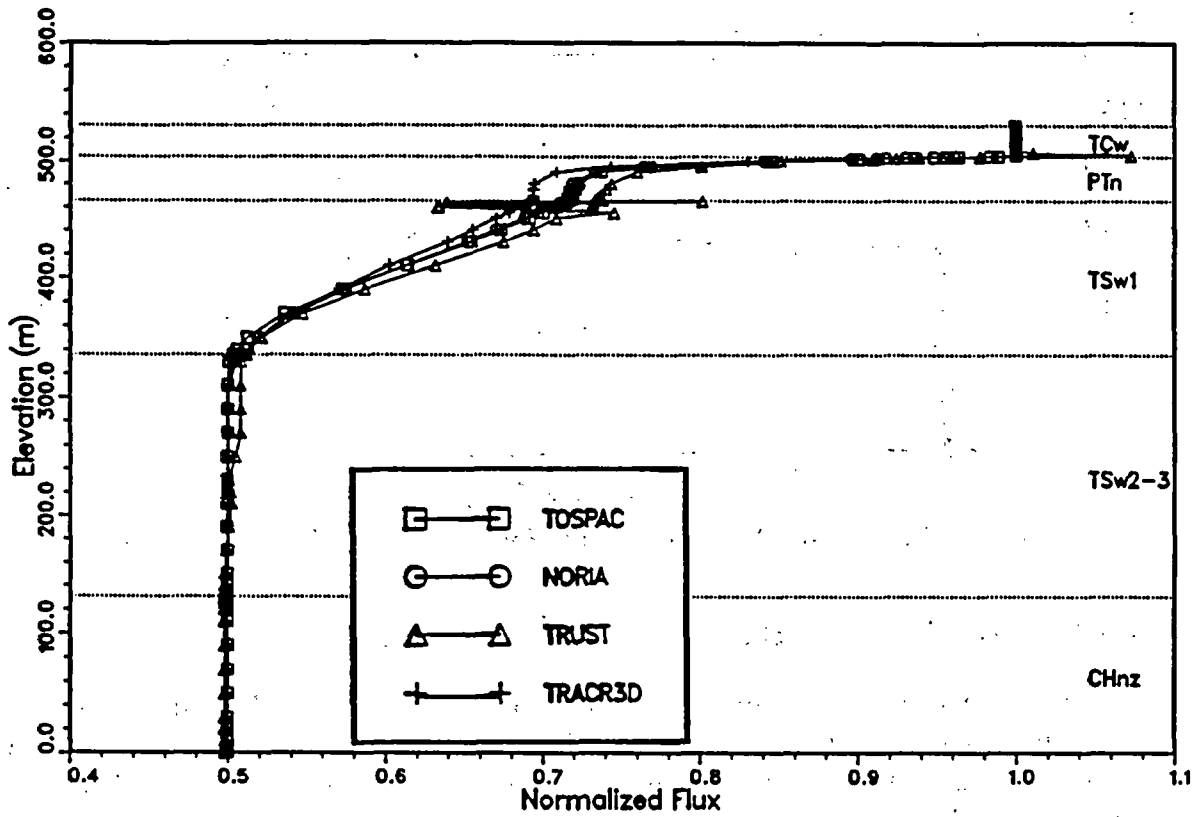


Figure 51. Case 11: Final Results for Normalized Flux at 0.5 Years

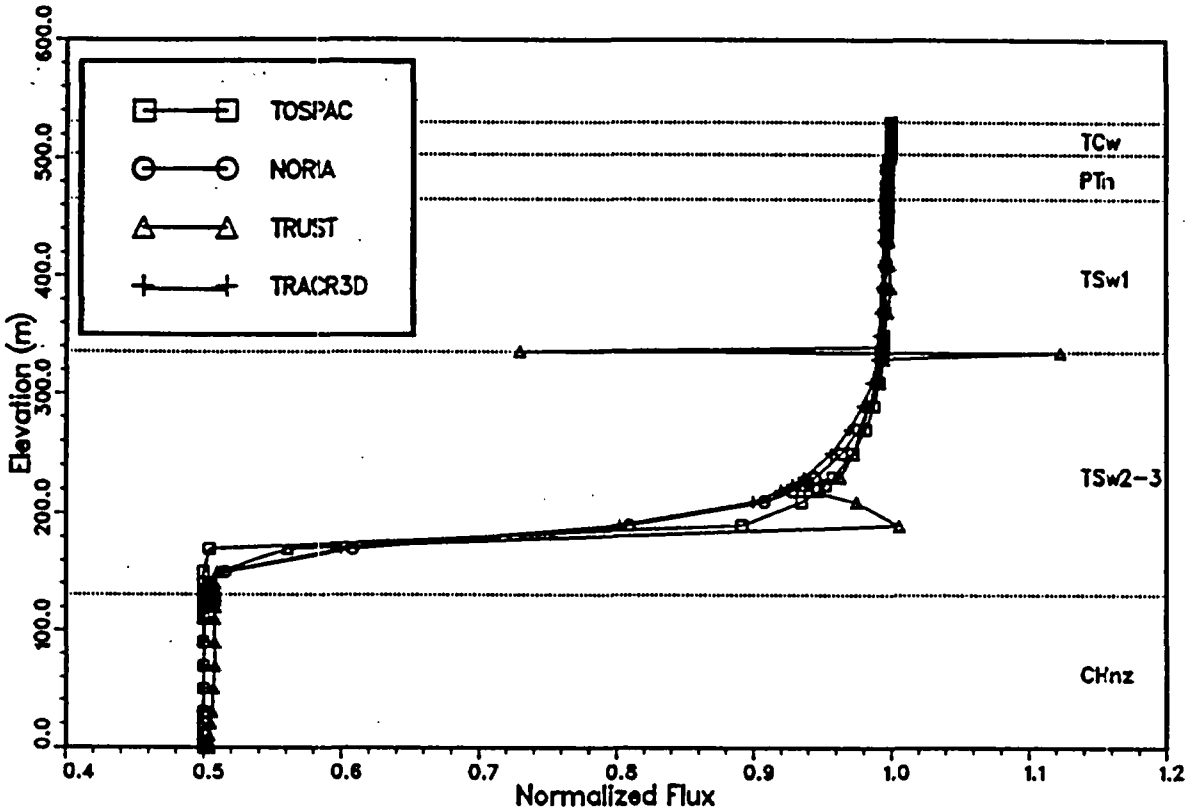


Figure 52. Case 11: Final Results for Normalized Flux at 1.5 Years

**Case 12: Transient step change from 4.0 to 8.0 mm/yr, vitric**

This transient is quite similar to that for Case 11. In fact, until the front reaches the Calico Hills geologic unit, the results are almost identical. Since the Calico Hills layer has an initial saturation much lower in this case, the entire transient takes much longer than Case 11. The majority of the time in this transient is spent saturating the Calico Hills unit. Figure 53 shows the location of the front in the Calico Hills unit at 100 years.

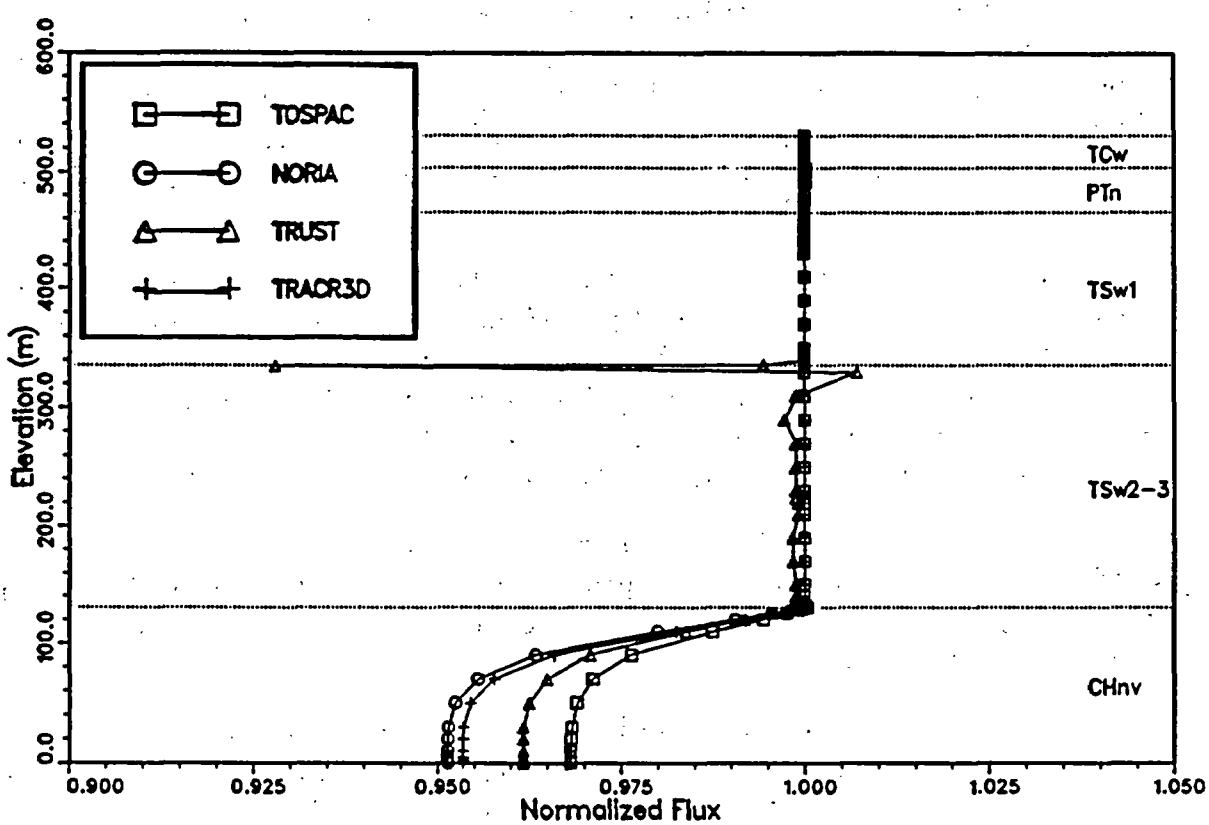


**Figure 53.** Case 12: Final Results for Normalized Flux at 100 Years

# 4 SUMMARY AND CONCLUSIONS

The initial results presented by the participants showed excellent agreement in the pressure profiles (the dependent variable of all the codes). The various distributions for saturation, that were derived directly from the pressure, also agreed well in the initial results. However, some of the secondary quantities derived from the gradient of the pressure were quite variable. The cause of these discrepancies was typically coding errors and differences in mesh refinement.

The post-processing routines (used to calculate parameters derived from pressure head) are critical for achieving useful performance-assessment parameters. The errors evident from the initial results and the efforts necessary to get acceptable final agreement indicate that more attention must be paid to ensuring that these routines work properly. Analysts must give much more attention to careful formulation of the problem and to critical review of their work to prevent the necessity for repeating analyses.

A second round of calculations was required to correct the errors in the codes identified in the initial round. Small discrepancies were still evident in the quantities derived from the gradient of the pressure. This is due to the large variation of hydraulic properties as a function of pressure.

The TRACR3D calculations (Birdsell and Travis, 1991) demonstrated that errors may occur in transient calculations if great care is not taken in assuring convergence in the calculations. For some cases, very small changes in the pressure level can have large effects on the fluxes and water contents. This, in turn, can significantly affect the progression of the flux perturbation through the domain in a transient. The TRACR3D report also demonstrated that small inaccuracies in tabulated hydraulic properties can also have large impacts on the calculated results (TRACR3D was the only code to use tabulated properties).

One of the difficulties in doing a comparison using several participants and several codes is the lack of consistency in reporting and results. Although each participant was requested to use the same input data and functional relationships, and to report on the same subjects, reporting styles were sufficiently different so that comparisons of techniques, successes and failures were not easily accomplished. For example, each code represented interfaces between two geologic media in slightly different ways. This resulted in significant local differences in numerical quantities at the interface. When shown graphically, some codes exhibited what appeared to be point discontinuities at the interfaces (especially where large property differences existed). These very localized discrepancies will have little effect on the calculated performance of the site, but they do distract from the otherwise good agreement among the codes. The participants should take more time in assuring a consistent formulation of the flux quantities at interfaces so that smooth results are obtained.

The current generation of computer codes is probably not efficient enough to allow

large-scale, multidimensional analyses of performance assessment to be performed. The execution times for many of the codes on the COVE-2A problems indicate that a more ambitious problem set would be difficult.

# 5 REFERENCES


Birdsell, K. H., and B. J. Travis, 1991. "Results of the COVE-2A Benchmarking Calculations Run with TRACR3D," LA-11513-MS, Los Alamos National Laboratory, Los Alamos, NM. (NNA.900213.0043)

Bixler, N. E., 1985. "NORIA - A Finite Element Computer Program for Analyzing Water, Vapor, Air, and Energy Transport in Porous Media," SAND84-2057, Sandia National Laboratories, Albuquerque, NM. (NNA.870721.0002)

Carrigan, C. R., N. E. Bixler, P. L. Hopkins, and R. R. Eaton, 1991. "COVE-2A Benchmarking Calculations Using NORIA," SAND88-0942, Sandia National Laboratories, Albuquerque, NM. (NNA.910904.0164)

Dudley, A. L., R. R. Peters, J. H. Gauthier, M. L. Wilson, M. S. Tierney, and E. A. Klavetter, 1988. "Total System Performance Assessment Code (TOSPAC) Volume 1: Physical and Mathematical Bases," SAND85-0002, Sandia National Laboratories, Albuquerque, NM. (NNA.881202.0211).

Dykhuizen, R. C., 1989. "Investigations into the Numerical Solution of Partially Saturated, Porous-Medium Flow," Comm. Appl. Num. Meth., Vol. 5, pp. 105-112. (NNA.910819.0009)

Gauthier, J. H., N. B. Zieman, and W. B. Miller, 1991. "TOSPAC Calculations in Support of the COVE-2A Benchmarking Activity," SAND88-2730, Sandia National Laboratories, Albuquerque, NM. (NNA.910821.0031)

Hayden, N. K., 1985. "Benchmarking NNWSI Flow and Transport Codes: COVE-1 Results," SAND84-0996, Sandia National Laboratories, Albuquerque, NM. (NNA.870721.0003).

Hopkins, P. L., 1989. "COVE-2A Benchmarking Calculations Using LLUVIA," SAND88-2511, Sandia National Laboratories, Albuquerque, NM. (NNA.900314.0236).

Hopkins, P. L. and R. R. Eaton, 1989. "LLUVIA - A One-Dimensional, Steady-State Program for Flow Through Partially Saturated Porous Media," SAND88-0558, Sandia National Laboratories, Albuquerque, NM. (NNA.900406.0001)

Narasimhan, T. N., A. L. Edwards, and P. A. Witherspoon, 1978. "Numerical Model for Saturated-Unsaturated Flow in Deformable Porous Media, Part II: The Algorithm," Water Resour. Res., Vol. 14(2), pp. 255-261. (NNA.890522.0216)

Peters, R. R., E. A. Klavetter, I. J. Hall, S. C. Blair, P. R. Heller, and G. W. Gee, 1984. "Fracture and Matrix Hydrologic Characteristics of Tuffaceous Materials from Yucca Mountain, Nye County, Nevada," SAND84-1471, Sandia National Laboratories, Albuquerque, NM. (NNA.870407.0036)

Peters, R. R., and E. A. Klavetter, 1988. "A Continuum Model for Water Movement in an Unsaturated Fractured Rock Mass," Water Resour. Res., Vol. 24(3), pp. 416-430. (NNA.890523.0319)

Prindle, R. W., January 8, 1986. "Benchmarking of Flow and Transport Codes, COVE-2A Yucca Mountain Hydrology," Sandia National Laboratories memorandum. (NNA.890523.0140)

Silling, S. A., 1983. "Final Technical Position on Documentation of Computer Codes for High-Level Waste Management," NUREG-0856, U. S. Nuclear Regulatory Commission, Washington, DC. (NNA.871104.0034)

Travis, B. J., 1984. "TRACR3D: A Model of Flow and Transport in Porous/Fractured Media," LA-9667-MS, Los Alamos National Laboratory, Los Alamos, NM. (HQS.880517.2072).

# Appendix A. Reference Information Base

### Information from the Reference Information Base Used in this Report

This report contains no information from the Reference Information Base.

### Candidate Information for the Reference Information Base

This report contains no candidate information for the Reference Information Base.

### Candidate Information for the Site & Engineering Properties Data Base

This report contains no candidate information for the Site and Engineering Properties Data Base.

DISTRIBUTION LIST

1 J. W. Bartlett, Director (RW-1)
Office of Civilian Radioactive
Waste Management
U.S. Department of Energy
1000 Independence Avenue, S.W.
Washington, D.C. 20585

1 F. G. Peters, Deputy Director (RW-2)
Office of Civilian Radioactive
Waste Management
U.S. Department of Energy
1000 Independence Avenue, S.W.
Washington, D.C. 20585

1 T. H. Isaacs (RW-4)
Office of Strategic Planning
and International Programs
Office of Civilian Radioactive
Waste Management
U.S. Department of Energy
1000 Independence Avenue, S.W.
Washington, D.C. 20585

1 J. D. Saltzman (RW-5)
Office of External Relations
Office of Civilian Radioactive
Waste Management
U.S. Department of Energy
1000 Independence Avenue, S.W.
Washington, D.C. 20585

1 Samuel Rousso (RW-10)
Office of Program and Resources
Management
Office of Civilian Radioactive
Waste Management
U.S. Department of Energy
1000 Independence Avenue, S.W.
Washington, D.C. 20585

1 J. C. Bresee (RW-10)
Office of Civilian Radioactive
Waste Management
U.S. Department of Energy
1000 Independence Avenue, S.W.
Washington, D.C. 20585

1 C. P. Gertz (RW-20)
Office of Geologic Disposal
Office of Civilian Radioactive
Waste Management
U.S. Department of Energy
1000 Independence Avenue, S.W.
Washington, D.C. 20585

1 S. J. Brocoum (RW-22)
Analysis and Verification Division
Office of Civilian Radioactive
Waste Management
U.S. Department of Energy
1000 Independence Avenue, S.W.
Washington, D.C. 20585

1 D. D. Shelor (RW-30)
Office of Systems and Compliance
Office of Civilian Radioactive
Waste Management
U.S. Department of Energy
1000 Independence Avenue, S.W.
Washington, D.C. 20585

1 J. Roberts (RW-33)
Office of Civilian Radioactive
Waste Management
U.S. Department of Energy
1000 Independence Avenue, S.W.
Washington, D.C. 20585

1 G. J. Parker (RW-332)
Office of Civilian Radioactive
Waste Management
U.S. Department of Energy
1000 Independence Avenue, S.W.
Washington, D.C. 20585

1 Associate Director (RW-40)
Office of Storage and Transportation
Office of Civilian Radioactive
Waste Management
U.S. Department of Energy
1000 Independence Avenue, S.W.
Washington, D.C. 20585

1 Associate Director (RW-50)
Office of Contract Business
Management
Office of Civilian Radioactive
Waste Management
U.S. Department of Energy
1000 Independence Avenue, S.W.
Washington, D.C. 20585

1 C. G. Russomanno (RW-52)
Office of Civilian Radioactive
Waste Management
U.S. Department of Energy
1000 Independence Avenue, S.W.
Washington, D.C. 20585

1 D. U. Deere, Chairman
Nuclear Waste Technical
Review Board
1100 Wilson Blvd. #910
Arlington, VA 22209-2297

1 Dr. John E. Cantlon
Nuclear Waste Technical Review Board
1795 Bramble Dr.
East Lansing, MI 48823

1 Dr. Melvin W. Carter
Nuclear Waste Technical Review Board
4621 Ellisbury Dr., N.E.
Atlanta, GA 30332

1 Dr. Donald Langmuir
Nuclear Waste Technical Review Board
109 So. Lookout Mountain Cr.
Golden, CO 80401

1 Dr. D. Warner North
Nuclear Waste Technical Review Board
Decision Focus, Inc.
4984 El Camino Real
Los Altos, CA 94062

1 Dr. Dennis L. Price
Nuclear Wast Technical Review Board
1011 Evergreen Way
Blacksburg, VA 24060

1 Dr. Ellis D. Verink
Nuclear Waste Technical Review Board
4401 N.W. 18th Place
Gainesville, FL 32605

5 C. P. Gertz, Project Manager
Yucca Mountain Project Office
U.S. Department of Energy
P.O. Box 98608--MS 523
Las Vegas, NV 89193-8608

1 C. L. West, Director
Office of External Affairs
DOE Field Office, Nevada
U.S. Department of Energy
P.O. Box 98518
Las Vegas, NV 89193-85180

12 Technical Information Officer
DOE Field Office, Nevada
U.S. Department of Energy
P.O. Box 98518
Las Vegas, NV 89193-8518

1 P. K. Fitzsimmons, Director
Health Physics & Environmental
Division
DOE Field Office, Nevada
U.S. Department of Energy
P.O. Box 98518
Las Vegas, NV 89193-8518

1 D. R. Elle, Director
Environmental Protection Division
DOE Field Office, Nevada
U.S. Department of Energy
P.O. Box 98518
Las Vegas, NV 89193-8518

1 Repository Licensing & Quality
Assurance Project Directorate
Division of Waste Management
U.S. Nuclear Regulatory Commission
Washington, D.C. 20555

1 Senior Project Manager for Yucca
Mountain Repository Project Branch
Division of Waste Management
U.S. Nuclear Regulatory Commission
Washington, D.C. 20555

1 NRC Document Control Desk
Division of Waste Management
U.S. Nuclear Regulatory Commission
Washington, D.C. 20555

1 P. T. Prestholt
NRC Site Representative
301 E. Stewart Ave.
Las Vegas, NV 89101

1 E. P. Binnall
Field Systems Group Leader
Building 50B/4235
Lawrence Berkeley Laboratory
Berkeley, CA 94720

1 Center for Nuclear Waste
Regulatory Analyses
6220 Culebra Road
Drawer 28510
San Antonio, TX 78284

3 L. J. Jardine
Technical Project Officer for YMP
Mail Stop L-204
Lawrence Livermore National
Laboratory
P.O. Box 808
Livermore, CA 94550

4 R. J. Herbst
Technical Project Officer for YMP
N-5, Mail Stop J521
Los Alamos National Laboratory
P.O. Box 1663
Los Alamos, NM 87545

1 H. N. Kalia
Exploratory Shaft Test Manager
Los Alamos National Laboratory
Mail Stop 527
101 Convention Center Dr.
Suite 820
Las Vegas, NV 89109

1 J. F. Divine
Assistant Director for
Engineering Geology
U.S. Geological Survey
106 National Center
12201 Sunrise Valley Dr.
Reston, VA 22092

6 L. R. Hayes
Technical Project Officer
Yucca Mountain Project Branch--MS 425
U.S. Geological Survey
P.O. Box 25046
Denver, CO 80225

1 V. R. Schneider
Asst. Chief Hydrologist--MS 414
Office of Program Coordination
& Technical Support
U.S. Geological Survey
12201 Sunrise Valley Drive
Reston, VA 22092

1 R. B. Raup, Jr.
Geological Division Coordinator
MS 913
Yucca Mountain Project
U.S. Geological Survey
P.O. Box 25046
Denver, CO 80225

1 D. H. Appel, Chief
Hydrologic Investigations Program
MS 421
U.S. Geological Survey
P.O. Box 25046
Denver, CO 80225

1 E. J. Helley
Branch of Western Regional Geology
MS 427
U.S. Geological Survey
345 Middlefield Road
Menlo Park, CA 94025

1 Chief
Nevada Operations Office
U.S. Geological Survey
101 Convention Center Drive
Suite 860, MS 509
Las Vegas, NV 89109

1 D. Zesiger
U.S. Geological Survey
101 Convention Center Dr.
Suite 860 - MS509
Las Vegas, NV 89109

1 R. V. Watkins, Chief
Project Planning and Management
U.S. Geological Survey
P.O. Box 25046
421 Federal Center
Denver, CO 80225

1 A. L. Flint
U.S. Geological Survey
MS 721
P.O. Box 327
Mercury, NV 89023

1 D. A. Beck
U.S. Geological Survey
1500 E. Tropicana, Suite 201
Las Vegas, NV 89119

1 P. A. Glancy
U.S. Geological Survey
Federal Building, Room 224
Carson City, NV 89701

1 Sherman S. C. Wu
Branch of Astrogeology
U.S. Geological Survey
2255 N. Gemini Dr.
Flagstaff, AZ 86001

1 J. H. Sass
Branch of Tectonophysics
U.S. Geological Survey
2255 N. Gemini Dr.
Flagstaff, AZ 86001

1 DeWayne A. Campbell
Technical Project Officer for YMP
Bureau of Reclamation
Code D-3790
P.O. Box 25007
Denver, CO 80225

1 K. W. Causseaux
NHP Reports Chief
U.S. Geological Survey
421 Federal Center
P.O. Box 25046
Denver, CO 80225

1 V. M. Glanzman
U.S. Geological Survey
913 Federal Center
P.O. Box 25046
Denver, CO 80225

1 J. H. Nelson
Technical Project Officer for YMP
Science Applications International Corp.
101 Convention Center Dr.
Suite 407
Las Vegas, NV 89109

2 SAIC-T&MSS Library
Science Applications International Corp.
101 Convention Center Dr.
Suite 407
Las Vegas, NV 89109

1 Elaine Ezra
YMP GIS Project Manager
EG&G Energy Measurements, Inc.
Mail Stop D-12
P.O. Box 1912
Las Vegas, NV 89125

1 R. E. Jackson, Program Manager
Roy F. Weston, Inc.
955 L'Enfant Plaza, Southwest
Washington, D.C. 20024

1 Technical Information Center
Roy F. Weston, Inc.
955 L'Enfant Plaza, Southwest
Washington, D.C. 20024

1 D. Hedges, Vice President,
Quality Assurance
Roy F. Weston, Inc.
4425 Spring Mountain Road, Suite 300
Las Vegas, Nevada 89102

1 D. L. Fraser, General Manager
Reynolds Electrical & Engineering Co.
Mail Stop 555
P.O. Box 98521
Las Vegas, NV 89193-8521

1 R. F. Pritchett
Technical Project Officer for YMP
Reynolds Electrical & Engineering Co.
MS 408
P.O. Box 98521
Las Vegas, NV 89193-8521

1 B. W. Colston
General Manager & President
Las Vegas Branch
Raytheon Services Nevada
Mail Stop 416
P.O. Box 95487
Las Vegas, NV 89193-5487

1 R. L. Bullock
Technical Project Officer for YMP
Raytheon Services Nevada
Suite P250, MS 403
101 Convention Center Dr.
Las Vegas, NV 89109

1 R. E. Lowder
Technical Project Officer for YMP
MAC Technical Services
101 Convention Center Drive
Suite 1100
Las Vegas, NV 89109

1 C. K. Hastings, Manager
PASS Program
Pacific Northwest Laboratories
P.O. Box 999
Richland, WA 99352

1 A. T. Tamura
Science and Technology Division
Office of Scientific and Technical Information
U.S. Department of Energy
P.O. Box 62
Oak Ridge, TN 37831

1 Carlos G. Bell, Jr.
Professor of Civil Engineering
Civil and Mechanical Engineering Department
University of Nevada, Las Vegas
4505 South Maryland Parkway
Las Vegas, NV 89154

1 C. F. Costa, Director
Nuclear Radiation Assessment Division
U.S. Environmental Protection Agency
Environmental Monitoring Systems Laboratory
P.O. Box 93478
Las Vegas, NV 89193-3478

1 ONWI Library
Battelle Columbus Laboratory
Office of Nuclear Waste Isolation
505 King Avenue
Columbus, OH 43201

1 T. Hay, Executive Assistant
Office of the Governor
State of Nevada
Capitol Complex
Carson City, NV 89710

3 R. R. Loux, Jr.
Executive Director
Nuclear Waste Project Office
State of Nevada
Evergreen Center, Suite 252
1802 North Carson Street
Carson City, NV 89710

1 C. H. Johnson
Technical Program Manager
Nuclear Waste Project Office
State of Nevada
Evergreen Center, Suite 252
1802 North Carson Street
Carson City, NV 89710

1 John Fordham
Water Resources Center
Desert Research Institute
P.O. Box 60220
Reno, NV 89506

1 Dr. Martin Mifflin
Water Resources Center
Desert Research Institute
2505 Chandler Avenue
Suite 1
Las Vegas, NV 89120

1 Eric Anderson
Mountain West Research-Southwest Inc.
2901 N. Central Ave. #1000
Phoenix, AZ 85012-2730

1 Department of Comprehensive Planning
Clark County
225 Bridger Avenue, 7th Floor
Las Vegas, NV 89155

1 Planning Department
Nye County
P.O. Box 153
Tonopah, NV 89049

1 Lincoln County Commission
Lincoln County
P.O. Box 90
Pioche, NV 89043

5 Judy Foremaster
City of Caliente
P.O. Box 158
Caliente, NV 89008

1 Economic Development Department
City of Las Vegas
400 East Stewart Avenue
Las Vegas, NV 89101

1 Community Planning & Development
City of North Las Vegas
P.O. Box 4086
North Las Vegas, NV 89030

1 Director of Community Planning
City of Boulder City
P.O. Box 367
Boulder City, NV 89005

1 Commission of the European Communities
200 Rue de la Loi
B-1049 Brussels
BELGIUM

2 M. J. Dorsey, Librarian
YMP Research and Study Center
Reynolds Electrical & Engineering
Co., Inc.
MS 407
P.O. Box 98521
Las Vegas, NV 89193-8521

1 Amy Anderson
Argonne National Laboratory
Building 362
9700 So. Cass Ave.
Argonne, IL 60439

2 L. D. Foust
Nevada Site Manager
TRW Environmental Safety Systems
101 Convention Center Drive
Suite 540 - MS 423
Las Vegas, NV 89109

| | | |
|---|---|---|
| 1 | 6300 | T. O. Hunter |
| 1 | 6310 | T. E. Blejwas, Actg. |
| 1 | 6312 | F. W. Bingham |
| 10 | 6312 | R. W. Barnard |
| 1 | 6312 | H. A. Dockery |
| 1 | 6313 | L. S. Costin |
| 1 | 6315 | F. B. Nimick, Actg. |
| 1 | 6316 | R. P. Sandoval |
| 2 | 6318 | R. J. Macer for 100/12149/SAND89-2558/QA |
| 1 | 6319 | R. R. Richards |
| 1 | 1510 | J. C. Cummings |
| 1 | 1511 | J. S. Rottler |
| 1 | 1511 | R. R. Eaton |
| 1 | 1511 | P. L. Hopkins |
| 1 | 1511 | M. J. Martinez |
| 1 | 1513 | R. C. Dykhuizen |
| 1 | 1513 | R. D. Skocypec |
| 5 | 3141 | S. A. Landenberger |
| 8 | 3145 | Document Processing for DOE/OSTI |
| 3 | 3151 | G. C. Claycomb |
| 20 | 6341 | WMT Library |
| 1 | 6410 | D. A. Dahlgren |
| 1 | 8523-2 | Central Technical Files |

SAND89-2558

The number in the lower right-hand corner is an accession number used for Office of Civilian Radioactive Waste Management purposes only. It should not be used when ordering this publication.

NNA.920130.0016

| Org. | Bldg. | Name | Rec'd by | Org. | Bldg. | Name | Rec'd by |
|---|---|---|---|---|---|---|---|
| | | | | | | | |
| | | | | | | | |
| | | | | | | | |
| | | | | | | | |
| | | | | | | | |
| | | | | | | | |
| | | | | | | | |
| | | | | | | | |
| | | | | | | | |
| | | | | | | | |
| | | | | | | | |
| | | | | | | | |
| | | | | | | | |
| | | | | | | | |
| | | | | | | | |

Sandia National Laboratories